On Perturbative Scattering Amplitudes in Maximally Supersymmetric Theories

by

Panagiotis Katsaroumpas

A report presented for the examination
for the transfer of status to the degree of
Doctor of Philosophy of the University of London.

Thesis Supervisors
Prof. Bill Spence and Dr. Gabriele Travaglini

Centre for Research in String Theory
Department of Physics
Queen Mary, University of London
Mile End Road, London E1 4NS, UK

I hereby declare that the material presented in this thesis is a representation of my own personal work, unless otherwise stated, and is a result of collaborations with Andreas Brandhuber, Paul Heslop, Dung Nguyen, Bill Spence, Marcus Spradlin and Gabriele Travaglini.

Panagiotis Katsaroumpas

Abstract

There has been substantial calculational progress in the last few years in maximally supersymmetric theories, revealing unexpected simplicity, new structures and symmetries. In this thesis, after reviewing some of the recent advances in $\mathcal{N} = 4$ super Yang-Mills and $\mathcal{N} = 8$ supergravity, we present calculations of perturbative scattering amplitudes and polygonal lightlike Wilson loops that lead to interesting new results.

In $\mathcal{N} = 8$ supergravity, we use supersymmetric generalised unitarity to calculate supercoefficients of box functions in the expansion of scattering amplitudes at one loop. Recent advances have presented tree-level amplitudes in $\mathcal{N} = 8$ supergravity in terms of sums of terms containing squares of colour-ordered Yang-Mills superamplitudes. We develop the consequences of these results for the structure of one-loop supercoefficients, recasting them as sums of squares of $\mathcal{N} = 4$ Yang-Mills expressions with certain coefficients inherited from the tree-level superamplitudes. This provides new expressions for all one-loop box coefficients in $\mathcal{N} = 8$ supergravity, which we check against known results in a number of cases.

In $\mathcal{N} = 4$ super Yang-Mills, we focus our attention on one of the many remarkable features of MHV scattering amplitudes, their conjectured duality to lightlike polygon Wilson loops, which is expected to hold to all orders in perturbation theory. This duality is usually expressed in terms of purely four-dimensional quantities obtained by appropriate subtraction of the infrared and ultraviolet divergences from amplitudes and Wilson loops respectively. By explicit calculation, we demonstrate the completely unanticipated fact that the equality continues to hold at two loops through $\mathcal{O}(\epsilon)$ in dimensional regularisation for both the four-particle amplitude and the (parity-even part of the) five-particle amplitude.

Contents

Chapter 1

Introduction

In this thesis we take a journey through maximal supersymmetry, with $\mathcal{N} = 4$ super Yang-Mills (SYM) and $\mathcal{N} = 8$ supergravity (SUGRA) being our two major destinations. We probe these theories by studying two central objects in quantum field theory, namely scattering amplitudes and Wilson loops. We do so in the framework of perturbation theory, where we also take a journey through the first three orders, from tree level to one and finally two loops.

Scattering amplitudes are windows to the theory giving us access to valuable information on its structure. They are the most direct channel for extracting predictions as they form a bridge between the formulation of the theory and the experiment. Amplitudes calculated in theory are directly related to cross-sections measured in experiment. At weak coupling, and when calculating the full amplitude analytically is an impossible task, we resort to perturbation theory, where one expands the amplitude in powers of the coupling constant and calculates the result order by order in this expansion. This way, one can obtain the answer to some degree of accuracy, and also catch a glimpse of the full amplitude, its properties and its symmetries.

Gauge theories are quantum field theories that have been extensively used to describe the elementary particles and their interactions. Non-abelian gauge theories or Yang-Mills (YM) theories form the backbone of the Standard Model, the theoretical model that unifies three out of the four fundamental forces in nature, the electromagnetic, the weak and the strong. The most complicated part of this model is Quantum Chromodynamics (QCD), the component gauge theory that describes the strong interactions, with gauge group $SU(3)$. The background of the Large Hadron Collider at CERN is dominated by QCD processes. It remains a challenge to deliver high precision theoretical predictions for such processes.

Maximally supersymmetric Yang-Mills (MSYM) or $\mathcal{N} = 4$ super-Yang-Mills (SYM) is an extension of Yang-Mills in a space with the maximum amount of supersymmetry for a theory without gravity. The extra symmetries, i.e. the supersymmetries, are restricting the form of the solutions which are simpler than those in pure Yang-Mills. The beta function vanishes identically for all values of the coupling constant giving us a conformal field theory that is ultraviolet finite [1, 2, 3, 4]. MSYM is an excellent laboratory for developing techniques that can be further applied to their non-supersymmetric cousin where things are more complicated, while the solution of the former is always part of the solution of the latter theory for any given process.

In a conformal field theory, due to scale invariance a scattering process cannot really be defined. While strictly speaking this fact is true, we are able to get around it in practice by regulating the theory in the infrared, and using dimensional regularization with $D = 4 - 2\epsilon$, with $\epsilon < 0$, and more specifically a version of it that preserves all the supersymmetries [5, 6]. Finally, the broken conformal invariance is recovered by performing a Laurent expansion around $\epsilon = 0$, up to and including the $\mathcal{O}(\epsilon^0)$ terms.

MSYM is very elegant and attractive even from a purely theoretical point of view, as hidden symmetries and interesting structures have emerged over the past few years. A specific class of amplitudes, called Maximally Helicity Violating (MHV), appear to be dual to a Wilson loop on a polygonal contour made out of lightlike segments living in a dual momentum space [7, 8, 9, 10, 11, 12, 13, 14]. Both objects involved in the duality, share a conformal symmetry acting in the dual momentum space, termed 'dual conformal symmetry'.

Moreover, the study of $\mathcal{N} = 4$ super-Yang-Mills gives us clues for String Theory and vice versa. Within the proposed weak-strong AdS/CFT duality [15, 16], four-dimensional $\mathcal{N} = 4$ super-Yang-Mills is dual to type IIB superstring theory in $AdS_5 \times S^5$. The mysterious MHV/Wilson loop duality first emerged in [17], where Alday and Maldacena argued using AdS/CFT that the prescription for computing scattering amplitudes at strong coupling was mechanically identical to that for computing the expectation value of a Wilson loop over the closed contour obtained by gluing the momenta of the scattering particles back-to-back to form a polygon with lightlike edges.

After the discovery of the duality at strong coupling, great progress was made on the weak side of the AdS/CFT correspondence. It was originally suggested in [7, 8] that MHV amplitudes and Wilson loops might be equal to each other order by order

in perturbation theory. This bold suggestion was confirmed by explicit calculations at one loop for four particles in [7] and for any number of particles in [8], and at two loops for four and five particles in [9, 10].

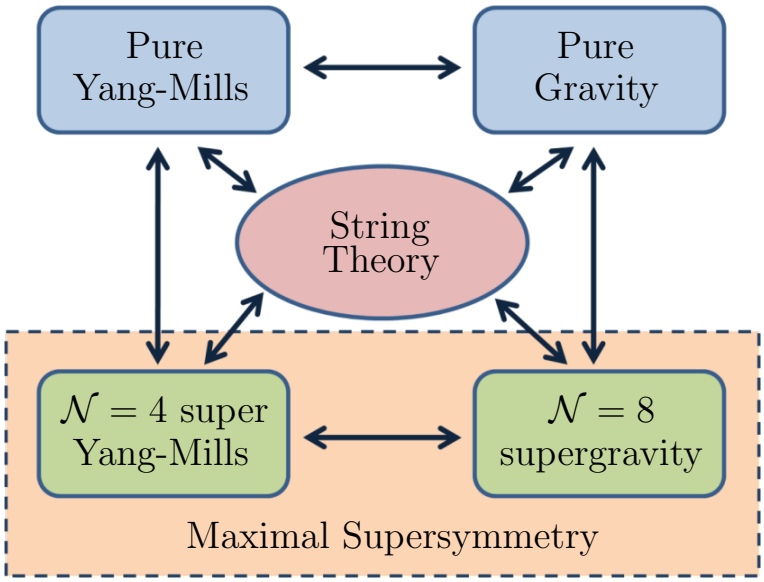

Figure 1.1: *Maximally supersymmetric theories and related theories. Scattering amplitudes in $\mathcal{N} = 4$ super Yang-Mills and $\mathcal{N} = 8$ supergravity are directly related to those in their non-supersymmetric versions. The relatively old KLT relations derived from String theory, and recently discovered relations within quantum field theory, express amplitudes in (super)gravity in terms of those in (super) Yang-Mills. Calculations on the exciting MHV amplitude/Wilson loop duality on both sides of AdS/CFT duality, i.e. in $\mathcal{N} = 4$ super Yang-Mills and string heory, are the latest example of the interplay between quantum field theory and string theory.*

There has been enormous progress in developing efficient techniques for calculating scattering amplitudes in pure and super Yang-Mills over the last two decades. Powerful new methods make use of the analytic properties of amplitudes to give us shortcuts to the final answer that is usually much simpler than any intermediate expression in Feynman diagram calculations. These techniques recycle information recursively to build more complicated amplitudes from simpler ones, even across the various orders of perturbation theory; as only on-shell quantities are used, no explicit Feynman diagram calculation needs to be performed. At tree level, on-shell recursion relations [18, 19], that rely on shifts of momenta of external particles in complex directions, have been widely used to calculate amplitudes in Yang-Mills and gravity, and very recently extended to superamplitudes in super Yang-Mills and supergravity. At loop level, generalised unitarity [20, 21] allows us to build one-loop

amplitudes in maximal supersymmetry from tree-level amplitudes without the need of performing any loop integration.

Turning our attention to the forth force in nature, recent advances have indicated that scattering amplitudes in a gravity theory based on the Einstein-Hilbert action are much simpler than what one would infer from the Feynman diagram expansion, very much like in Yang-Mills theory. In [22, 23], on-shell recursion relations were written down for graviton amplitudes at tree level, and a remarkably benign ultraviolet behaviour of the scattering amplitudes under certain large deformations along complex directions in momentum space was observed. This behaviour, not apparent from a simple analysis based on Feynman diagram considerations [22, 23] similar to those discussed in [19] for Yang-Mills amplitudes, was later re-examined and explained in [24, 25, 26].

Adding the maximum amount of supersymmetry to gravity we obtain $\mathcal{N} = 8$ supergravity (SUGRA). Recent computations show that unexpected cancellations take place in scattering amplitudes. The theory appears to have even better behaviour in the ultraviolet than pure gravity, suggesting that it could be even ultraviolet finite [27, 28, 29, 30]. If cancellations persist to all orders in perturbation theory, then $\mathcal{N} = 8$ supergravity will be the first consistent theory of quantum gravity, and the old idea of supersymmetry will be the new way to quantise gravity. Throughout this thesis we discuss many results that manifest the simplicity of supergravity.

At the quantum level, the unexpected cancellations occuring in maximal supergravity starting at one loop led to the conjecture [31, 32, 33, 34] and later proof [26, 35] of the "no-triangle hypothesis". According to this property, all one-loop amplitudes in $\mathcal{N} = 8$ supergravity can be written as sums of box functions times rational coefficients, similarly to one-loop amplitudes in $\mathcal{N} = 4$ super Yang-Mills (SYM). Interesting connections were established in [29] and [35, 36] between one-loop cancellations, and the large-z behaviour observed in [22, 23, 24, 25, 26], as well as the presence of summations over different orderings of the external particles typical of unordered theories such as gravity (and QED). There is therefore growing evidence of the remarkable similarities between the two maximally supersymmetric theories, $\mathcal{N} = 4$ super Yang-Mills and $\mathcal{N} = 8$ supergravity, culminating in the conjecture that the $\mathcal{N} = 8$ theory could be ultraviolet finite, just like its non-gravitational maximally supersymmetric counterpart. This is supported both by multi-loop perturbative calculations [29, 27, 28, 37], and string theory and M-theory considerations [38, 39, 40, 41].

In a recent paper [42], Elvang and Freedman were able to recast n-graviton MHV

amplitudes at tree level in a suggestive form in terms of sums of squares of n-gluon Maximally Helicity Violating (MHV) amplitudes. An analytical proof for all n of the agreement of their expression to that for the infinite sequence of MHV amplitudes conjectured from recursion relations in [22] was also presented, as well as numerical checks showing agreement with the Berends-Giele-Kuijf formula [43]. A direct proof of the formula of [42] was later given in [44]. In a related development at tree level, the authors of [45] used supersymmetric recursion relations [46, 26] of the BCFW type [18, 19], and the explicit solution found in the $\mathcal{N} = 4$ case in [47], to recast amplitudes in $\mathcal{N} = 8$ supergravity in a new simplified form which involves sums of $\mathcal{N} = 4$ amplitudes. More specifically, this sum involves squares of the SYM tree amplitudes times certain gravity "dressing factors".

Turning to loop amplitudes, it has been shown recently in [48] that four-dimensional generalised unitarity [20, 21] may be efficiently applied to calculate the supercoefficients of one-loop superamplitudes in $\mathcal{N} = 4$ SYM. One of the advantages of the use of superamplitudes is that it makes it particularly efficient to perform the sums over internal helicities [49, 50, 26, 48, 51, 52, 53, 54], which are converted into fermionic integrals. Furthermore, according to the no-triangle property of maximal supergravity [31, 32, 33, 34, 35, 26], one-loop amplitudes in the $\mathcal{N} = 8$ theory are expressed in terms of box functions only, therefore the coefficients of one-loop amplitudes can be calculated by using quadruple cuts. It is therefore natural to investigate how the new expressions for generic tree-level $\mathcal{N} = 8$ supergravity amplitudes found in [45] can be used together with supersymmetric quadruple cuts [48] in order to derive new formulae for one-loop amplitudes in $\mathcal{N} = 8$ supergravity. This is our main objective in [55], the results of which we present in detail in Chapter 3 of this thesis.

The structure of the relations between the tree-level amplitudes in the two maximally supersymmetric theories have very interesting consequences for the results we derive for the one-loop box supercoefficients. When the expressions for tree-level amplitudes are inserted into quadruple cuts, they give rise to new general formulae for the supercoefficients that are written as sums of squares of the result of the corresponding $\mathcal{N} = 4$ SYM calculation (apart from the four-mass case, this will be the square of an $\mathcal{N} = 4$ coefficient), multiplied by certain dressing factors. The one-loop supercoefficients therefore inherit the intriguing structure exhibited by the relations at tree level.

Specifically, we calculate supercoefficients for MHV amplitudes, next-to-MHV (NMHV) and next-to-next-to-MHV (N^2MHV) superamplitudes, and we show in a number of cases how these new expressions match known formulae. In particu-

lar, we show how our results agree with the expressions for the infinite sequence of MHV amplitudes obtained in [31] using unitarity, with the five-point NMHV amplitude [31], and with the six-point graviton NMHV amplitudes coefficients derived in [32, 33]. In the MHV case, we propose a correspondence between the "half-soft" functions introduced in [31] and particular sums of dressing factors, which we check numerically up to 12 external legs. In [31, 32, 33], the tree-level amplitudes entering the cut had been generated using KLT relations [56]. In our approach, we use instead the solution of the supersymmetric recursion relation expressing the tree-level amplitudes in supergravity in terms of squares of those in SYM [45]. Our results support the conjecture that all one-loop amplitude coefficients in $\mathcal{N} = 8$ supergravity may be written in terms of $\mathcal{N} = 4$ Yang-Mills expressions times known dressing factors.

Returning to the topic of the MHV amplitude/Wilson loop duality in $\mathcal{N} = 4$, we focus our attention to the class of MHV amplitudes. Already for a few years prior to the discover of this duality, planar MHV amplitudes in SYM had come under close scrutiny following the discovery of the ABDK relation [57], which expresses the four-point two-loop amplitude as a certain quadratic polynomial in the corresponding one-loop amplitude, a relation which was later checked to hold also for the five-point two-loop amplitude [58, 59]. The all-loop generalization of the ABDK relation, known as the BDS ansatz after the authors of [59], expresses an appropriately defined infrared finite part of the all-loop amplitude in terms of the exponential of the one-loop amplitude. This proposal has also been completely verified for the three-loop four-point amplitude [59], and partially explored for the three-loop five-point amplitude [60].

However, it was shown in [61] that the ABDK/BDS ansatz is incompatible with strong coupling results in the limit of a very large number of particles, and indeed it was found in [62] that starting from six particles and two loops the ansatz is incomplete and the amplitude is given by the ABDK/BDS expression plus a nonzero 'remainder function' (an analytic expression for which was obtained in [63, 64, 65, 66]). The breakdown of the ABDK/BDS ansatz beginning at six particles can be understood on the basis of dual conformal symmetry [67, 68], which completely determines the form of the four- and five-particle amplitudes but allows for an arbitrary function of conformal cross-ratios beginning at $n = 6$ [10, 12]. While dual conformal invariance of SYM scattering amplitudes remains a conjecture beyond one loop, it is necessary if the equality between amplitudes and Wilson loops is to hold in general since the symmetry translates to the manifest ordinary conformal

invariance of the corresponding Wilson loops.

Of course dual conformal symmetry alone does not imply the amplitude/Wilson loop equality since they could differ by an arbitrary function of cross-ratios, but miraculously precise agreement was found in [62, 12] between the two sides for $n = 6$ particles at two loops. Evidently some magical aspect of SYM theory is at work beyond the already remarkable dual conformal symmetry.

This series of developments has opened up a number of interesting directions for further work. In our paper [14], the results of which we present in Chapter 4, we turn our attention to a question which might have seemed unlikely to yield an interesting answer: does the amplitude/Wilson loop equality hold beyond $\mathcal{O}(\epsilon^0)$ in the dimensional regularization parameter ϵ? This question is motivated largely by the observation [8] that at one loop, the four-particle amplitude is actually equal to the lightlike four-edged Wilson loop to all orders in ϵ after absorbing an ϵ-dependent normalization factor. Furthermore, the parity-even part of the five-particle amplitude is equal to the corresponding Wilson loop to all orders in ϵ, again after absorbing the same normalisation factor. For $n > 5$ the Wilson loop calculation reproduces only the all orders in ϵ two-mass easy box functions, while the corresponding n-point amplitude contains additional parity-odd (as well as parity-even) terms which vanish as $\epsilon \to 0$. To our pleasant surprise we find a positive answer to this question at two loops: agreement between the $n = 4$ and the parity-even part of the $n = 5$ amplitude and the corresponding Wilson loop continues to hold at $\mathcal{O}(\epsilon)$ up to an additive constant which can be absorbed into various structure functions. To reach this answer, we perform precision tests of the duality, by means of numeric algorithms based on the Mellin-Barnes method, and powered by cluster computing.

Outline

This thesis is organised as follows.

Chapter 2 is devoted to tree-level scattering amplitudes in pure and maximally supersymmetric Yang-Mills and gravity. This chapter serves as an introduction to the technology needed in order to define and calculate amplitudes, and superamplitudes in the case of supersymmetric theories. After a short review of the colour decomposition in Yang-Mills, in Section 2.2 we present the kinematic variables with main focus on the spinor-helicity formalism. In Section 2.3, we introduce fermionic variables, that allow us to define superamplitudes. In Section 2.3, we present the seeds of our recursive methods, the three-point superamplitudes. Section 2.5 is de-

voted to on-shell recursion at tree-level, where we also familiarise ourselves with the use of all the technology with an explicit example. We conclude this chapter with a topic that has been the starting point for the research discussed in Chapter 3: we present expressions for supergravity tree amplitudes in terms of those in super Yang-Mills.

Chapter 3 is devoted to one-loop superamplitudes, where we present our results for supergravity one-loop coefficients as they appeared in [55]. In Section 3.1, we review the expansion of one-loop amplitudes in a basis of scalar integrals, and in Section 3.2 we present generalised unitarity, a method for calculating the coefficients in this basis in terms of tree superamplitudes. In the next section, we briefly discuss the behaviour of amplitudes in the infrared, while in Section 3.4 we present a discussion that combines three of the main themes of this thesis, namely tree-level recursion relations, generalised unitarity and the infrared behaviour of one-loop amplitudes. In section 3.5 we present supercoefficients in super Yang-Mills [48], the calculation of which motivated our work, and the expressions of which we use to check our formulae for gravity amplitudes against older results.

The remaining of Chapter 3, contains our calculations and results for the one-loop supergravity supercoefficients [55]. In Section 3.6.1, we study MHV superamplitudes at one loop, deriving a straightforward general expression for the supercoefficients in the n-point case. We propose a conjecture which enables an immediate correspondence to be made with the known general formula for these amplitudes, and test this explicitly, in Section 3.6.2, for the so-called two-mass easy coefficients with up to $n = 22$ external legs. Section 3.6.3 turns to consider NMHV amplitudes. We derive general expressions for the three-mass and two-mass easy box coefficients, and the related two-mass hard and one-mass coefficients. Similarly to the SYM case considered in [48], all the supercoefficients can be written in terms of the three-mass coefficients, which we are able to recast as sums of squares of the corresponding SYM three-mass coefficients, times certain bosonic dressing factors. In Section 3.6.4 we study an explicit example, the six-point NMHV case. In Section 3.6.5 we describe how this approach applies in general to N^pMHV amplitude coefficients.

Chapter 4 is dedicated to the MHV amplitude/polygonal lightlike Wilson loop duality. The main goal of that chapter is to present our results for this duality at $\mathcal{O}(\epsilon)$ as they appeared in [14]. We start with some background material on MHV amplitudes. After reviewing the ABDK/BDS ansatz, we present the formulation of the duality in Section 4.2. In the next section we discuss expressions for the MHV amplitude that will be needed later on in order to make the comparison with the

corresponding Wilson loops. In Section 4.5, we introduce the reader to Wilson loop calculations by discussing the one-loop case as an explicit example. In Section 4.6, we discuss dual conformal symmetry, a symmetry defined in dual momentum space that restricts the form of both amplitudes and Wilson loops. In Section 4.7, we present in detail all the integrals making up the two-loop Wilson loop. Sections 4.9 and 4.10 are devoted to the Mellin-Barnes method and its implementation in a computer algorithm. Finally, a presentation and analysis of our results can be found in Section 4.11. We compare amplitude and Wilson loops, showing the agreement between these two quantities up to and including $\mathcal{O}(\epsilon)$ terms.

In Chapter 5 we conclude this thesis and discuss open questions.

In Appendix A, we list all the scalar box integrals expanded in the dimensional regularisation parameter ϵ through $\mathcal{O}(\epsilon^0)$. In Appendix B, we present two different forms for the finite part of a the two-mass easy box functions, the only ingredients required for defining the one-loop MHV amplitude.

Chapter 2

Superamplitudes at tree level

We start our journey in maximal supersymmetry by studying perturbative scattering amplitudes, which are the main predictions one can extract from a theory and also the most common objects used to probe the theory and test its properties.

The first major destination we want to reach by the end of this chapter is to discuss tree-level superamplitudes in maximal supergravity and relate them to those in maximal super Yang-Mills. Our first destination is Yang-Mills, a theory of great importance, familiar to us from the Standard Model. From there we easily move on to its maximally supersymmetric extension, namely $\mathcal{N} = 4$ super Yang-Mills, where we study supersymmetric scattering amplitudes. We are able then to easily hop from one maximally supersymmetric theory to the other and land on $\mathcal{N} = 8$ supergravity. In addition, we take short trips to pure gravity to present older results for graviton amplitudes.

Apart from our journey through the four theories, we also start our journey through the first orders in perturbation theory and study their structure at tree level. Before doing so, we present the machinery we will need in the study of amplitudes, including the spinor-helicity formalism. Studying explicit examples we have the chance to see this machinery in action and familiarise ourselves with the use spinors and anticommuting superspace coordinates. Starting from superamplitudes of three particles, we discuss powerful recursion relations that allow us to build all tree-level superamplitudes in both maximally supersymmetric theories. Finally, we present relations that express tree-level superamplitudes in $\mathcal{N} = 8$ supergravity as a sum of squares of amplitudes in $\mathcal{N} = 4$ SYM. These relations motivated our work that is presented in Chapter 3.

2.1 Scattering amplitudes

In quantum field theory, the basic object calculated is the scattering amplitude of on-shell particles. For example, a scattering amplitude of n gluons in Yang-Mills theory with gauge group SU(N), is a function of the following form

$$\mathcal{A}_n = \mathcal{A}_n(p_1, h_1, a_1; p_2, h_2, a_2; \ldots; p_n, h_n, a_n), \tag{2.1}$$

where p_i, h_i and a_i are the momentum, the helicity and the colour of the i^{th} particle respectively. As a convention we choose to label all momenta when they are considered outgoing, while they satisfy total momentum conservation $\sum_i p_i = 0$.

In non-abelian gauge theory, external states carry colour, which increases the complexity of any calculation. The n-particle scattering amplitude $\mathcal{A}_n$ is in general a sum of terms that consist of a colour part and a kinematic part. The former is a combination of the generators t^a of the gauge group, while the latter is a function of the on-shell momenta satisfying $p_i^2 = 0$. The amplitudes depend also on the helicities of the external particles, but for the moment we can see each helicity configuration as labelling a different amplitude. Expanding in the space of the different colour structures that can appear in an amplitude, one obtains [69]

$$\mathcal{A}(\{p_i, h_i, a_i\}) = 2^{n/2} g^{n-2} \sum_{\sigma \in S_n/Z_n} \text{tr}\left[t^{a_{\sigma(1)}} \ldots t^{a_{\sigma(n)}}\right] A_n(\sigma(1^{h_1}, \ldots, n^{h_n})) + \mathcal{O}(\frac{1}{N^2}), \tag{2.2}$$

where we are summing over all non-cyclic permutations of the indices $\{1, 2, \ldots, n\}$ of the external particles and subleading terms in the number of colours N contain multi-traces of the generators t^a of the gauge group. Here, the generators t^a are in the fundamental representation of SU(N) and they are normalised according to $\text{tr}(t^a t^b) = \frac{1}{2}\delta^{ab}$, and g is the coupling constant of the theory. In the planar limit $N \to \infty$ while keeping $\lambda = g^2 N$ fixed, only the leading contribution survives, allowing us to strip off the colour part and reduce the problem to calculating the colour ordered partial amplitude A_n, that depends only on the momenta and the helicities of the external particles. We usually refer to this object as the amplitude, although it is not the full scattering amplitude. We study amplitudes at weak coupling and perform a perturbative expansion in the coupling constant g, or equivalently, the 't Hooft coupling $a = g^2 N/(8\pi^2)$. The leading term in this expansion is the tree-level contribution to the amplitude. The first subleading term gives us the one-loop correction, while terms with higher powers of the coupling constant give us multi-

loop corrections.

The standard textbook recipe for obtaining an amplitude in perturbation theory is an expansion in terms of Feynman diagrams. The colour-ordering is a very convenient property, as $A_n(1^{h_1}, 2^{h_2}, \ldots, n^{h_n})$ is a gauge-invariant object that contains only the planar Feynman diagrams where the external legs are cyclically ordered according to the ordering of the arguments of A_n. The Feynman rules for non-abelian gauge theory can be found in any quantum field theory textbook like [70, 71]. Due to the colour-ordering, these rules reduce to a simpler set of colour-ordered Feynman rules [69, 72] that contain only the terms that contribute to the colour structure with the right ordering. In what follows, we avoid any explicit Feynman diagram calculation. The number of Feynman diagrams one would have to calculate proliferates as the number of external particles or the order of perturbation increase, making such a calculation very inefficient. We resort to powerful techniques that make use of the analytic properties of amplitudes to give us shortcuts to the final answer that is much simpler than any intermediate expression in a Feynman diagram calculation. One other important characteristic of this technology, that makes it even more efficient, is that it recycles information recursively to build more complicated amplitudes from simpler ones. However, if one wants to understand these techniques and grasp their analytic essence, some Feynman diagram intuition is essential.

Scattering amplitudes can be directly translated to cross-sections that one measures in experiments. In order to obtain the total cross section for a given process with specific particle content, one just needs to square the corresponding scattering amplitudes and sum over all possible helicity configurations.

2.2 Kinematic variables

In the spinor-helicity formalism [73, 74, 75, 76, 77], which is currently the bread and butter of any amplitude calculation, one expresses kinematic objects in terms of spinors rather than momenta. The former are more fundamental than the latter and they lead to more compact expressions.

The complexified Lorentz group in four dimensions is locally isomorphic to

$$SO(3,1,\mathbb{C}) \cong Sl(2,\mathbb{C}) \times Sl(2,\mathbb{C}). \tag{2.3}$$

Due to this fact, a momentum four-vector p_i^μ can be written as a bispinor $p_i^{\alpha\dot{\alpha}}$; the former is obtained obtained from latter by means of the Hermitian 2×2 Pauli

matrices σ^μ, $\mu = 0, 1, 2, 3$,

$$p_{i\alpha\dot{\alpha}} = p_{i\mu}\sigma^\mu_{\alpha\dot{\alpha}}, \tag{2.4}$$

where $\sigma^0 = \mathbf{1}$ and the index μ lives in a space with signature $+---$. The antisymmetric tensors $\epsilon_{\alpha\beta}$ and $\epsilon_{\dot{\alpha}\dot{\beta}}$ (with $\epsilon_{12} = \epsilon_{\dot{1}\dot{2}} = 1$) act as metrics in the two distinct spinor spaces, and the masslessness of the momenta

$$p^{\alpha\dot{\alpha}}p_{\alpha\dot{\alpha}} = \epsilon_{\alpha\beta}\epsilon_{\dot{\alpha}\dot{\beta}}p^{\alpha\dot{\alpha}}p^{\beta\dot{\beta}} = \det(p^{\alpha\dot{\alpha}}) = 0, \tag{2.5}$$

allows us to factorise the momentum bispinor into two spinors. One proceeds by associating to each particle a pair of commuting Weyl spinors λ^α and $\tilde{\lambda}^{\dot{\alpha}}$, of positive and negative chirality respectively. These are complex-valued two-component objects, i.e. $\alpha, \dot{\alpha} = 1, 2$. More specifically, the momentum of the i^{th} particle in the bispinor form $p_{i\alpha\dot{\alpha}}$ can be written as the product of the two corresponding spinors

$$p_{i\alpha\dot{\alpha}} = \lambda_{i\alpha}\tilde{\lambda}_{i\dot{\alpha}}. \tag{2.6}$$

From (2.4), it follows that the reality of p_i^μ translates to the Hermiticy of $p_i^{\alpha\dot{\alpha}}$. This fact forces the two spinors to be complex conjugate to each other, i.e. $\overline{\lambda}_i^{\dot{\alpha}} = \pm\tilde{\lambda}_i^{\dot{\alpha}}$. However, as we are often working with complex momenta, one relaxes this constraint and takes the two spinors to be independent.

Lorentz invariant quantities written in spinor space must be functions of contractions of spinors only. To simplify the notation, we define the following objects for the inner products of positive and negative chirality spinors respectively

$$\langle ij\rangle \equiv \lambda_i^\alpha\lambda_{j\alpha} = \epsilon_{\alpha\beta}\lambda_i^\alpha\lambda_j^\beta, \tag{2.7}$$

$$[ij] \equiv \tilde{\lambda}_i^{\dot{\alpha}}\tilde{\lambda}_{j\dot{\alpha}} = \epsilon_{\dot{\alpha}\dot{\beta}}\tilde{\lambda}_i^{\dot{\alpha}}\tilde{\lambda}_j^{\dot{\beta}}. \tag{2.8}$$

By definition, these products are antisymmetric in their two arguments, i.e. $\langle ji\rangle = -\langle ij\rangle$ and $[ji] = -[ij]$, while they vanish if the two spinors are proportional, i.e. $\lambda_j^\alpha = c\lambda_i^\alpha$ or $\tilde{\lambda}_j^{\dot{\alpha}} = c\tilde{\lambda}_i^{\dot{\alpha}}$, with $c \in \mathbb{C}$.

As spinors are two-dimensional objects, we can span the whole space using any two spinors λ_i and λ_j, with $\langle ij\rangle \neq 0$. We can then express a third spinor λ_k in this basis

$$\lambda_k = c_1\lambda_i + c_2\lambda_j. \tag{2.9}$$

Contracting both sides with either λ_i or λ_j we can solve for the complex coefficients

c_1 and c_2 to obtain

$$\lambda_k = \frac{\langle kj\rangle\lambda_i + \langle ik\rangle\lambda_j}{\langle ij\rangle}. \tag{2.10}$$

Contracting with a fourth spinor λ_l we obtain the following identity

$$\langle ij\rangle\langle kl\rangle = \langle ik\rangle\langle jl\rangle + \langle il\rangle\langle kj\rangle, \tag{2.11}$$

which is known as the Schouten identity. An identical expansion to (2.10) exists for the $\tilde{\lambda}$ spinors, leading to an identical Schouten identity to (2.11) with the only difference that the spinor inner products are changed to $\langle \bullet\, \bullet\rangle \to [\bullet\, \bullet]$.

Kinematic invariants written in terms of spinor inner products take the form

$$s_{ij} = (p_i + p_j)^2 = 2p_ip_j = \langle ij\rangle[ji]. \tag{2.12}$$

In Yang-Mills planar amplitudes, due to the colour-ordering, one encounters two-particle channels of the form $s_{i(i+1)}$ only, where it is understood that in an n-particle process $n + 1 \equiv 1$.

We can also construct Lorentz invariant quantities by contracting the two indices of a momentum bispinor $P^{\alpha\dot{\alpha}}$ with two spinors, one of each kind,

$$\langle i|P|j] \equiv \lambda_i^{\alpha} P_{\alpha}{}^{\dot{\alpha}} \tilde{\lambda}_{j\dot{\alpha}}. \tag{2.13}$$

Note that P here is not necessarily lightlike, and therefore it cannot always be factorised into a product of spinors. If it is a sum of massless momenta, then the object in (2.13) can be written as

$$\langle i|\sum_{r\in R} p_r|j] = \sum_{r\in R}\langle ir\rangle[rj], \tag{2.14}$$

where R is a set of indices of external massless momenta. Making use of momentum conservation

$$\sum_{r\in\{1,2,\ldots,n\}} p_r = 0, \tag{2.15}$$

we can write down identities of the following form

$$\langle i|\sum_{r\in R} p_r|j] = -\langle i|\sum_{r\in\{1,2,\ldots,n\}\setminus R} p_r\,|j], \tag{2.16}$$

where the summation on the right-hand side is performed over the complement of

the set of indices R relatively to the set of all indices $\{1, 2, \ldots, n\}$.

Similarly, we can contract more momenta to build Lorentz invariant objects like $\langle i|PQ|j\rangle$. We give the following alternative notation for spinors and massless momenta bispinors

$$\lambda_i^\alpha = \langle i^\alpha|, \qquad \lambda_{i\alpha} = |i_\alpha\rangle, \tag{2.17}$$

$$\tilde{\lambda}_i^{\dot{\alpha}} = [i^{\dot{\alpha}}|, \qquad \tilde{\lambda}_{i\dot{\alpha}} = |i_{\dot{\alpha}}], \tag{2.18}$$

$$p_{i\alpha}{}^{\dot{\alpha}} = |i_\alpha\rangle[i^{\dot{\alpha}}|, \tag{2.19}$$

that allows us to fully understand the structure of any Lorentz invariant object we might write down.

The spinor-helicity formalism also allows us to define wavefunctions of particles in terms of spinors. For fermions with momentum $p_{\alpha\dot{\alpha}} = \lambda_\alpha \tilde{\lambda}_{\dot{\alpha}}$ we define

$$\psi_\alpha^{(-)} = \lambda_\alpha, \qquad \psi_{\dot{\alpha}}^{(+)} = \tilde{\lambda}_{\dot{\alpha}}. \tag{2.20}$$

One can easily show that these are solutions of the Dirac equation. For a gluon with momentum $p_{\alpha\dot{\alpha}} = \lambda_\alpha \tilde{\lambda}_{\dot{\alpha}}$ we define the polarisation vectors

$$\epsilon_{\alpha\dot{\alpha}}^{(-)} = \frac{\lambda_\alpha\, \tilde{\mu}_{\dot{\alpha}}}{[\tilde{\lambda}\, \tilde{\mu}]}, \qquad \epsilon_{\alpha\dot{\alpha}}^{(+)} = \frac{\mu_\alpha \tilde{\lambda}_{\dot{\alpha}}}{\langle \mu\, \lambda\rangle}, \tag{2.21}$$

where we have used a reference lightlike momentum q with the decomposition $q_{\alpha\dot{\alpha}} = \mu_\alpha \tilde{\mu}_{\dot{\alpha}}$. One can easily show that the polarisation vectors (2.21) are perpendicular to the momenta p and q, while the freedom in choosing q reflects the freedom of gauge transformations.

Amplitudes written in spinor space are functions of the $2n$ spinors and the n helicities h_i. As total momentum conservation must be satisfied, they are actually defined on the surface given by the following equation

$$\sum_{i=1}^{n} p_i^{\alpha\dot{\alpha}} = \sum_{i=1}^{n} \lambda_i^\alpha \tilde{\lambda}_i^{\dot{\alpha}} = 0, \tag{2.22}$$

where no summation is performed over the index i.

Amplitudes satisfy n auxiliary conditions [78], that for a given particle i they take the form

$$-\frac{1}{2}\left(\lambda_i^\alpha \frac{\partial}{\partial \lambda_i^\alpha} - \tilde{\lambda}_i^{\dot{\alpha}} \frac{\partial}{\partial \tilde{\lambda}_i^{\dot{\alpha}}}\right) \mathcal{A}(\{\lambda, \tilde{\lambda}, h_i\}) = h_i\, \mathcal{A}(\{\lambda, \tilde{\lambda}, h_i\}), \tag{2.23}$$

where h_i is the helicity of the i^{th} particle. It turns out that the absolute value of the total helicity $|h_{\text{tot}}|$ in an amplitude, with $h_{\text{tot}} = \sum_{i=1}^{n} h_i$, is a measure of its simplicity. In theories without gravity, the helicities h_i can take the values ± 1 for gluons, $\pm 1/2$ for fermions and 0 for scalar fields. Superamplitudes with $|h_{\text{tot}}| = n, n-2$ vanish, while the simplest non-vanishing amplitudes are the ones with $h_{\text{tot}} = n-4$ and $h_{\text{tot}} = -n+4$, called Maximally Helicity Violating (MHV) and anti-MHV (or $\overline{\text{MHV}}$) respectively.

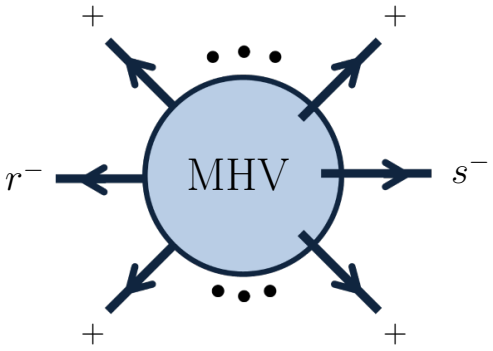

Figure 2.1: *The simplest non-vanishing amplitude corresponding to the MHV process.*

At tree-level, for a process of n gluons, the MHV amplitude is given by the Parke-Taylor formula [79]

$$A_n^{\text{MHV}}(1^+, 2^+, \ldots, r^-, \ldots, s^-, \ldots, n^+) = ig^{n-2} \frac{\langle r\, s\rangle^4}{\langle 1\, 2\rangle\langle 2\, 3\rangle \ldots \langle (n-1)\, n\rangle\langle n\, 1\rangle}, \quad (2.24)$$

where r and s are the labels of two negative helicity gluons. Note that (2.24) is a holomorphic function, i.e. it depends only on the positive chirality spinors λ_i. This result demonstrates, on one hand, the simplicity of the MHV amplitudes, and on the other hand, the power of the spinor-helicity formalism in producing compact expressions.

The formula (2.24) for the MHV amplitude was conjectured by Parke and Taylor and was later proven by Berends and Giele using their off-shell recursive technique [80]. In this method one uses off-shell gluonic currents as building blocks and a recursion formula based on the colour-ordered Feynman rules. Especially for the MHV case, one can guess the form of the gluonic current for arbitrary number of gluons and then prove it by induction.

The $\overline{\text{MHV}}$ amplitude has the same form as the MHV given in (2.24), with the only difference that it is an antiholomorphic function: it depends on the negative

chirality spinors $\tilde{\lambda}_i$ only. Therefore, to obtain the expression for the $\overline{\text{MHV}}$ amplitude, we have to modify (2.24) by changing the spinors of one type to the other $\lambda_i \to \tilde{\lambda}_i$, or, essentially, change the inner products of the one type to the other, i.e. $\langle \bullet\bullet \rangle \to [\bullet\bullet]$.

The next class of nonvanishing amplitudes in order of complexity are the next-to-MHV (NMHV) and $\overline{\text{NMHV}}$ with total helicities $h_{\text{tot}} = n - 6$ and $h_{\text{tot}} = -n + 6$ respectively. The general amplitude with total helicity $h_{\text{tot}} = n - 4 - 2m$ or $h_{\text{tot}} = -n + 4 + 2m$ is called N^mMHV or $\overline{\text{N}^m\text{MHV}}$ respectively.

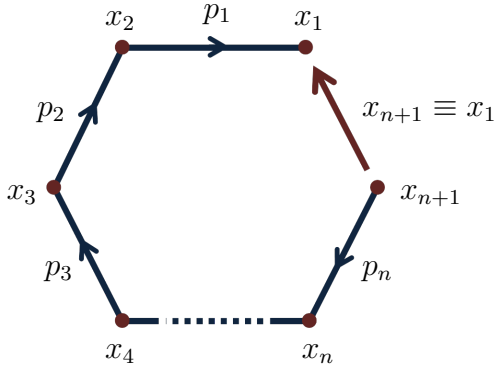

Figure 2.2: *A construction demonstrating the definition of the dual space and the dual momenta x_i. Due to momentum conservation, $x_{n+1} \equiv x_1$.*

At this point, we make a construction in order to introduce the notion of dual momenta x_i. These coordinates are present in our notation for several results, while the main object of Chapter 4, namely the lightlike polygonal Wilson loop, is defined in this dual momentum space. We define dual coordinates x_i [17, 67] according to the following equation

$$p_i = x_i - x_{i+1}. \tag{2.25}$$

As shown in Figure 2.2, starting from an arbitrary point x_{n+1}, each lightlike vector p_i takes us from the point x_{i+1} to the point x_i, to finally end up to the point x_1. From (2.25) it follows that

$$0 = \sum_{i=1}^{n} p_i = x_1 - x_{n+1}, \tag{2.26}$$

which vanishes due to momentum conservation. Therefore, the starting and ending points are identical, i.e. $x_1 \equiv x_{n+1}$.

The ambiguity on the selection of the starting point x_1 in the dual space is irrelevant, as all functions of the particle momenta p_i will be functions of differences

of dual coordinates

$$x_{ij} \equiv x_i - x_j = p_i + \ldots + p_{j-1}, \tag{2.27}$$

where it is understood that

$$x_{ij} \equiv x_i - x_j = p_i + \ldots + p_n + p_1 + \ldots + p_{j-1}, \qquad \text{if } i > j. \tag{2.28}$$

In Yang-Mills, due to colour ordering, the momenta invariants that one encounters are always squares of these differences x_{ij}^2, containing consecutive momenta. Finally, in this notation, momentum conservation is simply $x_{ij} + x_{ji} = 0$.

Planar scattering amplitudes in $\mathcal{N} = 4$ super Yang-Mills possess a superconformal symmetry in this dual x space [68, 46]. This surprising novel symmetry, termed 'dual superconformal symmetry', is exact at tree level but broken by quantum corrections [10]. Dual conformal symmetry was first observed in the context of the duality between MHV scattering amplitudes and Wilson loops [17, 7, 8], as Wilson loops also demonstrate this symmetry. We will return to discuss the MHV/Wilson loop duality in more detail in Chapter 4.

The graviton MHV amplitude, i.e. the amplitude with total helicity $h_{\text{tot}} = 2(n-4)$, was presented by Berends, Giele and Kuijf in [43]. The four-point amplitude is given by

$$\mathcal{M}_4^{\text{tree}}(1^-, 2^-, 3^+, 4^+) = \langle 12\rangle^8 \frac{[12]}{\langle 34\rangle N(4)}, \tag{2.29}$$

where we define

$$N(n) \equiv \prod_{i=1}^{n-1} \prod_{j=i+1}^{n} \langle ij\rangle. \tag{2.30}$$

For $n > 4$ the graviton MHV amplitudes is given by the BGK formula

$$\mathcal{M}_n^{\text{tree}}(1^-, 2^-, 3^+, \ldots, n^+) = \langle 12\rangle^8 \sum_{\mathcal{P}(2,3,\ldots,n-2)} \frac{[12][n-2\,n-1]}{\langle 1\,n-1\rangle N(n)} \left(\prod_{i=1}^{n-3} \prod_{j=i+2}^{n-1} \langle ij\rangle \right) \prod_{l=3}^{n-3} [l|x_{l+1,n}|n\rangle, \tag{2.31}$$

where the sum runs over all permutations of the labels in the set $\{2, \ldots, n-2\}$. The BGK formula was obtained from the KLT relations that we briefly discuss in Section 2.6. It was conjectured in [43] more than two decades ago, where the authors numerically verified its correctness for $n \leq 11$, while it has been proven only very recently by the authors of [81].

As gravity amplitudes are not colour-ordered, if one removes the factor $\langle 12\rangle^8$

containing the helicity information, we are left with a fully symmetric quantity

$$\frac{\mathcal{M}_n^{\rm MHV}(1^+,2^+,\ldots,i^-,\ldots,j^-,\ldots,n^+)}{\mathcal{M}_n^{\rm MHV}(1^+,2^+,\ldots,a^-,\ldots,b^-,\ldots,n^+)}=\frac{\langle ij\rangle^8}{\langle ab\rangle^8}. \tag{2.32}$$

However, we note that in the BGK formula (2.31) only part of this symmetry is manifest, namely the symmetry under permutations of the $n-3$ labels $\{2,\ldots,n-2\}$.

2.3 On-shell superspace

In maximal supersymmetric theories, the large number of species of external states leads to a proliferation of possible scattering amplitudes. It is extremely convenient to use the supersymmetric formalism of [82], where one also associates to each particle an anticommuting variable η_i^A, where $A=1,\ldots,\mathcal{N}$ is an SU($\mathcal{N}$) index. As we demonstrate in what follows, these extra variables are a very useful tool in bookkeeping all external states and amplitudes, packaged together into single objects, namely superwavefunctions and superamplitudes respectively.

In $\mathcal{N}=4$ SYM, all on-shell states can be assembled into a single superwavefunction

$$\begin{aligned}\Phi(p,\eta)=G^+(p)+\eta^A\Gamma_A(p)+\frac{1}{2}\eta^A\eta^B S_{AB}(p)+\frac{1}{3!}\eta^A\eta^B\eta^C\epsilon_{ABCD}\overline{\Gamma}^D(p)\\ +\frac{1}{4!}\eta^A\eta^B\eta^C\eta^D\epsilon_{ABCD}G^-(p),\end{aligned} \tag{2.33}$$

where, starting from the gluon G^+ with helicity $+1$ in the first term, each subsequent term contains a state with $1/2$ helicity less than the one in the previous term, up to the term containing the gluon G^- with helicity -1. The component states are purely kinematic functions, with no dependence on the η variable. As the helicity of the superwavefunction Φ and, therefore, the total helicity of each term on the right-hand side of (2.33) must be $+1$, it becomes natural to assign helicity $+1/2$ to the variables η^A. As discussed in [48], an alternative supermultiplet $\overline{\Phi}$ can be defined, expanded in terms of the variables $\overline{\eta}_A=(\eta^A)^*$. For real momenta, Φ and $\overline{\Phi}$ are complex conjugate to each other, while for complex momenta, they are related via a Grassmann Fourier transform. The discussion we just made generalises to $\mathcal{N}=8$ supergravity, with the only difference that the η^A variables have now eight components and the supermultiplet contains also fields with helicities ±2 and $\pm3/2$. In the rest of this section we continue the discussion refering to both theories by treating the number of supersymmetries as a free parameter that can take the values

$\mathcal{N} = 4, 8$ for super Yang Mills and supergravity respectively.

Having defined a superwavefunction, it is straightforward to define a superamplitude $\mathcal{A}_n(\{\lambda_i, \tilde{\lambda}_i, \eta_i\})$ as the scattering amplitude of superwavefunctions, where the symbol $\mathcal{A}$ refers to a superamplitude in either super Yang-Mills or supergravity. This is a function of the spinors λ_i and $\tilde{\lambda}_i$ and the Grassmann variables η_i of the external particles, while there is no reference to helicities because this object contains all amplitudes for all helicity configurations one can write down for all the particle species in the supermultiplet. We can expand the superamplitude in the η's, and keeping in mind the expansion of the supermultiplet (2.33), the various amplitudes will be the coefficients of the corresponding powers of η's. For example, in $\mathcal{N} = 4$ super Yang-Mills, the superamplitude expansion will contain terms like the following

$$(\eta_1)^4(\eta_2)^4 A_n(G^- G^- G^+ \dots G^+), \tag{2.34}$$

$$\frac{1}{3!}(\eta_1)^4 \eta_2^A \eta_2^B \eta_2^C \eta_3^E \epsilon_{ABCD} A_n(G^- \overline{\Gamma}_2^D \Gamma_{3E} G^+ \dots G^+ \dots G^+), \tag{2.35}$$

where $(\eta)^4 = \frac{1}{4!}\eta^A \eta^B \eta^C \eta^D \epsilon_{ABCD}$. The coefficient of the term (2.34) is the MHV all-gluon amplitude with gluons 1 and 2 of negative helicity. The coefficient of the term (2.35) is the MHV amplitude with two fermions and $n-2$ gluons, where particle 1 is a gluon of negative helicity, particles 2 and 3 are an antifermion and a fermion respectively, and all the remaining particles are gluons of positive helicity.

The Poincaré supersymmetry algebra generators satisfy

$$\{q_\alpha^A, \overline{q}_{B\dot{\alpha}}\} = \delta_B^A \, p_{\alpha\dot{\alpha}}, \tag{2.36}$$

and can be realised as

$$q_\alpha^A = \sum_{i=1}^n \lambda_{i\alpha} \eta_i^A, \qquad \overline{q}_{A\dot{\alpha}} = \sum_{i=1}^n \tilde{\lambda}_{i\dot{\alpha}} \frac{\partial}{\partial \eta_i^A}, \qquad p_{\alpha\dot{\alpha}} = \sum_{i=1}^n \lambda_{i\alpha} \tilde{\lambda}_{i\dot{\alpha}}. \tag{2.37}$$

Each term in the sums of (2.37) is the single particle generator for the corresponding symmetry.

To show how we arrive at (2.37) we focus for the moment on the generators of one particle. Writing down the momentum operator as the product of the corresponding spinors, the algebra (2.36) for one particle reads

$$\{q_\alpha^A, \overline{q}_{B\dot{\alpha}}\} = \delta_B^A \, p_{\alpha\dot{\alpha}} = \delta_B^A \, \lambda_\alpha \tilde{\lambda}_{\dot{\alpha}}. \tag{2.38}$$

We use λ_α and a second spinor ξ_α to decompose the two-component spinor q^A_α into

$$q^A_\alpha = \lambda_\alpha q^A_\parallel + \xi_\alpha q^A_\perp, \tag{2.39}$$

where $\langle\lambda\xi\rangle \neq 0$. A similar decomposition applies to $\overline{q}_{A\dot{\alpha}}$. Substituting these decompositions in (2.38), and contracting with either or both λ^α and $\tilde{\lambda}^{\dot{\alpha}}$, we can easily show that the projections $q^A_\perp$ and $\overline{q}_{\perp A}$ anticommute with each other and with the rest of the generators, and, therefore, they play no role; we will set them to zero. Substituting the parallel projections into (2.38), we obtain

$$\{q^A_\parallel, \overline{q}_{\parallel B}\} = \delta^A_B, \tag{2.40}$$

which is an algebra that can be realised in terms of Grassmann variables η^A, satisfying $\{\eta^A, \eta^B\} = 0$, and arrive at

$$q^A_\parallel = \eta^A, \qquad\qquad \overline{q}_{\parallel A} = \frac{\partial}{\partial \eta^A}. \tag{2.41}$$

The superamplitude $\mathcal{A}_n(\lambda, \tilde{\lambda}, \eta)$ must be invariant under the supersymmetry transformations in (2.37). In a similar fashion to total momentum conservation (2.22) confining amplitudes to a surface in spinor space, total supermomentum conservation constrains superamplitudes to a surface in superspace defined by the equation

$$q^A_\alpha = \sum_{i=1}^{n} \eta^A_i \lambda_{i\alpha} = 0. \tag{2.42}$$

A generic n-point superamplitude in maximal supersymmetry can be written as [82] [1]

$$\mathcal{A}_n(\lambda, \tilde{\lambda}, \eta) = i(2\pi)^4 \delta^{(4)}(p) \delta^{(2\mathcal{N})}(q) \mathcal{P}_n(\lambda, \tilde{\lambda}, \eta). \tag{2.43}$$

The bosonic delta function $(2\pi)^4\delta^{(4)}(p)$ ensures momentum conservation in the four distinct directions. The fermionic delta function $\delta^{(2\mathcal{N})}(q)$ ensures supermomentum conservation in $2\mathcal{N}$ directions since q carries two indices $A = 1, 2, \ldots, \mathcal{N}$ and $\alpha = 1, 2$. In what follows, we will often omit the bosonic delta function. Expression (2.43) makes explicit the q-supersymmetry, while acting with the $\overline{q}$-supersymmetry

[1] The three-point anti-MHV amplitude has a different form given in (2.66)

generator we obtain the constraint

$$\begin{aligned} 0 &= \overline{q}_{A\dot{\alpha}} \left(\delta^{(2\mathcal{N})}(q)\, \mathcal{P}_n(\lambda, \tilde{\lambda}, \eta) \right) \\ &= \left(\sum_{i=1}^{n} \tilde{\lambda}_{i\dot{\alpha}} \frac{\partial}{\partial \eta_i^A}\, \delta^{(2\mathcal{N})}(\sum_{i=1}^{n} \eta_i^A \lambda_{i\alpha}) \right) \mathcal{P}_n + \delta^{(2\mathcal{N})}(q) \left(\sum_{i=1}^{n} \tilde{\lambda}_{i\dot{\alpha}} \frac{\partial}{\partial \eta_i^A}\, \mathcal{P}_n \right). \end{aligned} \tag{2.44}$$

The first term on the right-hand side of (2.44) is proportional to $\sum_{i=1}^{n} \lambda_{i\alpha}\tilde{\lambda}_{i\dot{\alpha}}$, which vanishes due to the bosonic delta function present in (2.43). The second term on the right-hand side of (2.44), constrains the dependence of $\mathcal{P}_n$ on the superspace variables η

$$\delta^{(2\mathcal{N})}(q)\, \overline{q}_{A\dot{\alpha}}\, \mathcal{P}_n(\lambda, \tilde{\lambda}, \eta). \tag{2.45}$$

As we will see shortly, in the simple case of MHV superamplitudes, the only η-dependence is through the fermionic delta function, and the constraint $\overline{q}\, \mathcal{P}_n = 0$ is automatic, as $\mathcal{P}_n$ does not depend on any of the η's.

As a convention, we choose to label both momenta and supermomenta in an amplitude when all particles are considered outgoing. In the techniques that we discuss in the following sections, i.e. tree-level recursion relations and generalised unitarity at loop level, graphs contain intermediate propagators. As these propagators are attached to two amplitudes, for the corresponding particle we will have momentum p and q on one side and $-p$ and $-q$ on the other. In terms of spinors, changing the sign of momentum is equivalent to changing the sign of either spinor λ or $\tilde{\lambda}$. As a convention, we choose to change the sign of λ which results also to a change of sign for supermomentum q, without having to change the corresponding η. To summarise, in our conventions, the operation $\{p, q\} \to \{-p, -q\}$ written in terms of the superspace variables is $\{\lambda, \tilde{\lambda}, \eta\} \to \{-\lambda, \tilde{\lambda}, \eta\}$.

The supersymmetric amplitude can be expanded in powers of the $n \times \mathcal{N}$ superspace coordinates η_i^A, and the coefficient of each term in this expansion corresponds to a particular scattering amplitude with specific external states. In particular, and as a direct consequence of the expansion (2.33), the coefficient of the term containing m_i powers of η_i^A corresponds to a scattering process where the i^{th} particle has helicity $h_i = \mathcal{N}/4 - m_i/2$. The function $\mathcal{P}_n$ in (2.43) is of the form

$$\mathcal{P}_n = \mathcal{P}_n^{(0)} + \mathcal{P}_n^{(\mathcal{N})} + \mathcal{P}_n^{(2\mathcal{N})} + \ldots \mathcal{P}_n^{((n-4)\mathcal{N})}, \tag{2.46}$$

where $\mathcal{P}_n^{(\mathcal{N}k)}$ is an SU($\mathcal{N}$) invariant homogenous polynomial in the η variables of degree $\mathcal{N}k$. Each term appearing on the right-hand side of (2.46) contains all the

amplitudes of a specific class, starting from the MHV ones contained in $\mathcal{P}_n^{(0)}$, all the way to the $\overline{\text{MHV}}$ contained in the last term $\mathcal{P}_n^{((n-4)\mathcal{N})}$. Note that to get the full amplitude we need to include the fermionic delta function appearing in (2.43), which raises the degree of the term $\mathcal{P}_n^{(\mathcal{N}k)}$ to $\mathcal{N}(k+2)$.

We now have a closer look to the fermionic delta function $\delta^{(2\mathcal{N})}(q)$. In the same fashion that led us to (2.10) and the Schouten identities, we can decompose the spinor q_α^A in the basis of two linearly independent spinors $\lambda_{i\alpha}$ and λ_{ja}

$$q_\alpha^A = \frac{\langle iq^A\rangle\lambda_{j\alpha} - \langle jq^A\rangle\lambda_{i\alpha}}{\langle ij\rangle}, \tag{2.47}$$

where $\langle iq^A\rangle = \lambda_i^\alpha q_\alpha^A$. As a result, the fermionic delta function factorises as follows

$$\delta^{(2\mathcal{N})}(q_\alpha^A) = \langle ij\rangle^{\mathcal{N}}\delta^{(\mathcal{N})}\left(\frac{\langle iq^A\rangle\lambda_{j\alpha}}{\langle ij\rangle}\right)\delta^{(\mathcal{N})}\left(\frac{-\langle jq^A\rangle\lambda_{i\alpha}}{\langle ij\rangle}\right), \tag{2.48}$$

leading to the following useful relation

$$\delta^{(2\mathcal{N})}(q_\alpha^A) = \langle ij\rangle^{\mathcal{N}}\delta^{(\mathcal{N})}\left(\eta_i^A + \frac{1}{\langle ij\rangle}\sum_{s\neq i,j}\langle is\rangle\eta_s^\alpha\right)\delta^{(\mathcal{N})}\left(\eta_j^A - \frac{1}{\langle ij\rangle}\sum_{s\neq i,j}\langle js\rangle\eta_s^\alpha\right). \tag{2.49}$$

Because of the nature of the Grassmann integration obeying the rules

$$\int d\eta^A = 0, \qquad \int d\eta^A\eta^A = 1, \tag{2.50}$$

where no summation over A is implied in the last equation, the following relation holds

$$\delta^{(\mathcal{N})}\left(\sum_i c_i\eta_i^A\right) = \prod_{A=1}^{\mathcal{N}}\left(\sum_i c_i\eta_i^A\right). \tag{2.51}$$

On the left-hand side of (2.51), we have a Grassmann delta function whose argument is a sum of η variables with coefficients c_i that are bosonic quantities. On the right-hand side of the same equation, we have rewritten the Grassmann delta function as a product of the components of its argument for $A = 1, \ldots, \mathcal{N}$. Finally, one can easily show that the following useful identity holds

$$\delta^{(2\mathcal{N})}\left(\sum_{i\in I}\eta_i^A\lambda_{i\alpha}\right) = \frac{1}{\mathcal{N}^2}\prod_{A=1}^{\mathcal{N}}\sum_{i,j\in I, i\neq j}\eta_i^A\eta_j^A\,\langle ij\rangle. \tag{2.52}$$

More than twenty years ago, Nair wrote down the following expression for the

MHV superamplitude in $\mathcal{N}=4$ SYM [82]

$$A_n^{\text{MHV}} = \frac{\delta^{(8)}(\sum_{i=1}^n \eta_i \lambda_i)}{\langle 12\rangle\langle 23\rangle\cdots\langle n1\rangle}. \tag{2.53}$$

One can verify that this formula reproduces the Parke-Taylor formula (2.24). For the all-gluon MHV three-point amplitude with negative helicity gluons i and j, one needs to expand the fermionic delta function according to (2.49) and (2.51), and read off the coefficient of $(\eta_i)^4(\eta_j)^4$ which is $\langle ij\rangle^4$, giving us exactly the numerator we are missing in order to get the right result.

The generalisation of the auxiliary condition 2.23 to superamplitudes reads

$$-\frac{1}{2}\left(\lambda_i^\alpha \frac{\partial}{\partial \lambda_i^\alpha} - \tilde{\lambda}_i^{\dot\alpha}\frac{\partial}{\partial \tilde{\lambda}_i^{\dot\alpha}} - \eta_i^A \frac{\partial}{\partial \eta_i^A}\right) A(\{\lambda,\tilde{\lambda},\eta_i\}) = s\, A(\{\lambda,\tilde{\lambda},\eta_i\}), \tag{2.54}$$

where $s=1$ for $\mathcal{N}=4$ super-Yang-Mills and $s=2$ for $\mathcal{N}=8$ supergravity.

2.4 Three-point superamplitudes

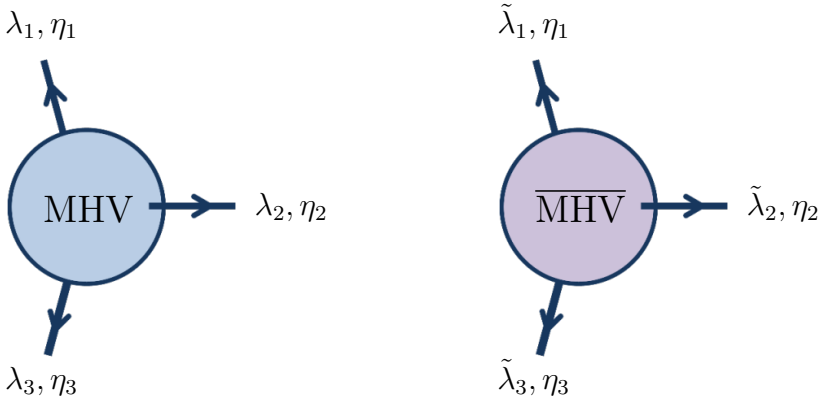

Figure 2.3: *The three-point MHV and $\overline{MHV}$ amplitudes can be defined for complex momenta in Minkowski space or real momenta in a spacetime with signature $(++--)$. The MHV amplitude is a holomorphic function, i.e. it does not depend on the $\tilde{\lambda}$'s, while it corresponds to kinematics where $\tilde{\lambda}_1 \propto \tilde{\lambda}_2 \propto \tilde{\lambda}_3$ and all $[ij]$'s vanish. The $\overline{MHV}$ is an anti-holomorphic function.*

The three-point amplitudes are the most fundamental objects upon which we build our recursion, to obtain first all tree amplitudes and then build one-loop supercoefficients. At three points, due to momentum conservation $p_1+p_2+p_3=0$ and the masslessness of the momenta $p_1^2=p_2^2=p_1^3=0$, we are led to the following

awkward situation

$$0 = p_i^2 = (p_j + p_k)^2 = 2p_j \cdot p_k, \tag{2.55}$$

where the set of indices $\{i, j, k\} = \{1, 2, 3\}$, leading to

$$\langle 12\rangle[21] = \langle 23\rangle[32] = \langle 31\rangle[13] = 0. \tag{2.56}$$

For real momenta in Minkowski space, the fact that $\overline{\lambda}_i^{\dot{\alpha}} = \pm\tilde{\lambda}_i^{\dot{\alpha}}$, (2.56) forces all spinor products of either type to vanish

$$\langle 12\rangle = [12] = \langle 23\rangle = [23] = \langle 31\rangle = [31] = 0, \tag{2.57}$$

which prohibit the existence of the three-point amplitude. However, we can still define these amplitudes if we relax the condition between the λ's and $\tilde{\lambda}$'s, which will take us either to complex momenta in Minkowski or to a spacetime with signature $(++--)$. This gives us the freedom to set either

$$[12] = [23] = [31] = 0, \qquad \text{or} \tag{2.58}$$

$$\langle 12\rangle = \langle 23\rangle = \langle 31\rangle = 0, \tag{2.59}$$

allowing us to define three-particle amplitudes. Note that these two sets of solutions do not mix. For example, if we set $[12] = 0$, i.e. $\tilde{\lambda}_1$ and $\tilde{\lambda}_2$ are proportional, then contracting the momentum conservation condition (2.22) with $\tilde{\lambda}_1$ we get

$$\langle 12\rangle\tilde{\lambda}_2 + \langle 13\rangle\tilde{\lambda}_3 = 0, \tag{2.60}$$

which means that all three $\tilde{\lambda}$'s are proportional and $[23] = [31] = 0$. The choice between the solutions (2.58) and (2.59) is actually a choice between the MHV and $\overline{\text{MVH}}$ amplitudes.

In the MHV case, the general three-point amplitude of particles with spin $|s|$ has the form

$$A^{\text{MHV}}(1^{-|s|}, 2^{-|s|}, 3^{+|s|}) = \langle 12\rangle^a\langle 23\rangle^b\langle 31\rangle^c. \tag{2.61}$$

The three auxiliary conditions (2.23) for $i = 1, 2, 3$, give us

$$a + b = +2|s|, \qquad b + c = -2|s|, \qquad c + a = +2|s|, \tag{2.62}$$

fixing completely the form of the amplitude to the following

$$A^{\rm MHV}(1^{-|s|},2^{-|s|},3^{+|s|}) = \left(\frac{\langle 12\rangle^3}{\langle 23\rangle\langle 31\rangle}\right)^{|s|}. \tag{2.63}$$

Similarly, for the anti-MHV three-point amplitude one finds

$$A^{\rm MHV}(1^{+|s|},2^{+|s|},3^{-|s|}) = \left(\frac{[12]^3}{[23][31]}\right)^{|s|}. \tag{2.64}$$

In $\mathcal{N}=4$ SYM, the three-point MHV superamplitude is [82]

$$A_3^{\rm MHV}(1,2,3) = \frac{\delta^{(8)}\left(\sum_{i=1}^3 \eta_i\lambda_i\right)}{\langle 12\rangle\langle 23\rangle\langle 31\rangle}. \tag{2.65}$$

This is a holomorphic function of the spinor variables, i.e. it depends only on the λ's and not on the $\tilde{\lambda}$'s. The presence of the spinor inner products $\langle ij\rangle$ in the denominator requires the choice of the solution (2.58).

The anti-MHV three-point superamplitude is given by [26, 46]

$$A_3^{\overline{\rm MHV}}(1,2,3) = \frac{\delta^{(4)}(\eta_1[23]+\eta_2[31]+\eta_3[12])}{[12][23][31]}. \tag{2.66}$$

This is an anti-holomorphic function, i.e. it does not depend on the λ's. Note in (2.66) the presence of an unusual fermionic delta function that is of degree 4 in the superspace variables η_i^A. This agrees with the general rule that n-point $\overline{\rm MHV}$ amplitudes in SYM have degree $4n-8$, which in the case $n=3$ prohibits the presence of the usual $\delta^{(8)}(\sum_{i=1}^3 \eta_i\lambda_i)$ of degree 8. This time, the presence of the spinor inner products $[ij]$ in the denominator of (2.66) requires the choice of the solution (2.59).

It is easy to show that the amplitude (2.66) is invariant under all supersymmetries. Indeed, we can use the fermionic delta function to solve for

$$\eta_1 = \frac{-\eta_2^A[31]-\eta_3^A[12]}{[23]}\,\lambda_1. \tag{2.67}$$

The q-supersymmetry operator becomes

$$\sum_{i=1}^3 \eta_i^A\lambda_{i\alpha} = \eta_2^A\frac{\lambda_{1\alpha}[13]+\lambda_{2\alpha}[23]}{[23]} - \eta_3^A\frac{\lambda_{1\alpha}[12]+\lambda_{3\alpha}[32]}{[23]} = 0, \tag{2.68}$$

which vanishes due to momentum conservation (2.22) resulting to

$$\lambda_{1\alpha}[13] + \lambda_{2\alpha}[23] = -\lambda_{3\alpha}[33] = 0, \tag{2.69}$$

$$\lambda_{1\alpha}[12] + \lambda_{3\alpha}[32] = -\lambda_{2\alpha}[22] = 0. \tag{2.70}$$

Therefore, we have proven that (2.66) is invariant under q-supersymmetry. To check the invariance under the $\overline{q}$-supersymmetry, all we have to do is act the corresponding operator to the argument of the fermionic delta function in (2.66), to obtain

$$\sum_{i=1}^{n} \tilde{\lambda}_i \frac{\partial}{\partial \eta_i} \Big(\eta_1[23] + \eta_2[31] + \eta_3[12] \Big) = \tilde{\lambda}_1[23] + \tilde{\lambda}_2[31] + \tilde{\lambda}_3[12] = 0, \tag{2.71}$$

which vanishes due to the antiholomorphic version of (2.10) that one obtains by sending $\lambda \to \tilde{\lambda}$ and $\langle \bullet\, \bullet \rangle \to [\bullet\, \bullet]$.

If, for example, one wants to reproduce the result for the all-gluon anti-MHV three-point amplitude with gluon 1 being the negative helicity one, one needs to expand the fermionic delta function in (2.66) according to (2.51) and read off the coefficient of $(\eta_1)^4$ which gives

$$A(1^-, 2^+, 3^+) = \frac{[23]^4}{[12][23][31]}, \tag{2.72}$$

which agrees with (2.64) after setting $|s| = 1$ and cyclically rotating the labels $i \to i + 1$.

At three-points, since the two superamplitudes (2.65) and (2.66) are defined for different kinematics, given in (2.58) and (2.59) respectively, one cannot combine them into a single amplitude.

In $\mathcal{N} = 8$ supergravity, the three-point amplitudes are given by [26]

$$\mathcal{M}_3^{\rm MHV}(1,2,3) = [A_3^{\rm MHV}(1,2,3)]^2 = \frac{\delta^{(16)}\left(\sum_{i=1}^{3} \eta_i \lambda_i\right)}{(\langle 12\rangle\langle 23\rangle\langle 31\rangle)^2}, \tag{2.73}$$

$$\mathcal{M}_3^{\overline{\rm MHV}}(1,2,3) = [A_3^{\overline{\rm MHV}}(1,2,3)]^2 = \frac{\delta^{(8)}(\eta_1[23] + \eta_2[31] + \eta_3[12])}{([12][23][31])^2}, \tag{2.74}$$

which are the squares of the corresponding superamplitudes in $\mathcal{N} = 4$ SYM. In squaring the corresponding MSYM expressions (2.65) and (2.66), it is understood that the square of the fermionic delta function in MSYM gives us the the corre-

sponding fermionic delta function in supergravity [45]

$$\left[\delta^{(8)}\left(\sum_{i=1}^{n}\eta_i\lambda_i\right)\right]^2 = \delta^{(16)}\left(\sum_{i=1}^{n}\eta_i\lambda_i\right), \tag{2.75}$$

where the η_i's on the left-hand side are the four-component superspace variables of SYM and those on the right-hand side are the eight-component superspace variables of supergravity. Note that the three-point MHV and $\overline{\text{MHV}}$ superamplitudes in supergravity, given in (2.73) and (2.74), are of degree 16 and 8 respectively in the superspace variables η_i^A.

Equation (2.75) works because we can break $SU(8)$ in $\mathcal{N}=8$ superagravity into $SU(4)_a \times SU(4)_b$ by taking $\eta_1,\ldots,\eta_4$ for $SU(4)_a$ and $\eta_5,\ldots,\eta_8$ for $SU(4)_b$. This means that every $d^8\eta$ integral can be rewritten as a product of two $\mathcal{N}=4$ super Yang-Mills integrals and the $SU(8)$ symmetry of our answers is restored by adopting the convention (2.75).

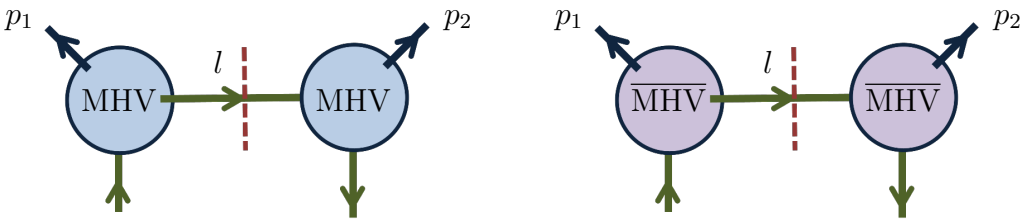

Figure 2.4: *A pair of adjacent three-point amplitudes both of MHV or $\overline{\text{MHV}}$ type would imply $(p_1+p_2)^2 = 0$ and, therefore, these configurations do not exist for general kinematics.*

When discussing one-loop amplitudes and the generalised unitarity method, we encounter pairs of three-point tree-level amplitudes glued together via an on-shell propagator with momentum l, as depicted in Figure 2.4. If these amplitudes are both of MHV type or both of $\overline{\text{MHV}}$ type, then we have $\tilde{\lambda}_1 \propto \tilde{\lambda}_{l_1} \propto \tilde{\lambda}_2$ or $\lambda_1 \propto \lambda_{l_1} \propto \lambda_2$ respectively, which means that $[12]=0$ or $\langle 12\rangle = 0$. In both cases, this means that $(p_1+p_2)^2 = \langle 12\rangle[21] = 0$ which is not true for general kinematics. Therefore, any pair of adjacent three-point superamplitudes should be an MHV-$\overline{\text{MHV}}$ pair.

2.5 Tree-level recursion relations

We now move on to present a supersymmetric generalisation [46, 26] of the BCFW recursion relations [18, 19], that allow us to calculate any tree-level superamplitude

in a recursive fashion. To seed the recursion process we need only the three-point amplitudes discussed in the previous section. In what follows, we present these relations in maximally supersymmetric theories, together with some extra 'bonus relations' special to supergravity. As an example, that also allows us to familiarise ourselves with the use of spinors, we derive the five-point $\overline{\text{MHV}}$ superamplitude.

2.5.1 Derivation

We will set up the formalism by reviewing the derivation of this technology, giving the reader more insight into the ingredients of the method, rather than just presenting a set of prescribed rules.

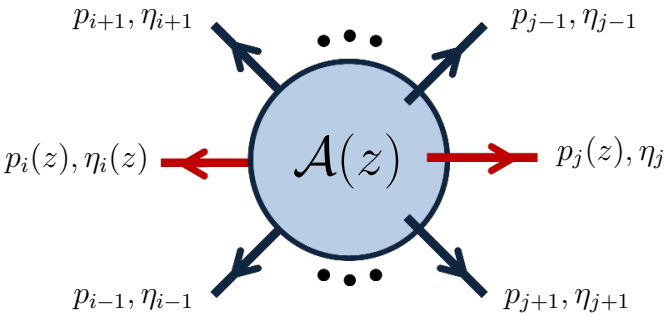

Figure 2.5: *In the deformed superamplitude $\mathcal{A}(z)$, the momenta of particles i and j are shifted in opposite directions. To satisfy supermomentum conservation, the superspace variable η_i is given a z-dependence as well.*

The first ingredient of our method is the two-particle shifts [19]. We consider a complex variable z labelling a family of deformed superamplitudes $\mathcal{A}(z)$. The deformation affects only two of the external particles, that we label i and j. The spinor variables of these particles are shifted according to [19]

$$\tilde{\lambda}_i \to \tilde{\lambda}_i(z) = \tilde{\lambda}_i + z\tilde{\lambda}_j, \qquad \lambda_j \to \lambda_j(z) = \lambda_j - z\lambda_i, \tag{2.76}$$

while λ_i, $\tilde{\lambda}_j$ and both spinors of all the remaining particles remain unchanged. We denote this pair of shifts by $[ij\rangle$. The deformation (2.76) is chosen in such a way so that they momenta p_i and p_j are shifted by the same quantity but in opposite directions

$$p_i(z) = \lambda_i\tilde{\lambda}_i(z) = p_i + z\lambda_i\tilde{\lambda}_j, \qquad p_j(z) = \lambda_j(z)\tilde{\lambda}_j = p_j - z\lambda_i\tilde{\lambda}_j. \tag{2.77}$$

Particles i and j are still on-shell, since their momenta are written down as prod-

ucts of spinors, but for general values of z these momenta are complex, as the reality condition $\overline{\lambda}^{\dot{\alpha}} = \pm\tilde{\lambda}^{\dot{\alpha}}$ is spoiled. Moreover, since $p_i(z) + p_j(z) = p_i + p_j$, total momentum conservation is preserved, and therefore, as far as momenta are concerned, the superamplitude $\mathcal{A}(z)$ is a well defined object.

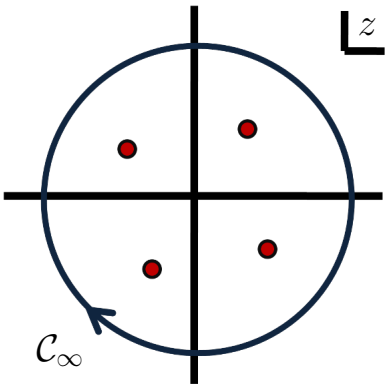

Figure 2.6: *The contour of integration for the integral (2.80) on the complex z-plane is a circle at infinity, encircling all the poles of the function $\mathcal{A}(z)$.*

As far as supermomentum is concerned, the shifts in spinors introduce a shift in q_α^A by an amount of $-z\eta_j\lambda_i$. In order to preserve supermomentum conservation (2.42), we introduce a shift to the superspace variable

$$\eta_i \to \eta_i(z) = \eta_i + z\eta_j, \tag{2.78}$$

which translates to the following shift for the supermomentum of the particle i

$$q_i \to q_i(z) = q_i + z\eta_j\lambda_i. \tag{2.79}$$

We then consider the contour integral

$$\mathcal{C}_\infty = \frac{1}{2\pi i}\oint_{\mathcal{C}} dz \frac{A(z)}{z}, \tag{2.80}$$

where C is a circle at infinity on the complex z-plane shown in Figure 2.6. At tree-level, the superamplitude $\mathcal{A}$ is a rational function of the spinor variables and a polynomial in the superspace variabels η_i^A. Therefore, the deformed superamplitude $\mathcal{A}(z)$ is a rational function of the variable z containing only poles and no branch cuts on the complex z-plane. The integrand in (2.80) contains all the poles of $A(z)$ plus the pole at $z = 0$, simply due to the fact that we have divided by z. Moreover, assuming that $A(z) \to 0$ as $z \to \infty$, the contour integral $\mathcal{C}_\infty = 0$. We return to this

point and discuss the large-z behaviour of amplitudes at infinity in more detail in Section 2.5.2. It follows from Cauchy's theorem that the vanishing integral (2.80) will be equal to the residues of the integrand at all its poles, giving us the following result

$$\mathcal{A}(0) = -\sum_{z_P} \text{Res}\left[\frac{\mathcal{A}(z)}{z}\right], \tag{2.81}$$

where z_P are the poles of the shifted superamplitude $A(z)$ only, as the residue at the pole $z = 0$ is giving us the term $A(0)$ appearing on the left-hand side. Note that $A(0)$ is the unshifted physical superamplitude we want to calculate.

The next key ingredient we are going to add to our method, is the well-studied factorisation of amplitudes on multi-particle or collinear poles, see for example the reviews [69, 72]. This means that near each pole, i.e. the points in momentum space where the momentum P of an intermediate propagator in Feynman diagrams becomes massless, the amplitude factorises into two on-shell subamplitudes times a Feynman propagator corresponding to P

$$\mathcal{A}(z) \to \mathcal{A}_L^{\text{tree}}(z)\frac{i}{P^2(z)}\mathcal{A}_R^{\text{tree}}(z). \tag{2.82}$$

In Yang-Mills, the momenta P one has to consider are always made up of consecutive external momenta due to colour-ordering, while in gravity it is the sum of any subset of all the external momenta.

Now back to constructing our recursion relations, the poles we have to consider are found by considering all diagrams having the form of the one appearing in Figure 2.7, where the labels of the external momenta on this figure are specific to Yang-Mills as they are colour-ordered. The two z-dependent momenta are always on opposite sides, and we have to consider all possible ways of distributing the remaining external legs to the left and right subamplitude A_L and A_R respectively. The momentum of the internal on-shell propagator is the sum of the external momenta on either side, with a factor of ± 1 depending on our convention for the flow of internal momentum on the graph. In super Yang-Mills, it is convenient to chose the shifted legs i and j to be adjacent, i.e. $j = i \pm 1$, as this reduces the number of diagrams one has to consider.

The location of the pole z_P, is found by setting the internal propagator $1/P^2(z)$ on shell. The condition $P^2(z) = 0$ gives us

$$(P + z\lambda_i\tilde{\lambda}_j)^2 = P^2 + 2z\langle i|P|j] = 0 \tag{2.83}$$

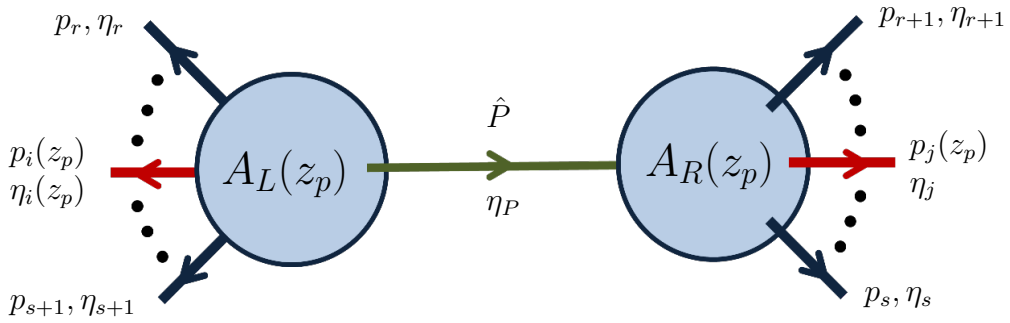

Figure 2.7: *Recursive diagram in super Yang-Mills. The shifted momenta are always on opposite sides, while we consider all choices of r and s with $i \leq r \leq j-1$ and $j \leq s \leq i-1$, keeping in mind the cyclicity condition $i \pm n \equiv i$ with $1 \leq i \leq n$. The subamplitudes are evaluated at the value $z = z_P$ of the corresponding pole. In supergravity, one is not restricted by colour-ordering and has to consider all ways of distributing the unshifted legs to the two subamplitudes. We also associate a superspace variable η_P to the internal propagator that we integrate over.*

where P is the sum of momenta $P = \sum_{m=s+1}^{r} p_m$. From (2.83) we can see that $\mathcal{A}(z)$ has only single poles in z and the location of the pole for each contributing diagram is given by

$$z_P = -\frac{P^2}{2\langle i|P|j]} \ . \tag{2.84}$$

Using the factorisation property (2.82), the contribution of a specific diagram becomes

$$\mathcal{A}_L^{\text{tree}}(z)\frac{-i/(2\langle i|P|j])}{z - P^2/(2\langle i|P|j])}\mathcal{A}_R^{\text{tree}}(z), \tag{2.85}$$

and the residue of $A(z)$ on the pole z_P is given by

$$\text{Res}\ A(z)\Big|_{z=z_P} = \mathcal{A}_L^{\text{tree}}(z_P)\frac{i}{-2\langle i|P|j]}\mathcal{A}_R^{\text{tree}}(z_P). \tag{2.86}$$

As a last step, we need to insert the residues (2.86) into (2.81) and divide by the values (2.84) of the corresponding poles z_P.

The final form of the supersymmetric recursion relations reads

$$\mathcal{A}^{\text{tree}} = \sum_{z_P} \int d^{\mathcal{N}}\eta_{\hat{P}}\, \mathcal{A}_L^{\text{tree}}(z_P)\frac{i}{P^2}\mathcal{A}_R^{\text{tree}}(z_P). \tag{2.87}$$

The superamplitude $\mathcal{A}$ has been expressed as a sum over the poles z_P of products of superamplitude $\mathcal{A}_L(z_P)$ and $\mathcal{A}_R(z_P)$, evaluated on the values of the poles, times a propagator i/P^2. We are also integrating over the superspace variables η_i^A, which

is equivalent to considering all possible helicity configurations for the intermediate leg.

The relations we have just presented are recursive because they express an n-point superamplitude in terms of products of lower-point superamplitudes, i.e. superamplitudes with less than n external legs. They enable us to build any tree-level superamplitude starting from the three-point ones that we presented in the previous section.

In (2.46) we decomposed a generic superamplitude into different contributions carrying different powers of the η's. Each subamplitude on the right-hand side of (2.87) also admits an expansion according to (2.46), while the Grassmann integration over $d^{\mathcal{N}}\eta_P$, which is equivalent to a differentiation, lowers the total degree of each term by $\mathcal{N}$. Therefore, the combined degrees of the subamplitudes reduced by an amount of $\mathcal{N}$ should equal the degree of the superamplitude we are calculating. When writing down the diagrams for the recursion, one has to consider all possible combinations of subamplitudes satisfying this condition. All these points are made clearer in the explicit example presented in the Section 2.5.3.

2.5.2 Large-z behaviour and bonus relations

In this section, we would like to expand on the behaviour of superamplitudes as the complex parameter $z \to \infty$ and discuss one of its implications in supergravity. The vanishing of the shifted amplitude in this limit is a necessary condition for the existence of recursion relations of the BCFW type. In maximal supersymmetry all superamplitudes vanish at infinite complex momentum defined in the naturally supersymmetric way given in (2.77) and (2.79) and for infinite z [26, 46]. More specifically, in $\mathcal{N} = 4$ super Yang-Mills superamplitudes vanish as

$$A(z) \propto \frac{1}{z} \qquad \text{while } z \to \infty, \tag{2.88}$$

and in $\mathcal{N} = 8$ supergravity they vanish as

$$\mathcal{M}(z) \propto \frac{1}{z^2} \qquad \text{while } z \to \infty. \tag{2.89}$$

In the original BCFW setup [19], where one deals with helicity amplitudes rather superamplitudes, the nonsupersymmetric version of the relations is almost identical to what we have described in the previous section, with the only difference that there are no superspace variables and therefore we do not consider the shift in η_i

given in (2.78). Moreover, amplitudes do not in general vanish under any choice of shifted legs. Amplitudes with shifted leg j of negative helicity (we shift the positive chirality spinor λ_j for this leg) do vanish at infinity [19, 22, 23, 24, 25], as it can be shown by simply inspecting how the ingredients of tree-level Feynman diagrams scale with z, i.e. how polarisation vectors and internal propagators behave at infinite z. This allows us to write down recursion relations for helicity amplitudes in pure gravity and pure Yang-Mills for specific choices of shifted legs.

In the supersymmetric version of the recursion relations, the authors of [26] proved the vanishing of any superamplitude by means of a q-supersymmetry translation. One can translate all the η's in a way that two of them can be set to zero. Choosing these two η's to be the ones of the shifted legs, the resulting amplitude is the one with shifted legs of negative helicity and this is known to vanish at infinite z.

Supergravity has better large-z behaviour than super Yang-Mills, which is a manifestation of the simplicity and the cancellations that take place in gravity. Due to the $1/z^2$ falloff of supergravity amplitudes we are able to consider the following contour integral, in addition to the one in (2.80)

$$\mathcal{C}'_{\infty} = \frac{1}{2\pi i} \oint_{\mathcal{C}} dz\, \mathcal{M}(z) = 0, \tag{2.90}$$

where the contour of integration is the same with the one in (2.80), i.e. a circle at infinity on the complex z-plane, as shown in Figure 2.6. In the same fashion we derived the recursion relations, using Cauchy's theorem on the integral (2.90) we obtain relations that involve the diagrams that appear on the recursion relations (2.87). More specifically, calling D_{z_P} the diagram corresponding to the pole z_P

$$D_{z_P} = \int d^{\mathcal{N}}\eta_{\hat{P}}\, \mathcal{M}_L(z_P)\frac{i}{P^2}\mathcal{M}_R(z_P), \tag{2.91}$$

(2.90) leads us to the 'bonus relations' [26, 44]

$$\sum_{z_P} z_P\, D_{z_P} = 0. \tag{2.92}$$

In [44], the bonus relations have been used to relate formulas for the MHV amplitude with $(n-2)!$ terms, related to the BGK formula (2.31), to formulas with $(n-2)!$ terms, typically obtained from recursion relations, like the following

expression presented in [22]

$$\mathcal{M}_n^{\text{MHV}} = \frac{1}{2}\sum_{\mathcal{P}(3,\ldots,n)} \frac{[1n]}{\langle 1n\rangle\langle 12\rangle^2}\frac{[34]}{\langle 23\rangle\langle 24\rangle\langle 34\rangle\langle 35\rangle\langle 45\rangle}\prod_{s=5}^{n-1}\frac{\langle 2|x_{3,s}|s]}{\langle s\ s+1\rangle\langle 2\ s+1\rangle}, \quad (2.93)$$

where we have promoted the presented helicity amplitude to a superamplitude by removing the factor of $\langle ij\rangle^8$ containing the helicity information for the negative helicity gluons i and j. This formula is valid for $n \geq 5$, where for $n = 5$ the product is equal to one.

2.5.3 Example

As an example we will calculate the $\overline{\text{MHV}}$ part of the five-point tree-level superamplitude in super Yang-Mills, using recursion relations. We choose to shift the two adjacent legs $i = 1$ and $j = 2$, i.e. a $[12\rangle$ shift, and the shifts for the spinors given in (2.76) become

$$\hat{\tilde{\lambda}}_1 \equiv \tilde{\lambda}_1(z) = \tilde{\lambda}_1 + z\tilde{\lambda}_2, \qquad \hat{\lambda}_2 \equiv \lambda_2(z) = \lambda_2 - z\lambda_1, \quad (2.94)$$

where from now on hatted quantities are shifted or z-dependent quantities. The Grassmann variable η_1 is the only superspace coordinate acquiring a z-dependence

$$\hat{\eta}_1 = \eta_1 + z\eta_2. \quad (2.95)$$

Using the prescription given in Figure 2.7, we draw the two contributing diagrams appearing in Figure 2.8. Since we are looking at the $\overline{\text{MHV}}$ contribution, the total degree of each diagram in the η's should be $(n-2)\,\mathcal{N} = 12$, which means that, before performing the superspace integration, the product of subamplitudes should have degree 16. In both diagrams, the four-point subamplitudes can only be of MHV type carrying degree 8 in the η's, which forces the three-point subamplitudes to have degree 8 and be of MHV type as well. The first diagram vanishes, as the chosen shifts (2.94) result to $\langle \hat{P}2\rangle = \langle \hat{2}3\rangle = \langle 3\hat{P}\rangle = 0$, making the three-point subamplitude to vanish.

We now focus on the second diagram in Figure 2.8, which is the only contribution

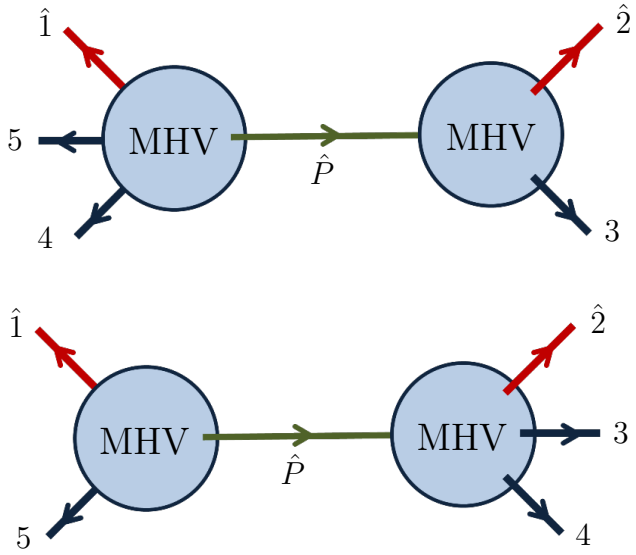

Figure 2.8: *Recursive diagrams for the $\overline{MHV}$ contribution to the five-point superamplitude in $\mathcal{N}=4$ super Yang-Mills. Power counting arguments force both subamplitudes to be of MHV type. The first diagram vanishes for the chosen shifts.*

to our recursion. The two subamplitudes are

$$A_L = \frac{\delta^{(4)}(\hat{p}_1 + \hat{P} + p_5)\,\delta^{(8)}(\hat{\eta}_1\lambda_1 + \eta_{\hat{P}}\lambda_{\hat{P}} + \eta_5\lambda_5)}{\langle 1\hat{P}\rangle\langle\hat{P}5\rangle\langle 51\rangle}, \tag{2.96}$$

$$A_R = \frac{\delta^{(4)}(\hat{p}_2 + p_3 + p_4 - \hat{P})\,\delta^{(8)}(\eta_2\hat{\lambda}_2 + \eta_3\lambda_3 + \eta_4\lambda_4 - \eta_{\hat{P}}\lambda_{\hat{P}})}{\langle\hat{2}3\rangle\langle 34\rangle\langle 4\hat{P}\rangle\langle\hat{P}\hat{2}\rangle}. \tag{2.97}$$

The bosonic delta functions impose momentum conservation on the two subamplitudes and their product combines in the final result into an overall momentum conservation delta function $\delta^{(4)}(\sum_{i=1}^{5} p_i)$. The product of the two fermionic delta functions gives us the overall supermomentum conservation delta function $\delta^{(8)}(\sum_{i=1}^{5}\eta_i\lambda_i)$. Using the momentum conservation on the right subamplitude we can easily show the following identities

$$\langle\hat{2}3\rangle[34] = \langle\hat{2}|3|4] = \langle\hat{2}|\hat{P}|4] = \langle\hat{2}\hat{P}\rangle[\hat{P}4], \tag{2.98}$$

$$\langle 34\rangle[34] = (p_3 + p_4)^2 = (\hat{p}_2 - \hat{P})^2 = -\langle\hat{2}\hat{P}\rangle[\hat{P}2], \tag{2.99}$$

$$[34]\langle 4\hat{P}\rangle = [3|4|\hat{P}\rangle = [3|\hat{2}|\hat{P}\rangle = [32]\langle\hat{2}\hat{P}\rangle. \tag{2.100}$$

Using the results of solving these equations for $\langle\hat{2}3\rangle$, $\langle 34\rangle$ and $\langle 4\hat{P}\rangle$, the denominator

of A_R becomes

$$\langle\hat{2}3\rangle\langle 34\rangle\langle 4\hat{P}\rangle\langle\hat{P}\hat{2}\rangle = \frac{[\hat{P}4][\hat{P}2][23][34]\langle\hat{2}\hat{P}\rangle^4}{[34]^4}. \tag{2.101}$$

Next we combine terms on the denominators of A_L and A_R and use momentum conservation for A_L to obtain the following identities

$$\langle 1\hat{P}\rangle[\hat{P}4] = \langle 1|\hat{P}|4] = -\langle 1|5|4] = -\langle 15\rangle[54], \tag{2.102}$$

$$\langle 5\hat{P}\rangle[\hat{P}4] = \langle 5|\hat{P}|2] = -\langle 5|1|2] = -\langle 51\rangle[12]. \tag{2.103}$$

The recursion relation (2.87), in our case gives

$$\begin{aligned} A_5^{\overline{\text{MHV}}} &= \int d^4\eta_{\hat{P}}\, A_L \frac{i}{P_{15}} A_R \\ &= \Bigg(\int d^4\eta_{\hat{P}}\, \delta^{(8)}(\eta_1\lambda_1 + z_P\eta_2\lambda_1 + \eta_{\hat{P}}\lambda_{\hat{P}} + \eta_5\lambda_5) \\ &\qquad\qquad \times \delta^{(8)}(\eta_2\hat{\lambda}_2 + \eta_3\lambda_3 + \eta_4\lambda_4 - \eta_{\hat{P}}\lambda_{\hat{P}}) \Bigg) \\ &\quad \times \delta^{(4)}\left(\sum_{i=1}^{5} p_i\right) \frac{i\,[34]^4}{\left(\prod_{i=1}^{5}[i\;i+1]\right)\langle 15\rangle^4\langle\hat{2}\hat{P}\rangle^4}. \end{aligned} \tag{2.104}$$

If we wish to extract amplitudes for specific helicity configurations from the result (2.104), all we need to do is use the identity (2.52) to expand the two fermionic delta functions in terms of the η's, perform the Grassmann integration and extract the coefficient of the corresponding term. For example, for the split-helicity gluonic $\overline{\text{MHV}}$ amplitude with gluons 3 and 4 of positive helicity, we need to extract the coefficient of the $(\eta_1)^4(\eta_5)^4(\eta_2)^4$. As far as the integration over $\eta_{\hat{P}}$ is concerned, only terms having exactly $(\eta_{\hat{P}})^4$ powers of this superspace coordinate survive. Therefore, the coefficient in question, is the coefficient in the expansion of the integrand of the term $(\eta_1)^4(\eta_2)^4(\eta_5)^4(\eta_{\hat{P}})^4$. Since the second fermionic delta function can only give us the $(\eta_2)^4(\eta_{\hat{P}})^4$ part, the first fermionic delta function has to give us the $(\eta_1)^4(\eta_5)^4$ part. Therefore, we pick up a factor of $\langle 15\rangle^4$ and $\langle\hat{2}\hat{P}\rangle^4$ from the expansion of each fermionic delta function according to (2.52), and the final result reads

$$A(1_g^-, 2_g^-, 3_g^+, 4_g^+, 5_g^-) = i\,\frac{[34]^4}{[12][23][34][45][51]}. \tag{2.105}$$

Similarly, in the case of the all-gluon $\overline{\text{MHV}}$ amplitude with gluons 2 and 4 of positive helicity we need to extract the coefficient of the term $(\eta_1)^4(\eta_3)^4(\eta_5)^4(\eta_{\hat{P}})^4$ in the integrand, giving us a factor $\langle 15\rangle^4\langle 3\hat{P}\rangle^4$. Using momentum conservation on the

right subamplitude we get $([43]\langle 3\hat{P}\rangle)^4 = ([42]\langle 2\hat{P}\rangle)^2$ and we arrive to the following result

$$A(1_g^-, 2_g^+, 3_g^-, 4_g^+, 5_g^-) = i\,\frac{[24]^4}{[12][23][34][45][51]}. \tag{2.106}$$

Both results (2.105) and (2.106) agree with the Parke-Taylor formula. Finally, we consider the following example involving fermions $A(1_g^-, 2_g^-, 3_f^+, 4_g^+, 5_f^-)$. Following a similar reasoning as in the previous examples, the four powers of η_1 can only come from the first fermionic delta function in (2.104), while the four powers of η_2 can only come from the second one, as in the first one η_1 and η_2 are both multiplied by λ_1. Continuing our reasoning, the single power of η_3 and the three powers of η_5 can come from the second and the first fermionic delta functions respectively. Finally, the powers of $\eta_{\hat{P}}$ are fixed to be one from the first and three from the second delta function. Therefore, we get a factor of $\langle 51\rangle^3\langle \hat{P}1\rangle\langle \hat{P}\hat{2}\rangle^3\langle \hat{2}3\rangle$, while momentum conservation on the right subamplitude gives $\langle \hat{2}3\rangle = -[54]\langle 43\rangle/[52]$, and manipulation $\langle 1\hat{P}\rangle/\langle 2\hat{P}\rangle$ after multiplying both numerator and denominator with $[\hat{P}2]$ gives us $\langle 1\hat{P}\rangle/\langle 2\hat{P}\rangle = -\langle 15\rangle[52]/(\langle 34\rangle[43])$. The final result reads

$$A(1_g^-, 2_g^-, 3_f^+, 4_g^+, 5_f^-) = i\,\frac{[34]^3[45]}{[12][23][34][45][51]}, \tag{2.107}$$

which agrees with the result given in [49]. Note that in the example we presented there has been no need to explicitly calculate the location of the pole z_P, as using momentum conservation we eliminate any z-dependent quantities by expressing them in terms of z-independent quantities.

2.6 Supergravity trees from SYM

Supergravity amplitudes can be expressed in terms of amplitudes in super Yang-Mills, and more specifically the former can be written down as a sum over products of the latter. All the results that we present in the current chapter support the ubiquitous pattern that gravity is the product of two copies of Yang-Mills. The first manifestation of this pattern is the three-point tree superamplitudes (2.73) and (2.74).

The three-point amplitudes has been discovered in the last few years, but more than two decades ago, Kawai, Lewellen and Tye wrote down the KLT relations [56] (see also [83] for a review) that express graviton tree amplitudes $\mathcal{M}_n$ as a sum of products of tree gluon amplitudes $A_n A_n^{'}$, where the momenta in $A_n^{'}$ are permuted

compared to the ones A_n. The KLT relations for four and five particles read

$$\mathcal{M}_4(1,2,3,4) = -s_{12}A_4(1,2,3,4)A_4(1,2,4,3), \tag{2.108}$$

$$\begin{aligned}\mathcal{M}_4(1,2,3,4) = {} & s_{23}s_{45}A_5(1,2,3,4,5)A_5(1,3,2,5,4) \\ & + s_{24}s_{35}A_5(1,2,4,3,5)A_5(1,4,2,5,3).\end{aligned} \tag{2.109}$$

A formula for general number of particles n exists, see for example Appendix A of [31]. The KLT relations were obtained from string theory relations between open and closed string amplitudes. Closed strings contain gravity and open strings contain gauge theories, while in the infinite tension limit, relations in string theory reduce to relations for the corresponding field theories. From a field theoretic point of view, the KLT relations are very surprising since the Lagrangian of Yang-Mills theory appears to be much simpler than the Einstein-Hilbert Lagrangian. The former contains only three- and four-point interactions only, while the latter contains complicated n-point two-derivative vertices.

In a recent paper [42], the n-point tree-level MHV supergravity amplitude has been expressed in terms of super Yang-Mills MHV tree amplitudes and certain 'dressing factors' $G^{\rm MHV}$. This result as given in [45] reads

$$\mathcal{M}_n^{\rm MHV} = \sum_{\mathcal{P}(2,\ldots,n-1)} \Big[A^{\rm MHV}(1,\ldots,n)\Big]^2 G^{\rm MHV}(1,\ldots,n), \tag{2.110}$$

where we sum over the permutations $\mathcal{P}(2,\ldots,n-1)$ of all the external legs apart from 1 and n, and the dressing factors are given by

$$G^{\rm MHV} = x_{13}^2 \prod_{s=2}^{n-3} \frac{\langle s|x_{s,s+2}x_{s+2,n}|n\rangle}{\langle sn\rangle}, \tag{2.111}$$

for $n \geq 4$. For $n = 4$ the product in the above formula is understood to be equal to one. Note that the dressing factors do not depend on the superspace variables η_i. This, together with the fact that two external legs do not participate in the permutations in the sum appearing in (2.110), will allow us in Section 3.6 to derive similar expressions at loop-level between supercoefficients in the two theories. An analytic proof of the agreement of formula (2.110) to the one given in (2.93) for all n was also presented in the same paper [45], as well as numerical checks showing agreement with the BGK formula (2.31). A direct proof of the formula (2.110) was later given in [44].

In a related development at tree level, the authors of [45] used supersymmetric

recursion to recast amplitudes of N^{m}MHV type in $\mathcal{N} = 8$ supergravity in a new simplified form involving squares of MHV amplitudes in $\mathcal{N} = 4$ super Yang-Mills. Specifically, according to [45] a generic supergravity amplitude can be written as

$$\mathcal{M}(1,2,\ldots,n) = \sum_{\mathcal{P}(2,\ldots,n-1)} M(1,2,\ldots,n), \tag{2.112}$$

where the ordered subamplitudes $M(1,2,\ldots,n)$ are [45]

$$M(1,2,\ldots,n) = \left[A^{\rm MHV}(1,2,\ldots,n)\right]^2 \sum_{\alpha} \left[R_\alpha(\lambda_i,\tilde{\lambda}_i,\eta_i)\right]^2 G_\alpha(\lambda_i,\tilde{\lambda}_i). \tag{2.113}$$

Here, $A^{\rm MHV}$ is the MHV superamplitude in SYM given in (2.53), R_α are certain dual superconformal invariant quantities [47], extending those introduced in [48, 68] for the NMHV superamplitudes. G_α are certain gravity 'dressing factors', which are independent of the superspace variables η_i. The summation in (2.113) over the index α denotes a summation over an appropriately chosen set of indices in each N^{m}MHV case. These relations differ from the KLT relations in that they relate supergravity amplitudes to squares of super Yang-Mills ones rather than products of them with permuted arguments. The fact that, in (2.112), two external legs do not participate in the permutations in the sum is very important in the construction we make in Section 3.6.

In the NMHV case the supergravity amplitude can be written as [45]

$$\mathcal{M}^{\rm NMHV}(1,2,\ldots,n) = \sum_{\mathcal{P}(2,\ldots,n-1)} \left(\left[A^{\rm MHV}(1,2,\ldots,n)\right]^2 \sum_{i=2}^{n-3} \sum_{j=i+2}^{n-1} R^2_{n;ij} G^{\rm NMHV}_{n;ij} \right). \tag{2.114}$$

where the dual superconformal invariants $R_{r;st}$ are given by [47, 48]

$$R_{r;st} = \frac{\langle s-1 s\rangle\langle t-1 t\rangle\, \delta^{(4)}\left(\Xi_{r;st}\right)}{x_{st}^2 \langle r|x_{rt}x_{ts}|s-1\rangle\langle r|x_{rt}x_{ts}|s\rangle\langle r|x_{rs}x_{st}|t-1\rangle\langle r|x_{rs}x_{st}|t\rangle}, \tag{2.115}$$

and we define

$$\Xi_{r;st} = \langle r| \left[x_{rs}x_{st} \sum_{k=t}^{r-1} |k\rangle\eta_k + x_{rt}x_{ts} \sum_{k=s}^{r-1} |k\rangle\eta_k \right]. \tag{2.116}$$

The explicit expressions for the dressing factors $G^{\rm NMHV}_{n;ij}$ are given in [45]. From the definition (2.115) of $R_{n;ij}$ one notices that it does not depend on either η_1 or η_n. This property simplifies drastically our calculation of supergravity supercoefficients

in Section 3.6 and is partially responsible for being able to write down the $\mathcal{N}=8$ supercoefficients ass sums of squares of $\mathcal{N}=4$ ones.

Lastly, the N^2MHV supergravity amplitude can be written as [45]

$$\mathcal{M}^{\mathrm{N}^2\mathrm{MHV}}(1,2,\ldots,n) = \sum_{\mathcal{P}(2,3,\ldots,n-1)} \Bigg(\left[A^{\mathrm{MHV}}(1,\ldots,n)\right]^2 \times \sum_{2\leq a,b\leq n-1} R^2_{n;ab} \left[\sum_{a\leq c,d<b} \left(R^{ba}_{n;ab;cd}\right)^2 H^{(1)}_{n;ab;cd} + \sum_{b\leq c,d<n} \left(R^{ab}_{n;cd}\right)^2 H^{(2)}_{n;ab;cd} \right] \Bigg). \tag{2.117}$$

Explicit formulae for the H and R functions are given in [45]. For our purposes we will only need to know the fact that the H functions are independent of the superspace variables η_i and the R functions do not depend on either η_1 or η_n. The latter can be seen from the fact that these extremal values are never taken by the subscripts in the R's, and their explicit form given in (2.14) of [45].

In Chapter 3, we make use of these relations at tree level to derive similar relations at one-loop level.

Chapter 3

One-loop supercoefficients

We continue our journey through maximal supersymmetry, while we move on, in perturbation theory, to loop level. One-loop superamplitudes can be expanded in a basis of known scalar integral, containing only the ones having the shape of a box. All the coefficients in this basis can be determined via a manifestly supersymmetric extension of the generalised unitarity method. This method is extremely efficient as it enables us to construct full one-loop superamplitudes by using ingredients solely from the tree-level land. Final destination of this chapter is to present our results that appeared in [55], that relate supercoefficients in the two maximally supersymmetric theories. We discover new relations that express one-loop coefficients in supergravity in terms of squares of coefficients in super Yang-Mills, similarly to the relations we discussed at tree level in section 2.6. Finally, we will take short trips to pure gravity to check that our results reproduce older results.

3.1 One-loop expansion

In maximally supersymmetric theories, four-dimensional one-loop scattering amplitudes can be expanded in a known basis of scalar box integrals $\mathcal{I}$ with rational coefficients [84, 85, 31, 32, 33, 34, 35, 26]

$$\mathcal{A}^{\text{1-loop}} = \sum_{\mathcal{P}(\{K_i\})} \mathcal{C}(K_1, K_2, K_3, K_4)\, \mathcal{I}(K_1, K_2, K_3, K_4). \tag{3.1}$$

The momenta K_i, with $i = 1, \ldots, 4$, are sums of external momenta, while we are summing over all possible ways of distributing these momenta to four clusters, one for each corner of the box. The general scalar box integral, depicted in Figure 3.1, contains four internal propagators and it is given by the following dimensionally

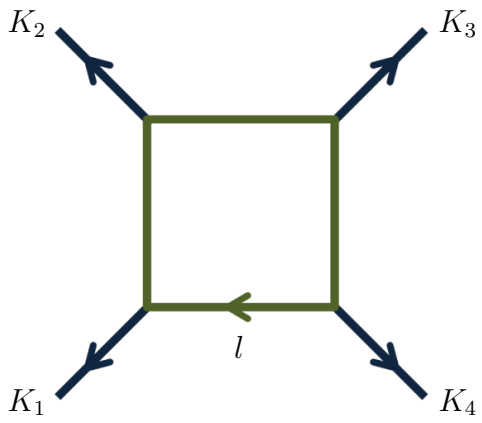

Figure 3.1: *The scalar box integral* $\mathcal{I}(K_1, K_2, K_3, K_4)$.

regularised integral

$$\mathcal{I}(K_1, K_2, K_3, K_4) = -i(4\pi)^{2-\epsilon} \int \frac{d^{4-2\epsilon}l}{(2\pi)^{4-2\epsilon}} \frac{1}{l^2(l-K_1)^2(l-K_1-K_2)^2(l+K_4)^2}. \tag{3.2}$$

Scattering amplitudes in four-dimensional theories with less supersymmetry are expandable in a larger basis containing also scalar integrals with less internal propagators, namely triangle and bubble scalar integrals together with a purely rational term. Maximal supersymmetry simplifies drastically the structure of amplitudes that acquire the no-triangle property, i.e. they contain boxes only. This has been shown in [84] in the SYM case, and in [86] for supergravity, while in [26] a proof identical for both maximally supersymmetric theories was presented.

When considering the expansion (3.1) in $\mathcal{N} = 4$ SYM, because of the colour-ordering, every cluster must contain consecutive momenta only, while this constraint is not present in supergravity amplitudes. The momenta K can be massless or massive; they are massless when they contain exactly one external momentum. The box integrals are classified according to the number of massive corners. For the class of 2m integrals, i.e. the ones with two massive corners, we distinguish two different cases depending on whether the massive corners are adjacent or not, giving us the two-mass hard and two-mass easy boxes respectively. The amplitude expanded in the basis of the different classes of scalar box integrals is

$$\mathcal{A}^{\text{1-loop}} = \sum \left(\mathcal{C}^{\text{1m}} \mathcal{I}^{\text{1m}} + \mathcal{C}^{\text{2me}} \mathcal{I}^{\text{2me}} + \mathcal{C}^{\text{2mh}} \mathcal{I}^{\text{2mh}} + \mathcal{C}^{\text{3m}} \mathcal{I}^{\text{3m}} + \mathcal{C}^{\text{4m}} \mathcal{I}^{\text{4m}} \right). \tag{3.3}$$

In the special case of four-particle scattering, the amplitude is expanded in terms of zero-mass integrals $\mathcal{I}^{0m}$ where all four momenta K are massless.

The scalar box integrals are purely kinematic objects, i.e. they depend only on the momenta of the external particles. Therefore, any helicity information of the external states that must be present in the amplitude, is encoded in the coefficients $\mathcal{C}$. Similarly, when we deal with superamplitudes, the same expansion (3.3) holds and any dependence on the superspace variables η is carried by the same objects $\mathcal{C}$, that we call supercoefficients. These objects, are rational functions of the spinors λ_i and $\tilde{\lambda}_i$ and polynomials in the superspace variables η_i.

An alternative basis of scalar box functions F can be defined, which is related to the $\mathcal{I}$'s via

$$F(K_1, K_2, K_3, K_4) = -\frac{2\sqrt{R(K_1, K_2, K_3, K_4)}}{r_\Gamma}\, \mathcal{I}(K_1, K_2, K_3, K_4), \tag{3.4}$$

where the constant r_Γ is given by

$$r_\Gamma = \frac{\Gamma(1+\epsilon)\Gamma^2(1-\epsilon)}{\Gamma(1-2\epsilon)}. \tag{3.5}$$

The kinematic function R is given by

$$\begin{aligned} R(K_1, K_2, K_3, K_4) = (x_{13}^2 x_{24}^2)^2 - 2x_{13}^2 x_{24}^2 x_{12}^2 x_{34}^2 \\ - 2x_{13}^2 x_{24}^2 x_{23}^2 x_{41}^2 + (x_{12}^2 x_{34}^2 - x_{23}^2 x_{41}^2)^2, \end{aligned} \tag{3.6}$$

where the x's are defined in a similar way to (2.27)-(2.28) but with the p_i's replaced by the momenta K_i. We can expand the one-loop amplitude to this alternative basis

$$\mathcal{A}^{\text{1-loop}} = \sum_{\mathcal{P}(\{K_i\})} \tilde{\mathcal{C}}(K_1, K_2, K_3, K_4)\, F(K_1, K_2, K_3, K_4). \tag{3.7}$$

The supercoefficients $\tilde{\mathcal{C}}$ are mapped one-to-one to the corresponding $\mathcal{C}$'s.

3.2 Generalised unitarity

The problem of calculating one-loop amplitudes is reduced to calculating the coefficients $\mathcal{C}$. The generalised unitarity method [21] is the most efficient way for calculating these unknown objects at one-loop level, as it recycles information from tree level. The analytic properties of scattering amplitudes lie in the heart of this method as well. At loop level, when amplitudes are seen as functions of the Mandelstam kinematic invariants, they also develop branch cuts apart from poles. Matching

the analytic properties on both sides of (3.3), i.e. using the known analytic properties of the scalar box integrals and the expected analytic properties, from Feynman diagram intuition, of the full one-loop amplitude, one can uniquely define the coefficients. More specifically, the analytic property one uses is the leading singularity, which in the case of box functions, is found by 'cutting' or putting on-shell all internal propagators as shown in Figure 3.2. As scattering amplitudes in maximal

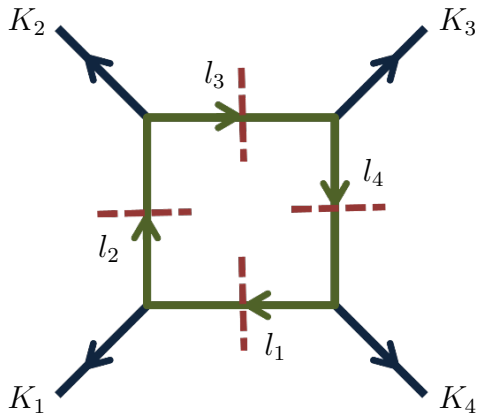

Figure 3.2: *Quadruple cut on the scalar box integral* $\mathcal{I}(K_1, K_2, K_3, K_4)$. *The fact that the four internal propagators* l_i *are put on-shell, combined with momentum conservation on the four corners of the box, freezes the* l_i*'s on two disconnected solutions* $\mathcal{S}_\pm$.

supersymmetry are cut-reconstructible [84, 85, 31, 32, 33, 34, 35, 26], we can evaluate the cuts in four dimensions. The two ingredients for finding the solutions of the cuts are the masslessness of all internal propagators and momentum conservation on each of the four corners of the box

$$\mathcal{S}_\pm : \quad l_i^2 = 0, \qquad l_{i+1} = l_i - K_i, \qquad (i = 1, 2, 3, 4). \tag{3.8}$$

Solving these constraints localises the loop integration to a discrete sum over the two solutions $\mathcal{S}_\pm$. The explicit solutions can be found in [21, 87]; we discuss some of them in what follows, see e.g. (3.22)-(3.24). However, in a lot of cases we do not need these solution, as we can use momentum conservation to eliminate any dependence on the l_i's from our results.

For our purposes, we present the supersymmetric extension of the quadruple unitarity cut method [48], presented and applied within $\mathcal{N} = 4$ super Yang-Mills. It turns out that all the details of this method carry over directly to $\mathcal{N} = 8$ supergravity, and that is the main subject of our work that appeared in [55] and we present in Section 3.6. In order to calculate the supercoefficient $\mathcal{C}(K_1, K_2, K_3, K_4)$

one needs to consider the diagram shown in Figure 3.3. One draws four tree-level amplitudes, with one cluster of momenta K_i attached to each one of them, while they are connected by four intermediate propagators with momenta l_i. As the momenta

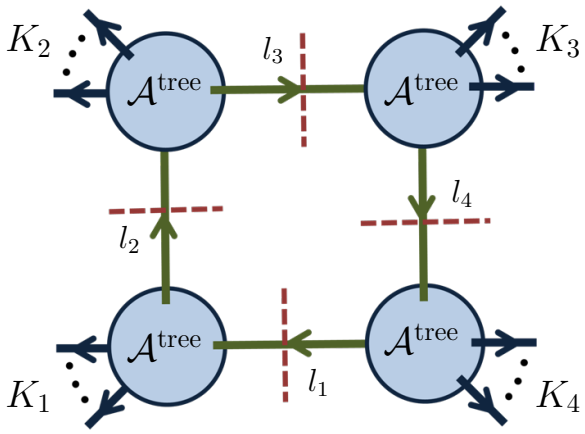

Figure 3.3: *Quadruple cut diagram for the supercoefficient* $\mathcal{C}(K_1, K_2, K_3, K_4)$.

of the cut propagators are on-shell, the four tree-level amplitudes are well-defined, although, in general, the solutions to the cuts give complex values to the momenta l_i.

In $\mathcal{N} = 4$ super Yang-Mills, the coefficients are given by

$$\begin{aligned}\mathcal{C}^{\mathcal{N}=4}(K_1, K_2, K_3, K_4) = \\ \frac{1}{2}\sum_{\mathcal{S}_\pm}\int\left(\prod_{i=1}^{4} d^4\eta_{l_i}\right) A^{\text{tree}}(-l_1, K_1, l_2)A^{\text{tree}}(-l_2, K_2, l_3) \\ \times A^{\text{tree}}(-l_3, K_3, l_4)A^{\text{tree}}(-l_4, K_4, l_1),\end{aligned} \tag{3.9}$$

where A^{tree} are tree-level superamplitudes and we are averaging over the two solutions $\mathcal{S}_\pm$ for the cut. We are integrating over the four superspace variables η_{l_i} corresponding to the intermediate propagators, which is essentially equivalent to a sum over all possible spin configurations for the internal legs, something one has to do when using the original nonsupersymmetric generalised unitarity method. Note that the tree amplitudes in (3.9) do not contain the bosonic momentum conservation delta function, although momentum conservation is still present in the solutions of the cuts. Due to colour-ordering, one needs to preserve the ordering in the clusters K_i when attached to the tree amplitudes.

Similarly, the supercoefficients in $\mathcal{N}=8$ supergravity are given by

$$\mathcal{C}^{\mathcal{N}=8}(K_1,K_2,K_3,K_4) = \frac{1}{2}\sum_{\mathcal{S}_\pm}\int\left(\prod_{i=1}^{4}d^8\eta_{l_i}\right)\mathcal{M}^{\text{tree}}(-l_1,K_1,l_2)\mathcal{M}^{\text{tree}}(-l_2,K_2,l_3) \times\mathcal{M}^{\text{tree}}(-l_3,K_3,l_4)\mathcal{M}^{\text{tree}}(-l_4,K_4,l_1), \tag{3.10}$$

where we are averaging over the same two solutions of the cut equations as in $\mathcal{N}=4$ SYM, but now we integrate over the eight superspace variables η^A, $A=1,\ldots,8$ and the integrand contains supergravity tree-level amplitudes.

What we have achieved is to be able to calculate one-loop quantities without having to perform any loop momentum integration. The Grassmann integration replaces the sum over internal helicity states and it is very easy to perform.

The decomposition (2.46) carries over to the supercoefficients as well and it is convenient to consider each class of them separately, as they carry different powers of η_i^A variables. In a similar fashion to the discussion for the supersymmetric recursion relations, when one looks at a term with a specific degree in the η's on the left-hand side of (3.9) or (3.10), one needs to consider all possible contribution on the right-hand side matching this degree. This time, the four integrations over the η_{l_i}'s lower the degree of the product of the four amplitudes by an amount of $4\mathcal{N}$. We will return and expand on this point with specific examples.

3.3 Infrared behaviour

The integral (3.2) are infrared (IR) divergent if at least one of the K_i's is null, which forces us to work in slightly more than four dimensions by an amount of -2ϵ where the infinitesimal IR expansion parameter $\epsilon<0$. One then proceeds by expanding in ϵ through $\mathcal{O}(\epsilon^0)$ order, which separates the desired finite part from the divergent part. The latter is the one that contains all the poles in ϵ and cancels when combined with other amplitudes in final infrared-safe quantities like cross-sections. The explicit expressions for the expanded scalar box integrals [88, 89, 90] through $\mathcal{O}(\epsilon^0)$ can be found in Appendix A. The infrared divergent parts of the scalar box

functions are

$$F^{1\text{m}}(p,q,r,P)\big|_{\text{IR}} = -\frac{1}{\epsilon^2}\left[(-s)^{-\epsilon} + (-t)^{-\epsilon} - (-P^2)^{-\epsilon}\right], \tag{3.11}$$

$$F^{2\text{me}}(p,P,q,Q)\big|_{\text{IR}} = -\frac{1}{\epsilon^2}\left[(-s)^{-\epsilon} + (-t)^{-\epsilon} - (-P^2)^{-\epsilon} - (-Q^2)^{-\epsilon}\right], \tag{3.12}$$

$$F^{2\text{mh}}(p,q,P,Q)\big|_{\text{IR}} = -\frac{1}{\epsilon^2}\left[\frac{1}{2}(-s)^{-\epsilon} + (-t)^{-\epsilon} - \frac{1}{2}(-P^2)^{-\epsilon} - \frac{1}{2}(-Q^2)^{-\epsilon}\right], \tag{3.13}$$

$$F^{3\text{m}}(p,P,R,Q)\big|_{\text{IR}} = -\frac{1}{\epsilon^2}\left[\frac{1}{2}(-s)^{-\epsilon} + \frac{1}{2}(-t)^{-\epsilon} - \frac{1}{2}(-P^2)^{-\epsilon} - \frac{1}{2}(-Q^2)^{-\epsilon}\right], \tag{3.14}$$

where lowercase momenta are massless and uppercase momenta are massive, and s is the square of the first two argument momenta, while t is the square of the sum of the second and the third. The four-mass box is infrared finite.

At one-loop level, amplitudes exhibit a well studied and understood universal behaviour at the infrared, where the leading IR divergent part is always proportional to the tree amplitude. In planar $\mathcal{N}=4$ super Yang-Mills this part is given by

$$A^{\text{1-loop}}\big|_{\text{IR}} = -\frac{1}{\epsilon^2}\sum_{i=1}^{n}(-s_{i,i+1})^{-\epsilon}\, A^{\text{tree}}. \tag{3.15}$$

In $\mathcal{N}=8$ supergravity the leading IR divergent part at one-loop is given by

$$\mathcal{M}^{\text{1-loop}}\big|_{\text{IR}} = -\frac{1}{\epsilon^2}\sum_{i,j}(-s_{ij})^{1-\epsilon}\, \mathcal{M}^{\text{tree}}. \tag{3.16}$$

One proceeds by expanding $(-s_{ij})^{1-\epsilon} = -s_{ij} + \mathcal{O}(\epsilon)$, and due to momentum conservation, the $1/\epsilon^2$ pole cancels in supergravity, leading to a softer IR behaviour. This is another manifestation of the better behaviour of supergravity as compared to super Yang-Mills.

The infrared part has been in many cases a blessing rather than a curse, as it constraints the form of amplitudes and it has been used for consistency checks on results.

From (3.11)-(3.14) we can see that each box function, and for specific momenta clusters as its arguments, has a unique infrared footprint. If we keep the infrared part of (3.3) we get

$$\mathcal{A}^{\text{1-loop}}\big|_{\text{IR}} = \sum\left(\tilde{\mathcal{C}}^{1\text{m}}\, F^{1\text{m}}\big|_{\text{IR}} + \tilde{\mathcal{C}}^{2\text{me}}\, F^{2\text{me}}\big|_{\text{IR}} + \tilde{\mathcal{C}}^{2\text{mh}}\, F^{2\text{mh}}\big|_{\text{IR}} + \tilde{\mathcal{C}}^{3\text{m}}\, F^{3\text{m}}\big|_{\text{IR}}\right), \tag{3.17}$$

where the coefficients $\tilde{\mathcal{C}}$ are finite quantities. As discussed in [26], plugging (3.15)

or (3.16) and (3.11)-(3.14) into (3.17), we can obtain linear equations between the coefficients, reducing the number of them that actually need to be calculated. One just needs to match the coefficients of each power of each momentum invariant $(-s_{ij})^{-\epsilon}$ on either side of the equation.

3.4 From IR equations to BCFW

In what follows we present a discussion combining three of the main themes of this thesis up to now, namely tree-level recursion relations, generalised unitarity and the infrared behaviour of one-loop amplitudes.

In $\mathcal{N}=4$ super Yang-Mills, the infrared equation corresponding to the two-particle channel $s_{12}=x_{13}^2$, i.e. the equation obtained from collecting the terms $-\frac{1}{\epsilon^2}(-(p_1+p_2)^2)^{-\epsilon}$, reads

$$\begin{aligned} A^{\text{tree}} &= \tilde{\mathcal{C}}^{\text{1m}}(p_1,p_2,p_3,x_{41})+\tilde{\mathcal{C}}^{\text{1m}}(p_n,p_1,p_2,x_{3n})-\tilde{\mathcal{C}}^{\text{2me}}(p_n,x_{13},p_3,x_{4n}) \\ &- \frac{1}{2}\tilde{\mathcal{C}}^{\text{2mh}}(p_{n-1},p_n,x_{13},x_{3,n-1})-\frac{1}{2}\tilde{\mathcal{C}}^{\text{2mh}}(p_3,p_4,x_{41},x_{13}) \\ &- \frac{1}{2}\sum_{i=5}^{n-2}\tilde{\mathcal{C}}^{\text{3m}}(p_n,x_{13},x_{3i},x_{in})-\frac{1}{2}\sum_{i=6}^{n-1}\tilde{\mathcal{C}}^{\text{3m}}(p_3,x_{4i},x_{i1},x_{13}), \end{aligned} \tag{3.18}$$

where x_{ij} is defined in (2.27)-(2.28). Note that we do not consider the coefficient $\mathcal{C}^{\text{2me}}(p_3,x_{4n},p_n,x_{13})$ since, due to the symmetry of the 2me box, it is identical to the one appearing in (3.18). Moving on to multi-particle channels, the infrared equation from the terms $-\frac{1}{\epsilon^2}(-x_{14}^2)^{-\epsilon}$ reads

$$\begin{aligned} 0 = &-\tilde{\mathcal{C}}^{\text{1m}}(p_1,p_2,p_3,x_{41})+\tilde{\mathcal{C}}^{\text{2me}}(p_1,x_{24},p_4,x_{51}) \\ &+\tilde{\mathcal{C}}^{\text{2me}}(p_n,p_{13},p_3,x_{4n})-\tilde{\mathcal{C}}^{\text{2me}}(p_n,p_{14},p_4,x_{5n})+\dots \end{aligned} \tag{3.19}$$

where the left-hand side of this equation vanishes, as there are no terms corresponding to multi-particle channels in (3.15), and the ellipses represent the 2mh and 3m coefficients. The coefficient $\tilde{\mathcal{C}}^{\text{1m}}(p_1,p_2,p_3,x_{41})$ is present due to momentum conservation $x_{14}^2=x_{41}^2$. Note that some of the terms appearing in (3.18) and (3.19) are the same but with different signs. Similarly, one can write down an infrared equation for any channel x_{ij}, which we denote by $[x_{ij}]$. As it was shown in [26], if we sum the following subset of the infrared equations labeled by j, and for a specific choice of

the index i,

$$\sum_{j=i+1}^{n+(i-2)} [x_{ij}], \tag{3.20}$$

numerous cancellations take place giving us the equation

$$A^{\text{tree}} = \frac{1}{2} \sum_{j=i+3}^{n+(i-1)} \tilde{\mathcal{C}}^{\text{1m/2mh}}(p_i, p_{i+1}, x_{i+2,j}, x_{ji}), \tag{3.21}$$

where, depending on the value of the index j and the number of massive momenta, the coefficients appearing are either of one-mass or two-mass hard type only. These equations were first presented in [91].

Each of the coefficients $\tilde{\mathcal{C}}$ appearing in (3.21), or equivalently, each supercoefficient $\mathcal{C}$ can be computed by means of the generalised unitarity method. The general diagram for the coefficient $\mathcal{C}^{\text{1m/2mh}}(p_i, p_{i+1}, x_{i+2,j}, x_{ji})$ is given in Figure 3.4, containing at least two three-point amplitudes, i.e. the ones on top. In the case of the one-mass coefficient, one of the amplitudes at the bottom is a three-point one as well. As we have discussed in Section 2.4, the two top three-point amplitudes should

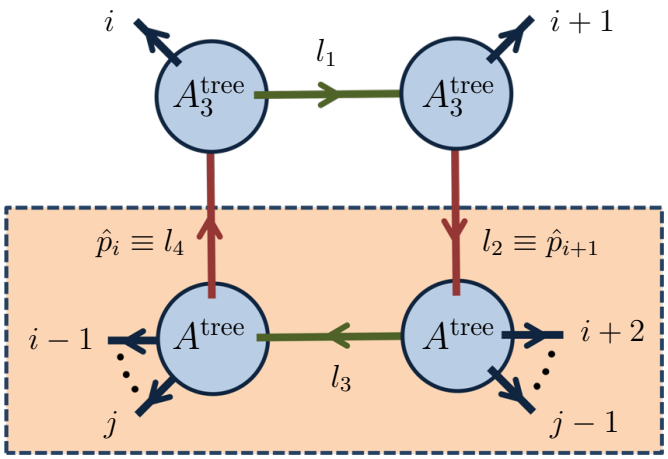

Figure 3.4: *The generic quadruple cut for the supercoefficients $\mathcal{C}(i, i+1, x_{i+2,j}, x_{j,i})$, of one-mass or two-mass easy type, in MSYM. The contribution of either solution $\mathcal{S}_\pm$ to the cut is identical (up to a kinematic factor taking us from the one basis of integrals to the other) to the super BCFW diagram shown within the frame.*

be a pair of MHV-$\overline{\text{MHV}}$ amplitudes. The two solutions for $l_1 = l$ corresponding to the two possible configurations are

$$l = z\lambda_i\tilde{\lambda}_{i+1}, \qquad l = z\lambda_{i+1}\tilde{\lambda}_i, \tag{3.22}$$

with z being a parameter to be determined. From momentum conservation we have

$$-l_2 = k_{i+1} - l, \qquad l_4 = k_i + l, \tag{3.23}$$

and

$$l_3 = k_j + k_{j+1} + \ldots + k_i + l, \tag{3.24}$$

while we determine z from the condition $l_3^2 = 0$. We see a lot of features of the tree-level recursion relations emerging. The shift in the momenta is given by l, with the momenta of legs i and $i+1$ shifted to l_4 and $-l_2$ respectively, while the location of the pole z is exactly the one we encounter in tree-level recursion. Finally the two different solutions (3.22) correspond to the two different ways for shifting legs i and $i+1$, i.e. shifts $[(i+1)i\rangle$ and $[i(i+1)\rangle$.

From (3.9) we have

$$\begin{aligned}\mathcal{C}^{\mathcal{N}=4}(i, i+1, x_{i+2,j}, x_{ji}) = \\ \frac{1}{2}\sum_{\mathcal{S}_\pm}\int\left(\prod_{i=1}^{4} d^4\eta_{l_i}\right) A_3^{\text{tree}}(-l_4, i, l_1) A_3^{\text{tree}}(-l_1, i+1, l_2) \\ \times A^{\text{tree}}(-l_2, x_{i+2,j}, l_3) A^{\text{tree}}(-l_3, x_{ji}, l_4).\end{aligned} \tag{3.25}$$

It turns out that one can substitute the two top three-point amplitudes and perform three out of the four Grassmann integrations in (3.25), arriving to an equation that is the sum of the two BCFW recursion relations for shifts $[(i+1)i\rangle$ and $[i(i+1)\rangle$ (see Appendix A of [26] for a more detailed discussion). The Grassmann integrations generate appropriate Jacobians that combine to give the BCFW relation (2.87), while they also fix $\eta_{l_2} = \eta_i + z\eta_{i+1}$, corresponding to the value of the shifted superspace variable needed in our BCFW prescription.

We now consider the first of the two solutions (3.22), i.e. $l = z\lambda_i\tilde{\lambda}_{i+1}$, and sketch the calculation. From (3.23) we get

$$l_2 = (z\lambda_i - \lambda_{i+1})\tilde{\lambda}_{i+1}, \qquad l_4 = \lambda_i(\lambda_i + z\tilde{\lambda}_{i+1}). \tag{3.26}$$

This means that we can make the following choice for the spinors of three of the l's

$$\begin{aligned} \lambda_{l_1} &= \lambda_i, & \tilde{\lambda}_{l_1} &= z\tilde{\lambda}_{i+1}, \\ \lambda_{l_2} &= z\lambda_i - \lambda_{i+1}, & \tilde{\lambda}_{l_2} &= \tilde{\lambda}_{i+1}, \\ \lambda_{l_4} &= \lambda_i, & \tilde{\lambda}_{l_4} &= \tilde{\lambda}_i + z\tilde{\lambda}_{i+1}, \end{aligned} \tag{3.27}$$

where any different normalisation of the spinors, i.e. $(\lambda, \tilde{\lambda}) \to (t\lambda, t^{-1}\tilde{\lambda})$ with $t \in \mathbb{C}^*$, would have been irrelevant in the final answer.

Since all λ's in $A_3^{\text{tree}}(-l_4, i, l_1)$ are proportional, this amplitude has to be of the $\overline{\text{MHV}}$ type, and (2.53) gives us

$$\begin{aligned} A_3^{\text{tree}}(-l_4, i, l_1) &= i\frac{\delta^{(4)}(\eta_i[l_1 l_4] + \eta_{l_1}[l_4 i] + \eta_{l_4}[i l_1])}{[i l_1][l_1 l_4][l_4 i]} \\ &= i\frac{(z[i\, i+1])^4\, \delta^{(4)}(\eta_i + \eta_{l_1} - \eta_{l_4})}{-z^3[i\, i+1]^3}, \end{aligned} \tag{3.28}$$

where we have pulled a common bosonic factor out of the fermionic delta function raised to the degree of the latter.

On the other hand, all $\tilde{\lambda}$'s in $A_3^{\text{tree}}(-l_1, i+1, l_2)$ are proportional, which means that this amplitude is of the MHV type, and (2.65) gives us

$$\begin{aligned} A_3^{\text{tree}}(-l_1, i+1, l_2) &= i\frac{\delta^{(8)}\left(\lambda_i(z\eta_{l_2} - \eta_{l_1}) + \lambda_{i+1}(\eta_{i+1} - \eta_{l_2})\right)}{\langle(-l_1)\, i+1\rangle\langle i+1\, l_2\rangle\langle l_2(-l_1)\rangle} \\ &= i\frac{\langle i\, i+1\rangle^4\, \delta^{(4)}(z\eta_{l_2} - \eta_{l_1})\delta^{(4)}(\eta_{i+1} - \eta_{l_2})}{z\langle i\, i+1\rangle^3}, \end{aligned} \tag{3.29}$$

where, because of the fact that the spinors λ_i and λ_{i+1} are independent, we are allowed to factorise the fermionic delta function in the same spirit with the discussion in (2.47)-(2.49).

Note that when multiplying the results (3.28) and (3.29) for the two three-point amplitude all factors of z cancel out. Moreover, one can easily perform the Grassmann integrations over η_{l_4}, η_{l_1} and η_{l_2}, and from the arguments of the delta functions one can easily read the following values for these superspace variables

$$\eta_{l_2} = \eta_{i+1}, \qquad \eta_{l_1} = z\eta_{l_2}, \qquad \eta_{l_4} = \eta_i + \eta_{l_1} = \eta_i + z\eta_{i+1}. \tag{3.30}$$

From (3.25) onwards we have been calculating the coefficients $\mathcal{C}$. Returning to (3.21), we need to convert our results into the coefficients $\tilde{\mathcal{C}}$ (see Section 3.1). For this purporse, in both the one-mass and two-mass hard boxes, the kinematic factor we need to divide by, given in (3.6), is simply

$$\sqrt{R(i, i+1, x_{i+2,j}, x_{ji})} = x_{i,i+2}^2 x_{i+1,j}^2. \tag{3.31}$$

The factor $x_{i,i+2}^2 = \langle i\, i{+}1\rangle[i{+}1\, i]$ cancels the factor we are left with after multiplying the two three-point amplitudes, while the factor $x_{i+1,j}^2$ gives us the propagator that

appears in the BCFW recursion relation (2.87). The final expression reads

$$A^{\text{tree}} = \sum_{j=i+3}^{n+(i-1)} \int d^4\eta_{l_3} A^{\text{tree}}(-\lambda_{l_2}, \tilde{\lambda}_{l_2}, \eta_{l_2}; \{i+2, \ldots, j-1\}; l_3, \eta_{l_3}) \times \frac{1}{x^2_{i+1,j}} A^{\text{tree}}(-l_3, \eta_{l_3}; \{j, \ldots, i-1\}; \lambda_{l_4}, \tilde{\lambda}_{l_4}, \eta_{l_4}), \quad (3.32)$$

where the shifted variables for legs l_2 and l_4 are given in (3.27) and (3.30). This is exactly the recursion relations we have presented in Section 2.5, with the shifted legs being i and $i+1$, which are replaced in (3.32) by l_4 and l_2. In a similar fashion, we calculate the contribution to the supercoefficients coming from the second solution in (3.22), which corresponds to the BCFW recursion relation with the roles of the shifted legs i and $i+1$ exchanged.

3.5 Supercoefficients in MSYM

Before discussing our results for the one-loop supergravity superamplitudes, we present some expressions for supercoefficients in $\mathcal{N}=4$ super Yang-Mills [48], the derivation of which motivated our work. More specifically, we discuss supercoefficients at MHV and NMHV level that we are going to use later on, in order to verify that our results reproduce older results.

The MHV part contains one-mass and two-mass easy scalar box integrals only. Without loss of generality we will consider the coefficient $\mathcal{C}^{\mathcal{N}=4}(1, P, s, Q)$, where in the one-mass case, one of the P, Q is massless, while in the exceptional case of four-point amplitudes both of them are massless. According to the quadruple cut prescription, we need to draw the diagram depicted in Figure 3.6, where we have distributed the four clusters of momenta to the four tree-level amplitudes. Since we are calculating the MHV contribution to the supercoefficient, or equivalently the supercoefficient of the MHV contribution to the one-loop amplitude, we need to consider all configurations with total degree in the Grassmann variables equal to 8. The Grassmann integration is reducing the total degree of the product of the four tree amplitudes by 16, which means that the later should be equal to 24. Since any non-three-point amplitude in MSYM has degree of at least 8, the two amplitudes attached to the clusters P and Q are fixed to the minimum degree of 8 each, corresponding to the MHV case, which leaves us with a maximum total degree of 8 for the two three-point amplitudes. This forces the three-point amplitudes to

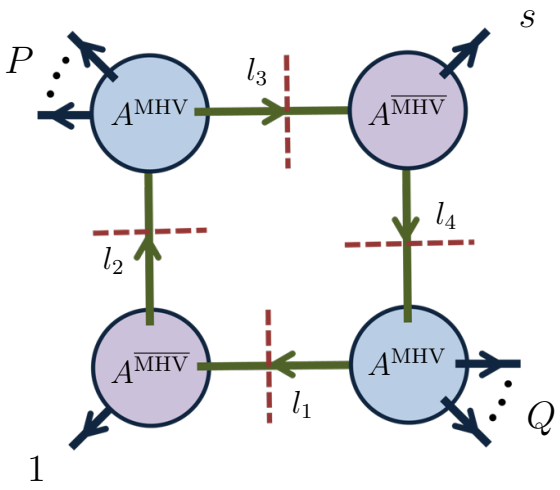

Figure 3.5: *The quadruple cut diagram determining the MHV part of the supercoefficient* $\mathcal{C}^{\mathcal{N}=4}(1,P,s,Q)$. *Simple power counting arguments for the Grassmann variables* η *force the tree-level amplitudes attached to massive corners to be of the MHV type, and the three-point ones to be of the anti-MHV type.*

be of the anti-MHV kind with a degree of 4 each.

Following a similar power counting argument we can show that we cannot construct any three-mass or four-mass configurations contributing to the MHV part, as there would be at least three non-three-point tree-level amplitudes exhausting all powers of η's we have available. Finally, in the case of the two-mass hard configuration, due to the fact that the three-point amplitudes are adjacent, and as we have explained in Section 2.4, one of them has to be MHV and the other $\overline{\text{MHV}}$ resulting to coefficients with minimum degree of 12, i.e. of at least NMHV type.

The generalised unitarity prescription (3.9) gives us the following initial expression for the supercoefficient we wish to calculate

$$\begin{aligned}\mathcal{C}^{\mathcal{N}=4}(1,P,s,Q) = \frac{1}{2}\Bigg[\int\left(\prod_{i=1}^{4} d^4\eta_{l_i}\right) \\ \times A_3^{\overline{\text{MHV}}}(-l_1,1,l_2)A^{\text{MHV}}(-l_2,2,\ldots,s-1,l_3) \\ \times A_3^{\overline{\text{MHV}}}(-l_3,s,l_4)A^{\text{MHV}}(-l_4,s+1,\ldots,n,l_1)\Bigg]_{\mathcal{S}_+},\end{aligned} \tag{3.33}$$

where due to the presence of the three-point amplitudes, only one solutions contributes to the cut, which we call $\mathcal{S}_+$. Using the results (2.65) and (2.53) for the

three-point anti-MHV and general MHV amplitudes respectively, we obtain

$$\begin{aligned}\mathcal{C}^{\mathcal{N}=4}(1,P,s,Q) = \frac{1}{2}\Bigg[\int\left(\prod_{i=1}^{4} d^4\eta_{l_i}\right) \\ \times \frac{\delta^{(4)}(\eta_1[l_2 l_1]+\eta_{l_2}[l_1 1]+\eta_{l_1}[1 l_2])}{[1 l_2][l_2 l_1][l_1 1]}\,\frac{\delta^{(8)}(\lambda_{l_2}\eta_{l_2}+\sum_2^{s-1}\lambda_i\eta_i-\lambda_{l_3}\eta_{l_3})}{\langle l_2 2\rangle\cdots\langle s-1\; l_3\rangle\langle l_3 l_2\rangle} \\ \times \frac{\delta^{(4)}(\eta_{l_3}[s l_4]+\eta_s[l_4 l_3]+\eta_{l_4}[l_3 s])}{[l_3 s][s l_4][l_4 l_3]}\,\frac{\delta^{(8)}(\lambda_{l_4}\eta_{l_4}+\sum_{s+1}^{n}\lambda_i\eta_i-\lambda_{l_1}\eta_{l_1})}{\langle l_4\; s+1\rangle\cdots\langle n l_1\rangle\langle l_1 l_4\rangle}\Bigg]_{\mathcal{S}_+}.\end{aligned} \tag{3.34}$$

It is straightforward to compute the four Grassmann integrals with the help of (2.49) to obtain [48]

$$\mathcal{C}^{\mathcal{N}=4}(1,P,s,Q) = \frac{1}{2}(P^2Q^2-st)\frac{\delta^{(8)}(\sum_{i=1}^{n}\eta_i\lambda_i)}{\langle 12\rangle\langle 23\rangle\cdots\langle n1\rangle}. \tag{3.35}$$

Incidentally, we notice that in order to arrive at (3.35) it is not necessary to know the explicit solutions to the cut equations, but only that the holomorphic spinors at the three-point anti-MHV corners are proportional, i.e. $\lambda_{l_1} \propto \lambda_{l_2} \propto \lambda_1$ and $\lambda_{l_3} \propto \lambda_{l_4} \propto \lambda_s$.

In the NMHV case, all coefficients appear up to three-mass. The three-mass NMHV coefficient is given by [68]

$$\mathcal{C}^{\mathcal{N}=4}_{3\text{m}}(r,P,Q,R) = \frac{\delta^{(8)}\left(\sum_{i=1}^{n}\eta_i\lambda_i\right)R_{r;st}}{\prod_{j=1}^{n}\langle j\,j+1\rangle}\,\Delta_{r,r+1,s,t}, \tag{3.36}$$

where the dual superconformal invariants $R_{r;st}$ are given in (2.115) and

$$\Delta_{r,r+1,s,t} = \frac{1}{2}\left(x_{rs}^2 x_{r+1t}^2 - x_{rt}^2 x_{r+1s}^2\right). \tag{3.37}$$

3.6 Supercoefficients in supergravity

We now move on to supergravity to present some of the main results of this thesis. We use supersymmetric generalised unitarity to express the one-loop supergravity supercoefficients in terms of gravity tree amplitudes. However, instead of substituting the final expressions for the tree amplitudes, we use the relations presented in Section 2.6 to express them in terms of tree amplitudes in MSYM, and then identify and reconstruct MSYM supercoefficients within our expressions. In several cases, we recast the $\mathcal{N}=8$ supercoefficient as a sum of permuted squares of $\mathcal{N}=4$ super-

coefficients times one-loop dressing factors, leading to new relations between these quantities in the two theories at one-loop level.

3.6.1 MHV case

We start by discussing the simplest case, namely the MHV case. The general diagram for this case appears in Figure 3.6, where using similar arguments to the $\mathcal{N}=4$ case, only 2me and 1m integrals are allowed, the corners attached to massive clusters are of MHV type and the three-point amplitudes are of $\overline{\text{MHV}}$ type. Again

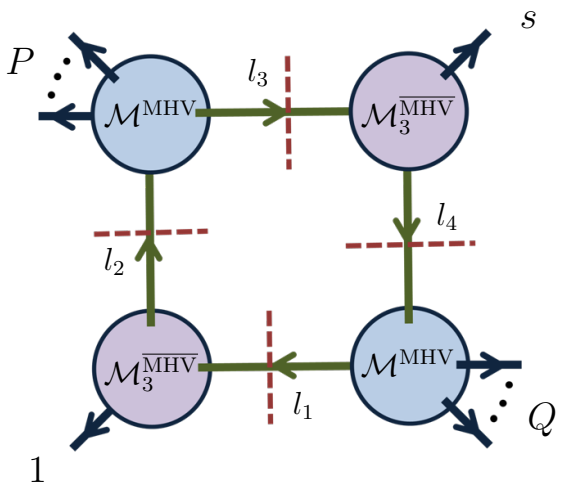

Figure 3.6: *The quadruple cut diagram determining the MHV part of the supercoefficient* $\mathcal{C}^{\mathcal{N}=4}(1,P,s,Q)$. *Similar arguments to the* $\mathcal{N}=4$ *case force the tree-level amplitudes attached to massive corners to be of the MHV type, and the three-point ones to be of the anti-MHV type.*

only one solution contributes and the cuts are identical to the ones in MSYM.

The generalised unitarity prescription (3.10) for the supergravity supercoefficients gives us

$$\begin{aligned}\mathcal{C}^{\mathcal{N}=8}(1,P,s,Q) = \frac{1}{2}\Bigg[\int\left(\prod_{i=1}^{4} d^8\eta_{l_i}\right) \\ \times \mathcal{M}_3^{\overline{\text{MHV}}}(-l_1,1,l_2)\mathcal{M}^{\text{MHV}}(-l_2,2,\ldots,s-1,l_3) \\ \times \mathcal{M}_3^{\overline{\text{MHV}}}(-l_3,s,l_4)\mathcal{M}^{\text{MHV}}(-l_4,s+1,\ldots,n,l_1)\Bigg]_{\mathcal{S}_+}. \end{aligned} \tag{3.38}$$

The solution to the cut is very easy to determine, as the two anti-MHV three-point superamplitudes simplify the kinematics. Firstly, for $n>4$, they allow only

one out of the two solutions to contribute. Secondly, they fix all the λ's in each of these two amplitudes to be parallel, so that the loop momenta become

$$l_1 = \lambda_1\tilde{\lambda}_{l_1}, \qquad l_2 = \lambda_1\tilde{\lambda}_{l_2}, \qquad l_3 = \lambda_s\tilde{\lambda}_{l_3}, \qquad l_4 = \lambda_s\tilde{\lambda}_{l_4}, \tag{3.39}$$

while the spinors $\tilde{\lambda}_{l_i}$, remain to be determined. This is accomplished by writing down the momentum conservation conditions on the two massive corners $l_2 = P + l_3$ and $l_4 = Q + l_1$ and contracting each one of them with either λ_1 or λ_s. The resulting values are

$$\tilde{\lambda}_{l_1} = -\frac{\langle s|Q}{\langle s1\rangle}, \qquad \tilde{\lambda}_{l_2} = \frac{\langle s|P}{\langle s1\rangle}, \qquad \tilde{\lambda}_{l_3} = -\frac{\langle 1|P}{\langle 1s\rangle}, \qquad \tilde{\lambda}_{l_4} = \frac{\langle 1|Q}{\langle 1s\rangle}, \tag{3.40}$$

and plugging them into (3.39) we obtain the cut momenta

$$l_1 = -|1\rangle\frac{\langle s|Q}{\langle s1\rangle}, \qquad l_2 = |1\rangle\frac{\langle s|P}{\langle s1\rangle}, \qquad l_3 = -|s\rangle\frac{\langle 1|P}{\langle 1s\rangle}, \qquad l_4 = |s\rangle\frac{\langle 1|Q}{\langle 1s\rangle}. \tag{3.41}$$

Returning to (3.38), we make use of the equations (2.66) and (2.110) to express the tree-level superamplitudes in supergravity in terms of those in SYM. For reasons that will soon become apparent, when considering the MHV amplitudes and the permutations in (2.110), we choose not to permute the legs corresponding to internal propagators, i.e. we choose these legs to be legs 1 and n. From (3.38) we arrive at

$$\begin{aligned}\mathcal{C}^{\mathcal{N}=8}(1,P,s,Q) = \frac{1}{2}\Bigg[\int\left(\prod_{i=1}^{4} d^8\eta_{l_i}\right) \\ \times\left[A_3^{\overline{\text{MHV}}}(-l_1,1,l_2)\right]^2\sum_{\mathcal{P}(P)}\left(\left[A^{\text{MHV}}(-l_2,P,l_3)\right]^2 G^{\text{MHV}}(-l_2,P,l_3)\right) \\ \times\left[A_3^{\overline{\text{MHV}}}(-l_3,s,l_4)\right]^2\sum_{\mathcal{P}(Q)}\left(\left[A^{\text{MHV}}(-l_4,Q,l_1)\right]^2 G^{\text{MHV}}(-l_4,Q,l_1)\right)\Bigg]_{\mathcal{S}_+},\end{aligned} \tag{3.42}$$

where P and Q denote the sets $\{2,\ldots,s-1\}$ and {s+1,...,n} respectively. The dressing factors are independent of the superspace variables and therefore we can pull them out of the Grassmann integrations. Moreover, since the two sums in (3.42) are over permutations of external legs only, we can chose to perform the summations

after the integrations, arriving at

$$\begin{aligned}
&\mathcal{C}^{\mathcal{N}=8}(1,P,s,Q) = \\
&\sum_{\mathcal{P}(P)}\sum_{\mathcal{P}(Q)}\Bigg(\Bigg[\frac{1}{2}\int\left(\prod_{i=1}^{4} d^4\eta_{l_i}\right) A_3^{\overline{\rm MHV}}(-l_1,1,l_2)A^{\rm MHV}(-l_2,P,l_3) \\
&\qquad\qquad \times A_3^{\overline{\rm MHV}}(-l_3,s,l_4)A^{\rm MHV}(-l_4,Q,l_1)\Bigg]^2_{\mathcal{S}_+} \\
&\qquad \times 2\left[G^{\rm MHV}(-l_4,Q,l_1)G^{\rm MHV}(-l_2,P,l_3)\right]_{\mathcal{S}_+}\Bigg),
\end{aligned} \tag{3.43}$$

where it is understood that the square of the integration measure over the four η^A's in $\mathcal{N}=4$ gives us the integration measure over the eight η^A's in $\mathcal{N}=8$. In (3.43), one immediately recognises the MSYM coefficient, and we can recast this equation to

$$\begin{aligned}
&\mathcal{C}^{\mathcal{N}=8}(1,P,s,Q) = \\
&\qquad \sum_{\mathcal{P}(P)}\sum_{\mathcal{P}(Q)}\left[\mathcal{C}^{\mathcal{N}=4}(1,P,s,Q)\right]^2 2\left[G^{\rm MHV}(-l_2,P,l_3)G^{\rm MHV}(-l_4,Q,l_1)\right]_{\mathcal{S}_+},
\end{aligned} \tag{3.44}$$

where the dressing factors $G^{\rm MHV}$ are evaluated on the cut given in (3.41).

We consider the dressing factor from $\mathcal{M}^{\rm MHV}(-l_4,s+1,\ldots,n,l_1)$, and from (2.111) we have

$$G^{\rm MHV}(-l_4,s+1,\ldots,n,l_1) = s_{-l_4,s+1}\prod_{r=s+1}^{n-2}\frac{\langle r|(r+1)\sum_{r+2}^{n} i|l_1\rangle}{\langle r l_1\rangle}. \tag{3.45}$$

From (3.41), the cut momenta l_1 and l_4 are

$$l_1 = \frac{1}{\langle 1s\rangle}\sum_{i=s+1}^{n}\langle si\rangle|1\rangle|i], \qquad l_4 = \frac{1}{\langle s1\rangle}\sum_{i=s+1}^{n}\langle i1\rangle|s\rangle|i]. \tag{3.46}$$

Inserting this solution into $G^{\rm MHV}(-l_4,s+1,\ldots,n,l_1)$, and denoting the corresponding quantity $G'(s,\{s+1,\ldots,n\},1)$, we find

$$\begin{aligned}
&G'(s,\{s+1,\ldots,n\},1) = \\
&\qquad \frac{1}{\langle 1s\rangle}\left(\sum_{i=s+2}^{n}\langle i1\rangle\langle s+1\ s\rangle[s+1\ i]\right)\prod_{r=s+1}^{n-2}\frac{\langle r|(r+1)\sum_{r+2}^{n} i|1\rangle}{\langle r1\rangle}.
\end{aligned} \tag{3.47}$$

Due to the symmetry of the 2me box and the cut solution, one can easily find the dressing factor $G'(1,\{2,\ldots,s-1\},s)$ corresponding to $G^{\rm MHV}(-l_2,2,\ldots,s-1,l_3)$ by just relabelling the last result.

Having inserted the solutions in (3.44) and defined G' we arrive at

$$\mathcal{C}^{\mathcal{N}=8}(1,P,s,Q)=\sum_{\mathcal{P}(P)}\sum_{\mathcal{P}(Q)}\left(\mathcal{C}^{\mathcal{N}=4}(1,P,s,Q)\right)^2 G'(1,\{P\},s)G'(s,\{Q\},1). \quad (3.48)$$

This expression gives a new form of the one-loop two-mass easy box integral coefficients in the supergravity MHV superamplitudes in terms of the ones in MSYM for any number of external legs. The MHV supercoefficients in $\mathcal{N}=4$ SYM are given in (3.35). As we have already discussed in (2.75) for the three-point amplitudes, the square of the $\mathcal{N}=4$ fermionic delta function contained in the MSYM coefficient on the right hand side of (3.48) gives us the $\mathcal{N}=8$ fermionic delta function that is present in the supergravity supercoefficient on the left-hand side of the same equation.

3.6.2 MHV examples and consistency checks

Next, we would like to compare our result (3.44) to previously known expressions for the MHV coefficients, and more specifically to the infinite sequence of graviton MHV amplitudes presented in [31]. The result of that paper for the two-mass easy coefficients written in terms of the "half-soft" functions $h(a,\{P\},b)$ is

$$\mathcal{C}^{\mathcal{N}=8}(1,P,s,Q)=\frac{1}{2}\left(P^2Q^2-st\right)^2 h(1,\{P\},s)\;h(s,\{Q\},1), \quad (3.49)$$

where we have supersymmetrised the MHV amplitude with negative helicity gluons i and j by removing a factor of $\langle ij\rangle^8$ and the usual fermionic delta function is implied. A factor of $(-1)^n$ in the result for the 2me coefficients as they appear in [31] is due to different conventions in the definition of the scalar box integrals. The first three

half-soft functions are given by

$$\begin{aligned} h(a,\{1\},b) &= \frac{1}{\langle a1\rangle^2\langle 1b\rangle^2}, \\ h(a,\{1,2\},b) &= \frac{[12]}{\langle 12\rangle\langle a1\rangle\langle 1b\rangle\langle a2\rangle\langle 2b\rangle}, \\ h(a,\{1,2,3\},b) &= \frac{[12][23]}{\langle 12\rangle\langle 23\rangle\langle a1\rangle\langle 1b\rangle\langle a3\rangle\langle 3b\rangle} + \frac{[23][31]}{\langle 23\rangle\langle 31\rangle\langle a2\rangle\langle 2b\rangle\langle a1\rangle\langle 1b\rangle} \\ &\quad + \frac{[31][12]}{\langle 31\rangle\langle 12\rangle\langle a3\rangle\langle 3b\rangle\langle a2\rangle\langle 2b\rangle}. \end{aligned} \tag{3.50}$$

There also exists a recursive form for the h functions given in [31] as well as the following explicit formula for the general half-soft function

$$\begin{aligned} h(a,\{1,2,\ldots,n\},b) &= \frac{[12]}{\langle 12\rangle}\frac{\langle a|K_{1,2}|3]\langle a|K_{1,3}|4]\cdots\langle a|K_{1,n-1}|n]}{\langle 23\rangle\langle 34\rangle\cdots\langle n-1n\rangle\ \langle a1\rangle\langle a2\rangle\cdots\langle an\rangle\ \langle 1b\rangle\langle nb\rangle} \\ &\quad + \mathcal{P}(2,3,\ldots,n), \end{aligned} \tag{3.51}$$

where $K_{i,j} = p_i + p_{i+1} + \ldots + k_j$, and we are summing over all permutations of the indices $\{2,3,\ldots,n\}$.

Now we want to show that the two expressions (3.48) and (3.49) for the one-loop MHV amplitude coefficients are equivalent. More specifically we want to match the latter to the bosonic part of the former. We consider a massive tree sub-amplitude in the loop diagram under consideration, for example that containing the set of momenta $Q = \{s+1,\ldots,n\}$. We now make the following conjecture relating the h functions in (3.49) to the dressing factors G' of (3.48)

$$\sum_{\mathcal{P}(s+1,\ldots,n)} \frac{G'(s,\{s+1,\ldots,n\},1)}{\big(\langle ss+1\rangle\langle s+1s+2\rangle\cdots\langle n-1n\rangle\langle n1\rangle\big)^2} = h(s,\{s+1,\ldots,n\},1). \tag{3.52}$$

If this relation is true, it follows directly that our formula (3.48) is identical to (3.49).

Let us first see how the equality (3.52) works in some simple cases. For the case where Q is a single momentum, the result is immediate since $G'(a,b,c) = 1$ and $h(a,\{b\},c) = 1/(\langle ab\rangle\langle bc\rangle)^2$.

The next check we perform is for the case when Q contains two momenta, for example we consider the the dressing factor $G'(3,\{4,5\},1)$ contained in the 1m coefficient $\mathcal{C}^{\mathcal{N}=8}(1,2,3,4+5)$. From (3.47) we find

$$G'(3,\{4,5\},1) = \frac{\langle 51\rangle\langle 43\rangle[45]}{\langle 13\rangle}, \tag{3.53}$$

while the left-hand side of the conjecture (3.52) becomes

$$\sum_{\mathcal{P}(4,5)} \frac{G'(3,\{4,5\},1)}{\big(\langle 34\rangle\langle 45\rangle\langle 51\rangle\big)^2} = \frac{[45]}{\langle 31\rangle\langle 45\rangle^2}\,\frac{\langle 34\rangle\langle 51\rangle + \langle 35\rangle\langle 14\rangle}{\langle 34\rangle\langle 35\rangle\langle 51\rangle\langle 14\rangle}$$
$$= \frac{[45]}{\langle 45\rangle}\,\frac{1}{\langle 34\rangle\langle 34\rangle\langle 14\rangle\langle 15\rangle}, \tag{3.54}$$

where in the last equation we have just used the Schouten identity (2.11). The result in (3.54) is precisely $h(3,\{4,5\},1)$.

For the next case we consider the dressing factor $G'(3,\{4,5,6\},1)$ and (3.47) gives us

$$G'(3,\{4,5,6\},1) = \frac{\langle 43\rangle\langle 61\rangle[56]}{\langle 13\rangle\langle 41\rangle}(\langle 51\rangle[45] + \langle 61\rangle[46]). \tag{3.55}$$

Inserting this into the left-hand side of (3.52) we find

$$\sum_{\mathcal{P}(4,5,6)} \frac{G'(3,\{4,5,6\},1)}{\big(\langle 34\rangle\langle 45\rangle\langle 56\rangle\langle 61\rangle\big)^2} = \frac{1}{\langle 13\rangle}\sum_{\mathcal{P}(4,5,6)} \frac{[56](\langle 51\rangle[45] + \langle 61\rangle[46])}{\langle 14\rangle\langle 34\rangle\langle 45\rangle^2\langle 16\rangle\langle 56\rangle^2}. \tag{3.56}$$

Adding the terms from the permutations (456) and (465) it is straightforward to obtain the first term of $h(3,\{4,5,6\},1)$ as given in the last formula in (3.50); the cyclically rotated terms are obtained in the same way.

We have checked numerically that our conjecture (3.52) holds for up to 12 legs, i.e. for n up to $s+10$. Note that an identical argument applies to the other massive corner with external legs $P = \{2,\ldots,s-1\}$ in the 2me box diagram. Therefore, this numerical check shows that the two expressions (3.48) and (3.49) for the 2me coefficients are equivalent for up to 22 external legs, whereas for the 1m diagrams, the equivalence is up to 13 legs.

Numeric checks

Finally, we want to give some more details on how one proceeds in checking numerically that two expressions are equivalent. This is done by using a mathematical package software like `MATHEMATICA`. One first needs to break all kinematic object down to the simplest possible entities, i.e. spinor inner products $\langle ij\rangle$ and $[ij]$. One does so by using the various identities we discussed in Section 2.2. Then, since

$$\langle ij\rangle = \lambda_i^1\lambda_j^2 - \lambda_i^2\lambda_j^1, \qquad [ij] = \tilde{\lambda}_i^{\dot{1}}\tilde{\lambda}_j^{\dot{2}} - \tilde{\lambda}_i^{\dot{2}}\tilde{\lambda}_j^{\dot{1}}, \tag{3.57}$$

our expressions become functions of the $4n$ spinor components λ_i^α and $\tilde{\lambda}_i^{\dot{\alpha}}$. Momentum conservation (2.22) gives

$$\begin{pmatrix} \sum_{i=1}^n \lambda_i^1 \tilde{\lambda}_i^{\dot{1}} & \sum_{i=1}^n \lambda_i^1 \tilde{\lambda}_i^{\dot{2}} \\ \sum_{i=1}^n \lambda_i^2 \tilde{\lambda}_i^{\dot{1}} & \sum_{i=1}^n \lambda_i^2 \tilde{\lambda}_i^{\dot{2}} \end{pmatrix} = \begin{pmatrix} 0 & 0 \\ 0 & 0 \end{pmatrix}, \tag{3.58}$$

reducing the number of independent components by four. We choose to give random values to all components apart from the ones of $\tilde{\lambda}_{n-1}$ and $\tilde{\lambda}_n$. We use (3.58) to solve for the four components of these two unknown spinors. More specifically, we chose to give random complex rational values to the $4n-4$ spinor components. Since, coefficients and tree-level amplitudes are rational functions of spinors, the results we will obtain will be rational numbers as well. These random objects have the form

$$\frac{RandInt(-r,r)}{RandInt(1,r)} + i\,\frac{RandInt(-r,r)}{RandInt(1,r)}, \tag{3.59}$$

where $RandInt(i,j)$ is a random integer in the range $[i,j]$ and r is a positive integer parameter controlling the number of choices for these random integers. For the specific choice of the unknown spinors to solve for, (3.58) gives us a system of linear equations in the components of $\tilde{\lambda}_{n-1}$ and $\tilde{\lambda}_n$ resulting to values for them that are also complex rational numbers.

Plugging these numeric values, that satisfy momentum conservation, into our two expressions gives us two numbers that should match. Instead of comparing the two values, it is wiser to consider their ratio because one can detect possible factors between the two expressions. If the two expressions match, up to a factor, one gets the same, usually simple answer, in different random kinematic points.

When checking our conjecture and as the number of legs grew bigger, we encountered computer memory limitations due to the fact that big analytic expressions were generated before substituting the numeric values. This issue was solved by substituting the numeric values in every term in the sums and products the moment they are generated rather than at the very end. Schematically, and for random values $\mathcal{R}$ for the spinors, we would compute

$$\sum_{\mathcal{P}} \prod_x \left[f_x(\{\lambda_i^\alpha, \tilde{\lambda}_i^{\dot{\alpha}}\}) \right]_{\mathcal{R}}, \tag{3.60}$$

rather than

$$\left[\sum_{\mathcal{P}} \prod_x f_x(\{\lambda_i^\alpha, \tilde{\lambda}_i^{\dot{\alpha}}\}) \right]_{\mathcal{R}}. \tag{3.61}$$

This has allowed us to overcome any memory limitations, and verify our conjecture (3.52) up to the number of legs allowed by computer time.

3.6.3 Next-to-MHV case

We now move on to consider NHMV superamplitudes. in $\mathcal{N} = 8$ supergravity. In this case, the three-mass and two-mass hard box functions also appear, in addition to the two-mass easy and one-mass ones. One can see this, using similar power counting arguments for the η's with the one we used in the MHV case. The relevant quadruple cut diagrams are the same as those appearing in [48] in the $\mathcal{N} = 4$ SYM case. In the following, we will give general expressions for the different box coefficients.

Three-mass coefficients

We begin by considering three-mass coefficients. In this case, there is one quadruple cut diagram, shown in Figure 3.7, containing three MHV amplitudes, and one anti-MHV, with each MHV amplitude containing more than three legs in general. For

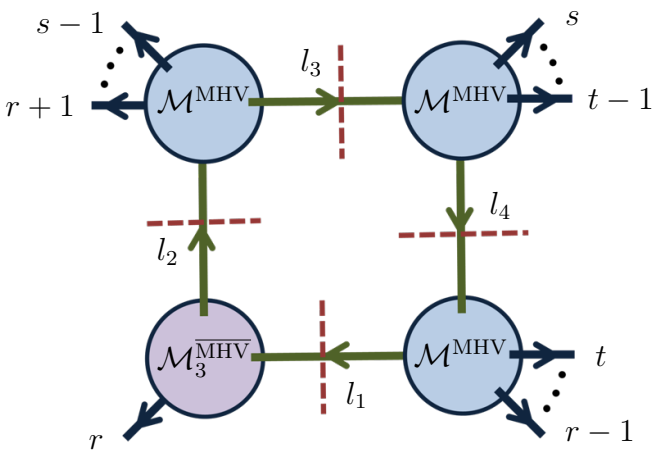

Figure 3.7: *The quadruple cut diagram determining the three-mass supercoefficient* $\mathcal{C}^{\mathcal{N}=8}(r, P, Q, R)$ *in the NMHV amplitude in* $\mathcal{N} = 8$ *supergravity. There is a single three-point anti-MHV amplitude participating in the cut. The remaining three superamplitudes are of the MHV type. We also define* $P := \sum_{l=r+1}^{s-1} p_l$, $Q := \sum_{l=s}^{t-1} p_l$, *and* $R := \sum_{l=t}^{r-1} p_l$.

the specific diagram, the quadruple cut formula (3.10) yields

$$\begin{aligned}\mathcal{C}_{3\mathrm{m}}^{\mathcal{N}=8}(r,P,Q,R) = \frac{1}{2}\sum_{\mathcal{S}_\pm}\int\prod_{i=1}^{4}d^8\eta_{l_i} \\ \times\,\mathcal{M}_3^{\overline{\mathrm{MHV}}}(-l_1,r,l_2)\mathcal{M}^{\mathrm{MHV}}(-l_2,r+1,\ldots,s-1,l_3) \\ \times\,\mathcal{M}^{\mathrm{MHV}}(-l_3,s,\ldots,t-1,l_4)\mathcal{M}^{\mathrm{MHV}}(-l_4,t,\cdots,r-1,l_1).\end{aligned} \tag{3.62}$$

The three-point anti-MHV amplitude is given in (2.74) and it is just the square of the corresponding SYM amplitude. The MHV superamplitudes may be written in terms of squares of super Yang-Mills amplitudes times dressing factors using (2.110) and (2.111). What is important in what follows is that in the sum over permutations in (2.110) there are always two missing legs. In applying this formula to write down explicitly the MHV superamplitudes entering the cut diagram in (3.62), we will arrange these two missing legs to be precisely the loop legs.

Since the dressing factors are independent of the superspace variables η, the fermionic integrations in (3.62) can then be done similarly to those for the SYM case in [48]. Moreover, the presence of the three-point amplitude allows only one of the two solutions $\mathcal{S}_\pm$ to contribute, we call this $\mathcal{S}_+$, and (3.62) becomes

$$\begin{aligned}\mathcal{C}_{3\mathrm{m}}^{\mathcal{N}=8}(r,P,Q,R) = \sum_{\mathcal{P}(P)}\sum_{\mathcal{P}(Q)}\sum_{\mathcal{P}(R)}\Big(\mathcal{C}_{3\mathrm{m}}^{\mathcal{N}=4}(r,P,Q,R)\Big)^2 \\ \times\;2\;\Big[G^{\mathrm{MHV}}(-l_2,P,l_3)G^{\mathrm{MHV}}(-l_3,Q,l_4)G^{\mathrm{MHV}}(-l_4,R,l_1),\Big]_{\mathcal{S}_+}\end{aligned} \tag{3.63}$$

where the corresponding super Yang-Mills supercoefficients $\mathcal{C}_{3\mathrm{m}}^{\mathcal{N}=4}(r,P,Q,R)$ are given in (3.36), and the dressing factors G^{MHV} in (2.111).

We have thus managed to express each three-mass coefficient as a sum of squares of SYM coefficients, weighted with bosonic dressing factors and summed over the appropriate permutations.

The product of the three tree-level dressing factors in (3.63) can in principle be further simplified by inserting the explicit solution to the cut expression. The generic solution to the cut (when the four corners are massive) has been worked out in [21]. One can however find rather simple expressions in terms of spinor variables when at least one of the four amplitudes participating in the quadruple cut is a three-point amplitude. For the three-mass configuration, the quadruple cut solutions have been presented in [92, 87] in a compact form. For the specific case in Figure 3.7, where

the three-point amplitude is anti-MHV, the solution is [92, 87]

$$
\begin{aligned}
l_1 &= \frac{|r\rangle\langle r|PQR|}{\langle r|PR|r\rangle}, & l_2 &= \frac{|r\rangle\langle r|RQP|}{\langle r|PR|r\rangle}, \\
l_3 &= \frac{|QR|r\rangle\langle r|P|}{\langle r|PR|r\rangle}, & l_4 &= \frac{|QP|r\rangle\langle r|R|}{\langle r|PR|r\rangle},
\end{aligned}
\tag{3.64}
$$

whereas the dressing factors given in (2.111), read

$$
G^{\rm MHV}(-l_2,\{P\},l_3) = s_{-l_2 r+1}\prod_{k=r+1}^{s-3}\frac{\langle k|x_{k,k+2}\,x_{k+2,l_3}|l_3\rangle}{\langle k l_3\rangle},
$$

$$
G^{\rm MHV}(-l_3,\{Q\},l_4) = s_{-l_3 s}\prod_{k=s}^{t-3}\frac{\langle k|x_{k,k+2}\,x_{k+2,l_4}|l_4\rangle}{\langle k l_4\rangle},
\tag{3.65}
$$

$$
G^{\rm MHV}(-l_4,\{R\},l_1) = s_{-l_4 t}\prod_{k=s}^{r-3}\frac{\langle k|x_{k,k+2}\,x_{k+2,l_1}|l_1\rangle}{\langle k l_1\rangle}.
\tag{3.66}
$$

Two-mass hard coefficients

We now turn to the two-mass hard coefficients. There are two quadruple cut diagrams contributing here. These are shown in Figure 3.8, where the two adjacent three-point amplitudes are MHV and anti-MHV (or vice versa). Similarly to the

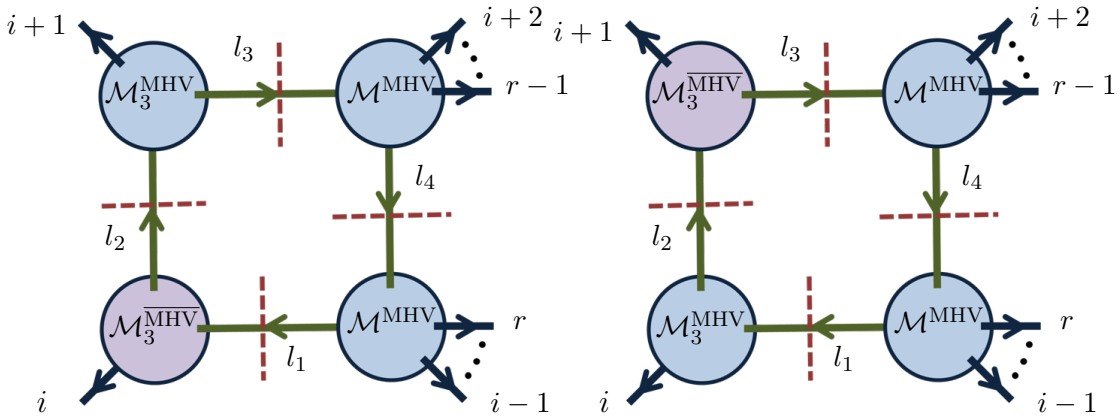

Figure 3.8: *The two quadruple cut diagrams determining the two-mass hard supercoefficient* $\mathcal{C}^{\mathcal{N}=8}(i,j,P,Q)$ *in the NMHV amplitudes in* $\mathcal{N}=8$ *supergravity. The three-point amplitudes are a pair of MHV and anti-MHV, while the remaining two amplitudes are of MHV type.*

$\mathcal{N}=4$ case discussed in [48], these two diagrams can be regarded as special cases of the three-mass diagrams in Figure 3.7. The result for the first diagram is simply

given by $\mathcal{C}_{3\mathrm{m}}^{\mathcal{N}=8}(i, i+1, P, Q)$, whereas for the second one is $\mathcal{C}_{3\mathrm{m}}^{\mathcal{N}=8}(i+1, i, Q, P)$, where $P := \{p_{i+2}, \ldots, p_{r-1}\}$ and $Q := \{p_r, \ldots, p_{i-1}\}$. The two-mass hard coefficients are then equal to

$$\mathcal{C}_{2\mathrm{mh}}^{\mathcal{N}=8}(i, i+1, P, Q) = \mathcal{C}_{3\mathrm{m}}^{\mathcal{N}=8}(i, i+1, P, Q) + \mathcal{C}_{3\mathrm{m}}^{\mathcal{N}=8}(i+1, i, Q, P). \tag{3.67}$$

We will present in Section 3.6.4 some numerical checks of (3.67) for the case of six-point NMHV superamplitudes, finding agreement with the results of [32, 33].

Two-mass easy coefficients

We now move on to consider the two-mass easy coefficients, and as a particular case of these, the one-mass coefficients. In the two-mass easy case there are two diagrams, as in the SYM case considered in [48], related to each other by a simple exchange of labels. Each cut diagram has two anti-MHV amplitudes, one NMHV amplitude and one MHV amplitude, as depicted in Figure 3.9. An additional quadruple cut can

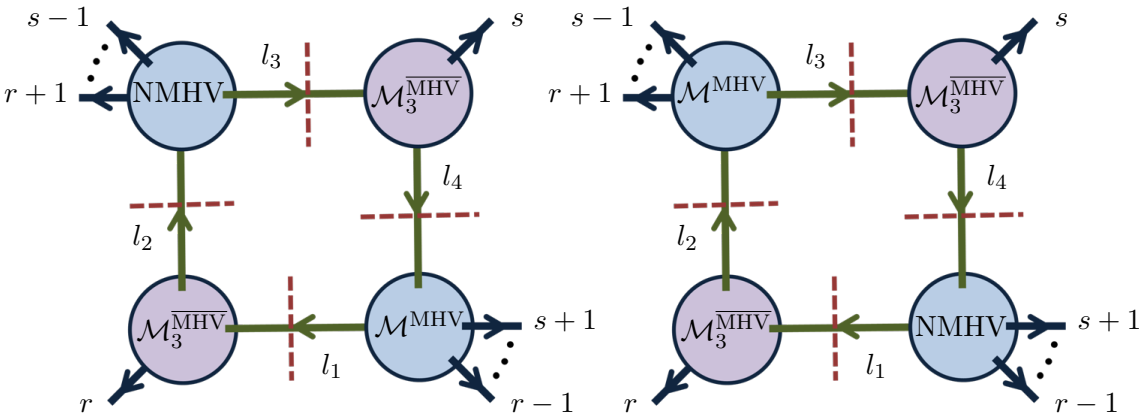

Figure 3.9: *The two quadruple cut diagrams determining the two-mass easy supercoefficient* $\mathcal{C}^{\mathcal{N}=8}(r, P, s, Q)$ *in the NMHV amplitudes in* $\mathcal{N} = 8$ *supergravity. The three-point amplitudes have the anti-MHV helicity configuration, whereas on the two massive corners we have an MHV and an NMHV amplitude. We also define* $P := \sum_{l=r+1}^{s-1} p_l$, *and* $Q := \sum_{l=s+1}^{r-1} p_l$.

actually be constructed by replacing one of the two three-point anti-MHV amplitude with a three-point MHV one, and compensating this by replacing further the NMHV amplitude by an MHV one. It can easily be shown [48] that this particular quadruple cut would lead to constraints on the external kinematics, and hence can be ignored.

We consider the first diagram, and from (3.10), the result for this quadruple cut

is

$$\mathcal{C}_{\rm 2me}^{\mathcal{N}=8}(r,P,s,Q)\Big|_1 = \frac{1}{2}\sum_{\mathcal{S}_\pm}\int\prod_{i=1}^{4}d^8\eta_{l_i} \qquad (3.68)$$
$$\times\ \mathcal{M}_3^{\overline{\rm MHV}}(-l_1,r,l_2)\mathcal{M}^{\rm NMHV}(-l_2,r+1,\ldots,s-1,l_3)$$
$$\times\ \mathcal{M}_3^{\overline{\rm MHV}}(-l_3,s,l_4)\mathcal{M}^{\rm MHV}(-l_4,s+1,\ldots,r-1,l_1).$$

Here we may use the expression for NMHV tree amplitudes given in (2.114). In writing explicitly the amplitude $\mathcal{M}^{\rm NMHV}(-l_2,p_{r+1},\ldots,p_{s-1},l_3)$ in (3.68) using (2.114), we will pick the loop legs $-l_2$ and l_3 to be 1 and n appearing in the latter formula. Two important consequences of this are that, firstly, the sum over permutations in (2.114) will not involve the cut-loop legs $-l_2$ and l_3; and, secondly, that the supermomenta $\eta_{l_2}\lambda_{l_2}$ and $\eta_{l_3}\lambda_{l_3}$ of the cut legs will appear only through the overall supermomentum conservation delta functions. Therefore, the fermionic integrations over η_{l_2} and η_{l_3} will proceed as in the case of the supergravity MHV superamplitude discussed previously.

We now proceed with the calculation. Inserting (2.114) into (3.68), as well as the expressions for the three-point anti-MHV amplitude (2.74) and for the MHV amplitude in (2.110), we find

$$\mathcal{C}_{\rm 2me}^{\mathcal{N}=8\ ({\rm NMHV})}(r,P,s,Q) =$$
$$\frac{1}{2}\sum_{S_\pm}\int\prod_{i=1}^{4}d^8\eta_{l_i}\left[A_3^{\overline{\rm MHV}}(-l_1,r,l_2)\right]^2\left[A_3^{\overline{\rm MHV}}(-l_3,s,l_4)\right]^2$$
$$\times\sum_{\mathcal{P}(P)}\left(\left[A^{\rm MHV}(-l_2,\{P\},l_3)\right]^2\sum_{i=r+1}^{s-3}\sum_{j=i+2}^{s-1}(R_{l_3;ij})^2G^{\rm NMHV}_{l_3;ij}\right)$$
$$\times\sum_{\mathcal{P}(Q)}\left[A^{\rm MHV}(-l_4,\{Q\},l_1)\right]^2G^{\rm MHV}(-l_4,\{Q\},l_1) + \ r\leftrightarrow s, \qquad (3.69)$$

where the first $(r\leftrightarrow s)$ term corresponds to the cut diagram on the left (right) of Figure 3.9. By $\{P\}$, $\{Q\}$, we mean the ordered sets of momenta $\{p_{r+1},\ldots,p_{s-1}\}$, and $\{p_{s+1},\ldots,p_{r-1}\}$. The explicit expressions for the dressing factors $G^{\rm NMHV}$ are given in [45].

Next we observe that only one of the two cut solutions contributes, namely the

solution we have calculated in (3.41). We can then recast (3.69) to

$$\mathcal{C}_{\text{2me}}^{\mathcal{N}=8\ (\text{NMHV})}(r,P,s,Q) = 2\sum_{\mathcal{P}(\{P\})}\sum_{\mathcal{P}(\{Q\})}\left[\mathcal{C}_{\text{2me}}^{\mathcal{N}=4\ (\text{MHV})}(r,P,s,Q)\right]^2 \times\left[\left(\sum_{i=r+1}^{s-3}\sum_{j=i+2}^{s-1}(R_{l_3;ij})^2 G_{l_3;ij}^{\text{NMHV}}\right)G^{\text{MHV}}(-l_4,Q,l_1)\right]_{\mathcal{S}_+} + r\leftrightarrow s. \tag{3.70}$$

The dual superconformal invariant R-functions appearing in (3.69) are given in (2.115), and in this case they read

$$R_{l_3,ij} = \frac{\langle i-1i\rangle\langle j-1j\rangle\delta^{(4)}(\Xi_{l_3;ij})}{x_{ij}^2\langle l_3|x_{r+1,i}x_{ij}|j\rangle\langle l_3|x_{r+1,i}x_{ij}|j-1\rangle\langle l_3|x_{r+1,j}x_{ji}|i\rangle\langle l_3|x_{r+1,j}x_{ji}|i-1\rangle}, \tag{3.71}$$

where

$$\Xi_{l_3;ij} = -\langle l_3|\left(x_{r+1,i}x_{ij}\sum_{m=j}^{s-1}|m\rangle\eta_m + x_{r+1,j}x_{ji}\sum_{m=i}^{s-1}|m\rangle\eta_m\right). \tag{3.72}$$

A few comments are in order here. Firstly, we need to insert the cut solutions into the previous expressions. These are obtained from (3.41) by just replacing $1\to r$. Furthermore, when the minimum value of i, i.e. $i=r+1$ is attained in the sum appearing in (3.70), the corresponding spinor for $i-1$ is actually $|i-1\rangle\equiv|-l_2\rangle$, since the R-function comes from the NMHV amplitude with legs $(-l_2,r+1,\ldots,s-1,l_3)$. However, the expression for R in (3.71) is invariant under rescalings of $|i-1\rangle$. Hence, since $|l_2\rangle\propto|r\rangle$ because of the cut condition, we conclude that we can set $|i-1\rangle\to|r\rangle$ when the minimum value in the sum over i in (3.70) is attained.

Furthermore, we notice that $|l_3\rangle\propto|s\rangle$ because of the cut condition. By expanding the fermionic delta function $\delta^{(4)}(\Xi_{l_3;ij})$ we see that this will contribute four powers of $\langle l_3|$. Inspecting (3.71), we conclude that $R_{l_3,ij}$ will eventually be invariant under rescalings of $\langle l_3|$ as well. We can then replace $\langle l_3|\to\langle s|$ inside the expression for $R_{l_3;ij}$ or, equivalently, $R_{l_3;ij}\to R_{s;ij}$ and $\Xi_{l_3;ij}\to\Xi_{s;ij}$, so that the explicit loop solutions are not present in these quantities.

Taking into account the previous remarks, we arrive at

$$\mathcal{C}_{\text{2me}}^{\mathcal{N}=8\ (\text{NMHV})}(r,P,s,Q) = 2\sum_{\mathcal{P}(P)}\sum_{\mathcal{P}(Q)}\left[\mathcal{C}_{\text{2me}}^{\mathcal{N}=4\ (\text{MHV})}(r,P,s,Q)\right]^2 \times\left[\left(\sum_{i=r+1}^{s-3}\sum_{j=i+2}^{s-1}(R_{s;ij})^2 G_{l_3;ij}^{\text{NMHV}}\right)G^{\text{MHV}}(-l_4,Q,l_1)\right]_{\mathcal{S}_+} + r\leftrightarrow s. \tag{3.73}$$

The general expressions for the MHV dressing factors are given in (2.111), from which one can obtain $G^{\rm MHV}(-l_4, Q, l_1)$.

One-mass coefficients

Finally we consider one-mass coefficients. As explained in [48] in the Yang-Mills case, the two relevant diagrams are special cases of other diagrams. In the first of them, the three three-point corners are MHV-$\overline{\rm MHV}$-MHV and the fourth corner is MHV, which is a special case of the NMHV two-mass easy coefficient. In the second diagram, the three three-point corners are $\overline{\rm MHV}$-MHV-$\overline{\rm MHV}$ and the fourth corner is NMHV, which is a special case of the NMHV three-mass coefficient. Therefore, one finds

$$\mathcal{C}^{\mathcal{N}=8}_{\rm 1m}(s+2,P,s,s+1)=\mathcal{C}^{\mathcal{N}=8}_{\rm 2me}(s+2,P,s,s+1)+\mathcal{C}^{\mathcal{N}=8}_{\rm 3m}(s+1,s+2,P,s). \quad (3.74)$$

3.6.4 NMHV examples and consistency checks

In this section we will consider (3.67) in the case of six-point NMHV superamplitudes, and perform some numerical checks comparing our results to those derived in [32, 33] for six-point NMHV graviton scattering amplitudes. Specifically, we will compare our results to the following coefficients [32, 33]

$$\mathcal{C}^{\mathcal{N}=8}_{\rm 2mh}(1^+,2^-,\{3^-,4^-\},\{5^+,6^+\}) \quad (3.75)$$
$$=\frac{1}{2}\,\frac{s_{34}s_{56}s_{12}^2(x_{25}^2)^8}{[23][34][24][43]\langle 56\rangle\langle 61\rangle\langle 65\rangle\langle 51\rangle[2|x_{25}|5\rangle[2|x_{25}|6\rangle[3|x_{25}|1\rangle[4|x_{25}|1\rangle},$$

and

$$\mathcal{C}^{\mathcal{N}=8}_{\rm 2mh}(3^+,4^-,\{5^+,6^+\},\{1^-,2^-\}) \quad (3.76)$$
$$=\frac{1}{2}\,\frac{([3|x_{14}|4\rangle)^8 s_{12}s_{56}(s_{34})^2}{\langle 45\rangle\langle 46\rangle\langle 56\rangle\langle 65\rangle[12][13][21][23][1|x_{14}|4\rangle[2|x_{14}|4\rangle[3|x_{14}|5\rangle[3|x_{14}|6\rangle}$$
$$+\frac{1}{2}\frac{\langle 12\rangle^6[56]^6 s_{12}s_{56}s_{34}^2}{\langle 13\rangle\langle 23\rangle[45][46][4|x_{14}|1\rangle[4|x_{14}|2\rangle[5|x_{14}|3\rangle[6|x_{14}|3\rangle}\ . \quad (3.77)$$

At six points, (3.67) is

$$\mathcal{C}^{\mathcal{N}=8}_{\rm 2mh}(i,i+1,P,Q)=\mathcal{C}^{\mathcal{N}=8}_{\rm 3m}(i,i+1,P,Q)+\mathcal{C}^{\mathcal{N}=8}_{\rm 3m}(i+1,P,Q,i), \quad (3.78)$$

where $P=p_{i+2}+p_{i+3}$ and $Q=p_{i+4}+p_{i+5}$. The three-mass supercoefficients given

in (3.63) become in this case

$$\mathcal{C}_{3\mathrm{m}}^{\mathcal{N}=8}(i,i+1,P,Q) = \sum_{\mathcal{P}(P)}\sum_{\mathcal{P}(Q)} \left(\mathcal{C}_{3\mathrm{m}}^{\mathcal{N}=4}(i,i+1,P,Q)\right)^2 \times\ 2\,\frac{\langle i+2|P\,Q|i\rangle\langle i|i+1|i+2]}{\langle i|(i+1)\,Q|i\rangle}\,\frac{\langle i+4|P\,(i+1)|i\rangle\langle i|Q|i+4]}{\langle i|(i+1)\,Q|i\rangle}, \tag{3.79}$$

and

$$\mathcal{C}_{3\mathrm{m}}^{\mathcal{N}=8}(i+1,P,Q,i) = \sum_{\mathcal{P}(P)}\sum_{\mathcal{P}(Q)} \left(\mathcal{C}_{3\mathrm{m}}^{\mathcal{N}=4}(i+1,P,Q,i)\right)^2 \times\ 2\,\frac{\langle (i+2)\,(i+1)\rangle\langle i+1|i\,Q\,P|i+2]}{\langle i+1|P\,i|i+1\rangle}\,\frac{\langle i+4|Q\,i|i+1\rangle\langle i+1|P|i+4]}{\langle i+1|P\,i|i+1\rangle}, \tag{3.80}$$

where dressing factors involving one external leg are equal to one, and the general expression for the $\mathcal{N}=4$ three-mass supercoefficient entering (3.79) and (3.80) is given in (3.36). Thus, we arrive at

$$\begin{aligned}
&\mathcal{C}_{2\mathrm{mh}}^{\mathcal{N}=8}(i,i+1,P,Q)\\
&\quad=\sum_{\mathcal{P}(P)}\sum_{\mathcal{P}(Q)}\Bigg[\left(\frac{\delta^{(8)}\left(\sum_{i=1}^n \eta_i\lambda_i\right)R_{i;i+2\,i+4}}{\prod_{j=1}^n\langle jj+1\rangle}\,\Delta_{i,i+1,i+2,i+4}\right)^2\\
&\qquad\times\ 2\,\frac{\langle i+2|P\,Q|i\rangle\langle i|i+1|i+2]}{\langle i|(i+1)\,Q|i\rangle}\,\frac{\langle i+4|P\,(i+1)|i\rangle\langle i|Q|i+4]}{\langle i|(i+1)\,Q|i\rangle}\\
&\quad+\left(\frac{\delta^{(8)}\left(\sum_{i=1}^n \eta_i\lambda_i\right)R_{i+1;i+4\,i}}{\prod_{j=1}^n\langle jj+1\rangle}\,\Delta_{i+1,i+2,i+4,i}\right)^2\\
&\qquad\times\ 2\,\frac{\langle (i+2)(i+1)\rangle\langle i+1|i\,Q\,P|i+2]}{\langle i+1|P\,i|i+1\rangle}\,\frac{\langle i+4|Q\,i|i+1\rangle\langle i+1|P|i+4]}{\langle i+1|P\,i|i+1\rangle}\Bigg].
\end{aligned} \tag{3.81}$$

In order to be able to extract the coefficients for graviton amplitudes, we need to analyse the η-dependence of the R-functions in (3.81). The dependence on the supermomenta of the external particles is contained in the product $[\delta^{(4)}(\Xi_{r;st})\delta^{(8)}(q)]^2$. Since we are going to compare to NMHV graviton amplitudes, we will only need the coefficients of terms of the form $(\eta_i)^8(\eta_j)^8(\eta_k)^8$.

Consider now the helicity assignment for the coefficient in (3.75). In (3.81), we encounter the quantities $\Xi_{i;i+2\,i+4}$ and $\Xi_{i+1;i+4\,i+6}$. We consider the expressions $\delta^{(8)}(\Xi_{1;35})\delta^{(16)}(q)$ and $\delta^{(8)}(\Xi_{2;51})\delta^{(16)}(q)$. From (2.116), we have, setting $i=1$,

$$\Xi_{1;35} = \langle 1|(5+6)\,4|3\rangle\eta_3 + \langle 1|(5+6)\,4|4\rangle\eta_4 + \langle 34\rangle[34]\langle 15\rangle\eta_5 + \langle 34\rangle[34]\langle 16\rangle\eta_6, \tag{3.82}$$

and

$$\Xi_{2;51} = \langle 21\rangle\langle 56\rangle\ ([61]\eta_5 + [15]\eta_6 + [56]\eta_1). \tag{3.83}$$

In the expansion of

$$\delta^{(8)}(\Xi_{1;35})\,\delta^{(16)}(\sum_{i=1}^{6}\eta_i\lambda_i), \tag{3.84}$$

we need to pick the coefficient of $(\eta_2)^8(\eta_3)^8(\eta_4)^8$, which is

$$(\langle 1|5+6|3+4|2\rangle\langle 43\rangle)^8, \tag{3.85}$$

and in the expansion of

$$\delta^{(8)}([61]\eta_5 + [15]\eta_6 + [51]\eta_1)\,\delta^{(16)}(\sum_{i=1}^{6}\eta_i\lambda_i), \tag{3.86}$$

the coefficient of $(\eta_2)^8(\eta_3)^8(\eta_4)^8$ vanishes. In performing the sum in (3.81) one will also need to include permutations of the above quantities.

Now we turn to the coefficient in (3.77) and compare to (3.81). In considering the latter for the specific helicity assignment, we encounter the quantities $\Xi_{3;51}$ and $\Xi_{4;13}$. These can be simply obtained by permuting indices in the expressions for $\Xi_{1;35}$ and $\Xi_{2;51}$ given above. The corresponding coefficients for $(\eta_1)^8(\eta_2)^8(\eta_4)^8$ are

$$(\langle 12\rangle\langle 34\rangle s_{56})^8, \tag{3.87}$$

from $\Xi_{3;51}$, and

$$\langle 4|1+2|3]^8, \tag{3.88}$$

from $\Xi_{4;13}$.

Finally, we compare (3.75) and (3.77) to the expansions of the supercoefficients $\mathcal{C}^{\mathcal{N}=8}_{2\text{mh}}(1,2,\{3,4\},\{5,6\})$ and $\mathcal{C}^{\mathcal{N}=8}_{2\text{mh}}(3,4,\{5,6\},\{1,2\})$ which one derives from (3.81). Summing over the appropriate permutations, we get

$$\begin{aligned}\mathcal{C}^{\mathcal{N}=8}_{2\text{mh}}(1^+,2^-,\{3^-,4^-\},\{5^+,6^+\}) &= \frac{\langle 34\rangle^3[56]\langle 1|(5+6)\,(3+4)|2\rangle^6(s_{12}s_{234})^2}{2\langle 12\rangle^6\langle 56\rangle^2\langle 1|5+6|2]^2(s_{34})^2} \\ &\times\left[\frac{1}{\langle 16\rangle[23]\langle 5|3+4|2]\langle 1|5+6|4]} + \frac{1}{\langle 51\rangle[23]\langle 6|3+4|2]\langle 1|5+6|4]}\right. \\ &\left. + \frac{1}{\langle 61\rangle[24]\langle 5|3+4|2]\langle 1|5+6|3]} + \frac{1}{\langle 15\rangle[24]\langle 6|3+4|2]\langle 1|5+6|3]}\right],\end{aligned} \tag{3.89}$$

and

$$\mathcal{C}_{2\text{mh}}^{\mathcal{N}=8}(3^+,4^-,\{5^+,6^+\},\{1^-,2^-\}) = -\frac{\langle 34\rangle^4[34]^2(s_{456})^2}{2\langle 3|(1+2)\,(5+6)|4\rangle^2}$$
$$\times\ \Bigg[\frac{\langle 12\rangle^6[12]\langle 56\rangle[56]^6}{\langle 3|1+2|4]^2}$$
$$\times\left(\frac{1}{\langle 23\rangle[45]\langle 1|5+6|4]\langle 3|1+2|6]} - \frac{1}{\langle 13\rangle[45]\langle 2|5+6|4]\langle 3|1+2|6]}\right.$$
$$\left.-\frac{1}{\langle 23\rangle[46]\langle 1|5+6|4]\langle 3|1+2|5]} + \frac{1}{\langle 13\rangle[46]\langle 2|5+6|4]\langle 3|1+2|5]}\right)$$
$$+\ \frac{\langle 12\rangle[56]\langle 4|1+2|3]^6}{\langle 56\rangle^2[12]^2}$$
$$\times\left(\frac{1}{\langle 45\rangle[23]\langle 4|5+6|1]\langle 6|1+2|3]} - \frac{1}{\langle 45\rangle[13]\langle 4|5+6|2]\langle 6|1+2|3]}\right.$$
$$\left.-\frac{1}{\langle 46\rangle[23]\langle 4|5+6|1]\langle 5|1+2|3]} + \frac{1}{\langle 46\rangle[13]\langle 4|5+6|2]\langle 5|1+2|3]}\right)\Bigg]. \quad (3.90)$$

We have checked numerically that (3.89) and (3.90) agree with (3.75) and (3.77), respectively. In Section 5.1 of [55], we consider one extra example, the five-point NMHV superamplitude and verify that it reproduces known results.

3.6.5 General case

Let us now consider going beyond NMHV. For the N^{2}MHV amplitudes we seek degree 16 contribtuions for $\mathcal{N} = 4$ SYM, or degree 32 contributions for $\mathcal{N} = 8$ supergravity. In the quadruple cuts for the case we encounter the following possibilities for the four tree amplitudes entering into the quadruple cuts: one can have four MHV amplitudes, leading to four-mass, three-mass and two-mass coefficients, or two MHV amplitudes, one anti-MHV amplitude and one NMHV amplitude, leading to three-mass and two-mass hard coefficients, or two NMHV and two anti-MHV amplitudes leading to two-mass easy coefficients, or finally one can have one MHV amplitude, two anti-MHV amplitudes and one N^{2}MHV amplitude, leading to the two-mass easy and one-mass coefficients.

Four-mass coefficients

For the four-mass coefficients, the obvious quadruple cut diagram, represented in Figure 3.10, has four MHV tree-level superamplitudes, and is given by

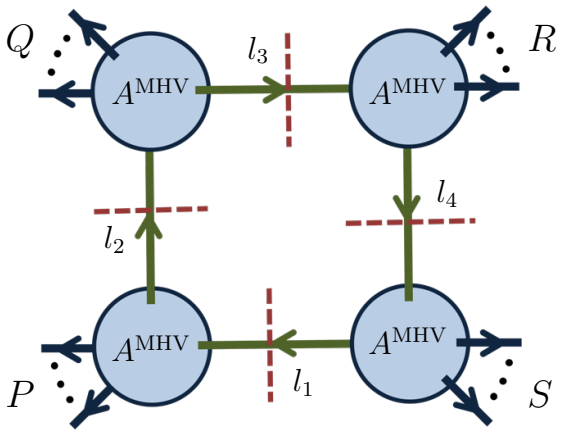

Figure 3.10: *A quadruple cut diagram determining the four-mass supercoefficient in an N^2MHV amplitude. The four tree-level superamplitudes entering the cut are of the MHV type.*

$$\mathcal{C}_{4\mathrm{m}}^{\mathcal{N}=8}(P,Q,R,S) = \frac{1}{2}\sum_{\mathcal{S}_\pm}\int\prod_{i=1}^{4} d^8\eta_{l_i}\,\mathcal{M}^{\rm MHV}(-l_1,P,l_2)\,\mathcal{M}^{\rm MHV}(-l_2,Q,l_3) \times \mathcal{M}^{\rm MHV}(-l_3,R,l_4)\,\mathcal{M}^{\rm MHV}(-l_4,S,l_1). \tag{3.91}$$

Using (2.110) this is equal to

$$\begin{aligned}&\mathcal{C}_{4\mathrm{m}}^{\mathcal{N}=8}(P,Q,R,S)\\ &= \frac{1}{2}\sum_{\mathcal{S}_\pm}\int\prod_{i=1}^{4} d^8\eta_{l_i}\sum_{\mathcal{P}(P)}\sum_{\mathcal{P}(Q)}\sum_{\mathcal{P}(R)}\sum_{\mathcal{P}(S)} \\ &\times \left[A^{\rm MHV}(-l_1,P,l_2)\right]^2 G^{\rm MHV}(-l_1,P,l_2)\left[A^{\rm MHV}(-l_2,Q,l_3)\right]^2 G^{\rm MHV}(-l_2,Q,l_3) \\ &\times \left[A^{\rm MHV}(-l_3,R,l_4)\right]^2 G^{\rm MHV}(-l_3,R,l_4)\left[A^{\rm MHV}(-l_4,S,l_1)\right]^2 G^{\rm MHV}(-l_4,S,l_1).\end{aligned} \tag{3.92}$$

Since the dressing factors $G^{\rm MHV}$ are independent of the superspace variables η, the superspace integrals will only act on the square of the product of the four tree MHV superamplitudes in the expression above. This is the same calculation as (the square of) the corresponding $\mathcal{N}=4$ Yang-Mills four-mass coefficient, and hence one

deduces that

$$\begin{aligned}\mathcal{C}_{4\mathrm{m}}^{\mathcal{N}=8}(P,Q,R,S) = \frac{1}{2}\sum_{\mathcal{S}_\pm}\sum_{\mathcal{P}(P)}\sum_{\mathcal{P}(Q)}\sum_{\mathcal{P}(R)}\sum_{\mathcal{P}(S)}\left(\mathcal{P}_{n;1}^{4\mathrm{m}}\right)^2 \\ \times G^{\mathrm{MHV}}(-l_1,P,l_2)G^{\mathrm{MHV}}(-l_2,Q,l_3) \\ \times G^{\mathrm{MHV}}(-l_3,R,l_4)G^{\mathrm{MHV}}(-l_4,S,l_1),\end{aligned} \tag{3.93}$$

where $\mathcal{P}_{n;1}^{4\mathrm{m}}$ is the coefficient function given in equation (5.11) of [48]. This depends on the external momenta and in addition on the loop variables l_i, the solutions for which must be substituted.

A comment is in order here. We observe that, in contradistinction with the coefficients considered so far, because of the presence in (3.93) of a sum over the two solutions, we cannot recast immediately the right-hand side of this equation in terms of squares of $\mathcal{N}=4$ supercoefficients; this appears to be a general feature of four-mass box coefficients.

Three-mass and two-mass hard coefficients

For the three-mass case, we have two possibilities. The first one corresponds to a special case of a four-mass coefficient, where one of the four tree superamplitudes in Figure 3.10 is a three-point MHV amplitude. In addition, there are three new diagrams, represented in Figure 3.11. We focus our attention for instance on the second diagram in Figure 3.11. This gives

$$\begin{aligned}\mathcal{C}_{3\mathrm{m}}^{\mathcal{N}=8}(r,P,Q,R)\big|_2 = \frac{1}{2}\sum_{\mathcal{S}_\pm}\int\prod_{i=1}^{4}d^8\eta_{l_i}\,\mathcal{M}_3^{\overline{\mathrm{MHV}}}(-l_1,r,l_2)\,\mathcal{M}^{\mathrm{MHV}}(-l_2,P,l_3) \\ \times\ \mathcal{M}^{\mathrm{NMHV}}(-l_3,Q,l_4)\,\mathcal{M}^{\mathrm{MHV}}(-l_4,R,l_1)\ ,\end{aligned} \tag{3.94}$$

where $P=\sum_{i=r+1}^{s-1}p_i$, $Q=\sum_{i=s}^{t-1}p_i$ and $R=\sum_{i=t}^{r-1}p_i$.

Because of the presence of a three-point anti-MHV amplitude, only one of the two cut solutions contributes, and therefore one can then drop the sum over solutions in (3.94). The explicit expressions (2.110) and (2.114) may be inserted into this

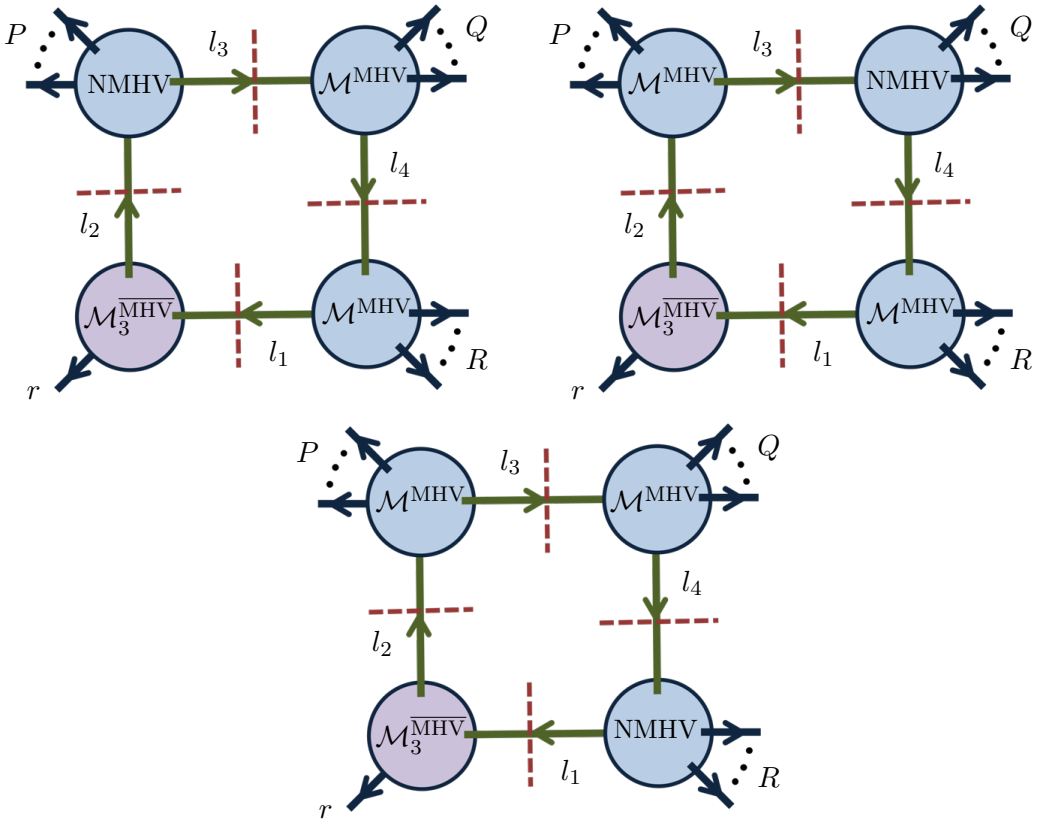

Figure 3.11: *Quadruple cut diagrams contributing to the three-mass supercoefficient in an N^2MHV amplitude. Additional quadruple cut diagrams contributing to this coefficient are obtained as special cases of the four-mass quadruple cut diagram in Figure 3.10.*

relation, yielding

$$\begin{aligned}\mathcal{C}_{3\rm m}^{\mathcal{N}=8}(r,P,Q,R)\big|_2 = \frac{1}{2}\int\prod_{i=1}^{4} d^8\eta_{l_i} \sum_{\mathcal{P}(P,Q,R)} &[A_3^{\overline{\rm MHV}}(-l_1,r,l_2)]^2 \\ &\times [A^{\rm MHV}(-l_2,P,l_3)]^2\, G^{\rm MHV}(-l_2,P,l_3) \\ &\times [A^{\rm MHV}(-l_3,Q,l_4)]^2 \left(\sum\sum R^2(-l_3,Q,l_4) G^{\rm NMHV}(-l_3,Q,l_4)\right) \\ &\times \ [A^{\rm MHV}(-l_4,R,l_1)]^2\, G^{\rm MHV}(-l_4,R,l_1), \end{aligned} \tag{3.95}$$

where we indicate the NMHV summation schematically for simplicity. Again, the key point, as noted in the discussion of NMHV amplitudes earlier, is that the fermionic variables corresponding to the loop momenta do not appear in the dressing factors or the R-functions. Hence one can perform these superspace integrations

ignoring these functions - and this corresponds to performing the same steps as in the corresponding $\mathcal{N} = 4$ Yang-Mills case, with the difference that the result is squared. Thus we obtain

$$\mathcal{C}_{3\mathrm{m}}^{\mathcal{N}=8}(r,P,Q,R)\big|_2 = 2\sum_{\mathcal{P}(P)}\sum_{\mathcal{P}(Q)}\sum_{\mathcal{P}(R)}\left(\mathcal{C}_{3\mathrm{m}}^{\mathcal{N}=4}(r,P,Q,R)\big|_2\right)^2 G^{\mathrm{MHV}}(-l_2,P,l_3) \times\left(\sum\sum R^2(-l_3,Q,l_4)G^{\mathrm{NMHV}}(-l_3,Q,l_4)\right)G^{\mathrm{MHV}}(-l_4,R,l_1), \tag{3.96}$$

where by $\mathcal{C}_{3\mathrm{m}}^{\mathcal{N}=4}(r,P,Q,R)\big|_2$ we mean the result of the same quadruple cut diagram evaluated for $\mathcal{N}=4$ SYM. The two-mass hard discussion goes along similar lines.

Two-mass easy coefficients

Finally, we consider the two-mass easy case. There are four types of diagrams possible here. A first non-vanishing contribution is obtained as a special case of the four-mass quadruple cut (see Figure 3.10), when two opposite corners of the diagram are three-point MHV amplitudes.

A second possibility is a special case of the three-mass contributions considered earlier in Figure 3.11, where the MHV amplitude opposite to the anti-MHV three-point amplitude is also a three-point amplitude. This particular quadruple cut diagram will in general vanish as it would entail constraints on the external kinematics (this is not specific to the particular amplitudes considered here, but is a general feature of two-mass easy quadruple cuts where the two opposite three-point amplitudes cannot be one MHV and one anti-MHV).

The third contribution comes from diagrams with two anti-MHV amplitudes at opposite corners and two NMHV amplitudes at the other two corners (see the third diagram on Figure 3.12). This gives

$$\mathcal{C}_{2\mathrm{me}}^{\mathcal{N}=8}(1,P,s,Q)\big|_3 = \frac{1}{2}\sum_{\mathcal{S}_\pm}\int\prod_{i=1}^{4}d^8\eta_{l_i}\,\mathcal{M}_3^{\overline{\mathrm{MHV}}}(-l_1,1,l_2)\,\mathcal{M}^{\mathrm{NMHV}}(-l_2,P,l_3) \times\mathcal{M}_3^{\overline{\mathrm{MHV}}}(-l_3,s,l_4)\,\mathcal{M}^{\mathrm{NMHV}}(-l_4,Q,l_1), \tag{3.97}$$

where $P=\sum_{i=2}^{s-1}p_i$ and $Q=\sum_{i=s+1}^{n}p_i$. Now we insert the expressions for the

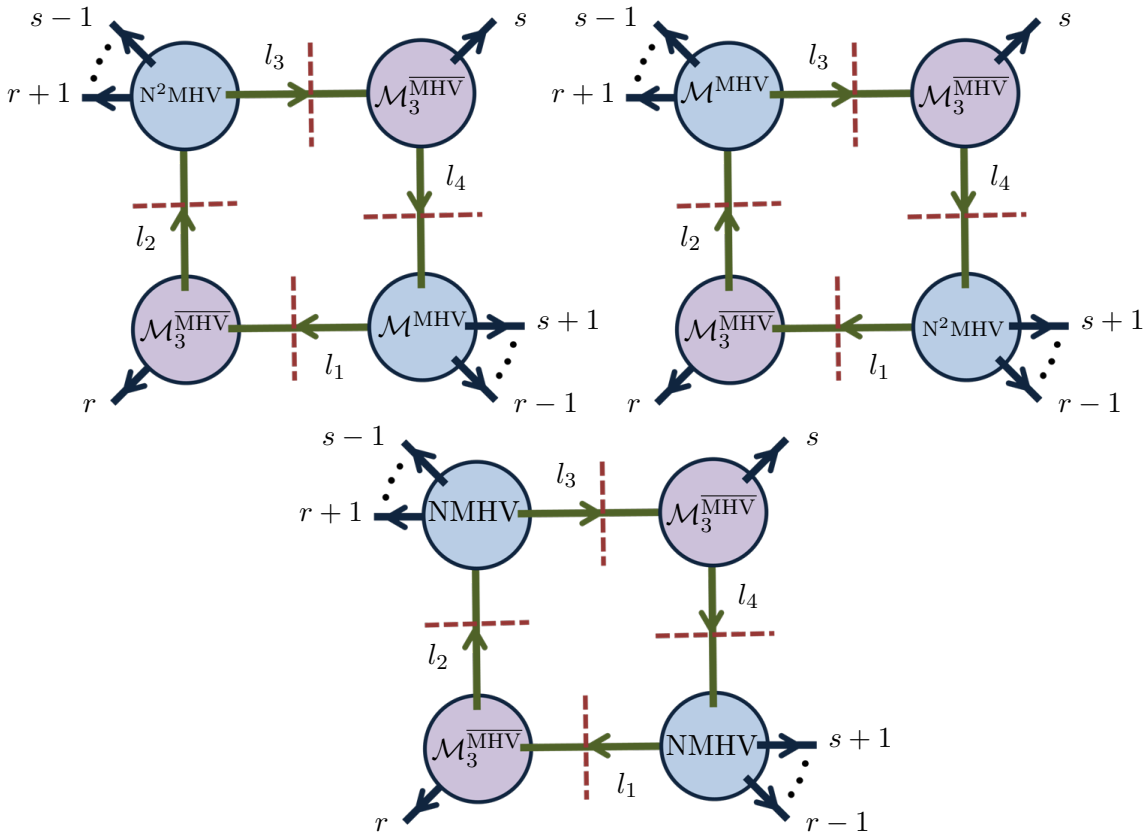

Figure 3.12: *Quadruple cut diagrams contributing to the two-mass easy coefficients of an N^2MHV superamplitude.*

anti-MHV amplitudes and the NMHV amplitudes, obtaining

$$\begin{aligned}\mathcal{C}_{\mathrm{2me}}^{\mathcal{N}=8}(1,P,s,Q)\big|_3 = \frac{1}{2}\sum_{\mathcal{S}_\pm}\sum_{\mathcal{P}(P)}\sum_{\mathcal{P}(Q)}\int\prod_{i=1}^{4}d^8\eta_{l_i} \qquad (3.98)\\ \times\left(A_3^{\overline{\mathrm{MHV}}}(-l_1,1,l_2)\,A^{\mathrm{MHV}}(-l_2,P,l_3)A_3^{\overline{\mathrm{MHV}}}(-l_3,s,l_4)\,A^{\mathrm{MHV}}(-l_4,Q,l_1)\right)^2\\ \times\left(\sum\sum R^2G^{\mathrm{NMHV}}\right)(-l_2,P,l_3)\left(\sum\sum R^2G^{\mathrm{NMHV}}\right)(-l_4,Q,l_1),\end{aligned}$$

using a shorthand notation as previously. Only one solution to the loop momenta conditions contributes, and one may perform the η integrals directly. This is the same calculation as for the MHV two-mass easy case, and thus we find the result

$$\begin{aligned}\mathcal{C}_{\mathrm{2me}}^{\mathcal{N}=8}(1,P,s,Q)\big|_3 = \frac{1}{2}\sum_{\mathcal{P}(P)}\sum_{\mathcal{P}(Q)}\left(\mathcal{C}_{\mathrm{2me}}^{\mathcal{N}=4}(1,P,s,Q)\right)^2\left(\sum\sum R^2G^{\mathrm{NMHV}}\right)(-l_2,P,l_3)\\ \times\left(\sum\sum R^2G^{\mathrm{NMHV}}\right)(-l_4,Q,l_1), \qquad (3.99)\end{aligned}$$

where the solutions for the loop momenta need to be inserted into the terms containing the dressing functions R and G.

Lastly, we consider two-mass easy cases for the first two diagrams in Figure 3.12, where a new ingredient is the presence of a tree-level $\mathrm{N^2MHV}$ amplitude. This amplitude is expressed in terms of MHV tree SYM amplitudes in (2.117), we write this equation in the short-hand form

$$\mathcal{M}^{\mathrm{N^2MHV}}(1,\ldots,n) = \sum_{\mathcal{P}(2,\ldots,n-1)} [A^{\mathrm{MHV}}(1,\ldots,n)]^2 \sum\sum R^2 R^2 H(1,\ldots,n). \quad (3.100)$$

As we have already discussed, the H functions are independent of the superspace variables η, and the R functions do not depend on η_1 or η_n. Now we may write the quadruple cut for the two-mass easy diagrams as

$$\begin{aligned}\mathcal{C}^{\mathcal{N}=8}_{\mathrm{2me}}(r,P,s,Q)\big|_4 = \frac{1}{2}\sum_{\mathcal{S}_\pm}\int\prod_{i=1}^{4} d^8\eta_{l_i}\, \mathcal{M}_3^{\overline{\mathrm{MHV}}}(-l_1,r,l_2)\, \mathcal{M}^{\mathrm{N^2MHV}}(-l_2,P,l_3) \\ \times \mathcal{M}_3^{\overline{\mathrm{MHV}}}(-l_3,s,l_4)\, \mathcal{M}^{\mathrm{MHV}}(-l_4,Q,l_1). \quad (3.101)\end{aligned}$$

As for the corresponding NMHV and MHV two-mass coefficients, only one of the two solutions to the cut condition contributes, given explicitly in (3.41). Taking this into account, we get

$$\begin{aligned}\mathcal{C}^{\mathcal{N}=8}_{\mathrm{2me}}(r,P,s,Q)\big|_4 = \frac{1}{2}\int\prod_{i=1}^{4} d^8\eta_{l_i}\sum_{\mathcal{P}(P)}\sum_{\mathcal{P}(Q)}[A^{\overline{\mathrm{MHV}}}(-l_1,r,l_2)]^2\,[A_3^{\mathrm{MHV}}(-l_2,P,l_3)]^2 \\ \times\sum\sum R^2R^2H(-l_2,P,l_3)\,[A^{\overline{\mathrm{MHV}}}(-l_3,s,l_4)]^2 \\ \times [A^{\mathrm{MHV}}(-l_4,Q,l_1)]^2\, G^{\mathrm{MHV}}(-l_4,Q,l_1). \quad (3.102)\end{aligned}$$

We may perform the loop superspace integrals and the final answer is

$$\begin{aligned}\mathcal{C}^{\mathcal{N}=8}_{\mathrm{2me}}(r,P,s,Q)\big|_4 = 2\sum_{\mathcal{P}(P)}\sum_{\mathcal{P}(Q)}(\mathcal{C}^{\mathcal{N}=4}_{\mathrm{2me}}(r,P,s,Q)\big|_4)^2\, G^{\mathrm{MHV}}(-l_4,Q,l_1) \\ \times\sum\sum R^2R^2H(-l_2,P,l_3), \quad (3.103)\end{aligned}$$

where the loop momenta are replaced by the cut solution in (3.41). For the one-mass case, the only contribution comes from the special case of the last two-mass easy case discussed immediately above - that where Q contains only one external momentum.

Having given some details of how the calculation proceeds for the N^2MHV case, one can see how the general case will work. One can see from [45] that the generalised R-functions and dressing factors which arise in any quadruple cut do not depend upon the η variables corresponding to the loop momenta; hence one may perform the superspace integrals with these functions as spectators. This calculation is however precisely the same as the corresponding $\mathcal{N} = 4$ Yang-Mills case, except that the coefficient is squared in the result. The outcome is that the $\mathcal{N} = 8$ supergravity coefficient is given by a sum of the squares of the result of the corresponding $\mathcal{N} = 4$ Yang-Mills calculation, factored into sums and products of R-functions and dressing factors. There is also in general a sum over solutions of the cut equation, which need to be inserted into these expressions. Thus we see how this approach yields $\mathcal{N} = 8$ supergravity coefficients in terms of squares of the results of $\mathcal{N} = 4$ Yang-Mills calculations.

Chapter 4

Wilson Loops

We now stay within $\mathcal{N} = 4$ super Yang-Mills and focus our attention on the MHV amplitudes. These amplitudes demonstrate an intriguingly simple iterative structure at any loop. In addition, a fascinating new duality relates them to specific Wilson loops over polygonal contours defined in dual momentum space. In this chapter, we make a step further in perturbation theory and present calculation up to two loops. Moreover, within dimensional regularisation, we travel beyond the finite terms in the expansion in ϵ and perform precision tests of the duality at $O(\epsilon)$. Using computer algorithms that take advantage of the Mellin-Barnes method, we probe both amplitudes and Wilson loops at various kinematic points. We discover that the duality persists at $O(\epsilon)$ for four and five points, and it has a surprisingly simple form.

4.1 The ABDK/BDS ansatz

We have already demonstrated the simplicity of MHV amplitudes in $\mathcal{N} = 4$ super Yang-Mills at tree level and one-loop level, while this remarkable simple structure persists at higher loop orders. Supersymmetric Ward identities [93, 94, 69, 72], dictate that, at any loop order L, the MHV amplitude can be expressed as the tree-level amplitude, times a scalar, helicity-blind function $\mathcal{M}_n^{(L)}$

$$A_n^{(L)} = A_n^{\text{tree}} \, \mathcal{M}_n^{(L)}. \tag{4.1}$$

At one loop, the function $\mathcal{M}_n^{(1)}$, expanded in the basis of scalar box functions,

contains two-mass-easy boxes F^{2me} only, with all the coefficients being equal to one

$$\mathcal{M}_n^{(1)} = \sum_{p,q} F^{\text{2me}}(p, P, q, Q). \tag{4.2}$$

The scalar box functions F are related to the scalar box integrals $\mathcal{I}$ via (3.4). In (A.6) we give the expansion of $\mathcal{I}^{\text{2me}}$ in ϵ through $\mathcal{O}(\epsilon)$.

In [57], ABDK discovered an intriguing iterative structure in the two-loop expansion of the four-point MHV amplitude. This relation can be written as

$$\mathcal{M}_4^{(2)}(\epsilon) - \frac{1}{2}\left(\mathcal{M}_4^{(1)}(\epsilon)\right)^2 = f^{(2)}(\epsilon)\mathcal{M}_4^{(1)}(2\epsilon) + C^{(2)} + \mathcal{O}(\epsilon), \tag{4.3}$$

where

$$f^{(2)}(\epsilon) = -\zeta_2 - \zeta_3\epsilon - \zeta_4\epsilon^2, \tag{4.4}$$

and

$$C^{(2)} = -\frac{1}{2}\zeta_2^2. \tag{4.5}$$

The ABDK relation (4.3) is built upon the known exponentiation of infrared divergences [95, 96], which guarantees that the singular terms must agree on both sides of (4.3), as well as on the known behavior of amplitudes under collinear limits [97, 98]. The highly nontrivial content of the ABDK relation is that (4.3) holds exactly as written at $\mathcal{O}(\epsilon^0)$, while ABDK observed that the $\mathcal{O}(\epsilon)$ terms do not satisfy the same iteration relation [57].

Scattering amplitudes with more than four gluons normalised by the tree amplitude may contain odd powers of the Levi-Civita tensor contracted with the external momenta. These terms flip sign under a parity transformation, which exchanges λ's with $\tilde{\lambda}$'s and reverses all helicities. We refer to them as parity-odd terms, and to the remaining terms as parity-even.

In [57], it was conjectured that (4.3) should hold for two-loop amplitudes with an arbitrary number of external particles, with the same quantities (4.4) and (4.5) for any n. For five-points, this conjecture was confirmed first in [58] for the parity-even part of the two-loop amplitude, and later in [59] for the complete amplitude. Notice that for the iteration to be satisfied, parity-odd terms that enter on the left-hand side of the relation (4.3) must cancel up to and including $\mathcal{O}(\epsilon^0)$ terms, since the right-hand side is parity even up to this order in ϵ. So far, this has been checked and confirmed at two loops for five and six particles [59, 99]. This is also crucial for the duality with Wilson loops, that is the main subject of this Chapter, which by

construction cannot produce parity-odd terms at two loops.

It has been found that starting from six particles and two loops, the ABDK/BDS ansatz (4.3) needs to be modified by allowing the presence of a remainder function $\mathcal{R}_n$ [62, 12],

$$\mathcal{M}_n^{(2)}(\epsilon) - \frac{1}{2}\left(\mathcal{M}_n^{(1)}(\epsilon)\right)^2 = f^{(2)}(\epsilon)\mathcal{M}_n^{(1)}(2\epsilon) + C^{(2)} + \mathcal{R}_n + E_n(\epsilon), \tag{4.6}$$

where $\mathcal{R}_n$ is ϵ-independent and $E_n(\epsilon)$ vanishes as $\epsilon \to 0$. We parameterize the latter as

$$E_n(\epsilon) = \epsilon\, \mathcal{E}_n + \mathcal{O}(\epsilon^2). \tag{4.7}$$

Ultimate goal of this Chapter is to discuss in detail $\mathcal{E}_n$ for $n = 4, 5$ and present a remarkable relation to the same quantity calculated from the Wilson loop, as it appeared in [14]. Hitherto this relation was only expected to hold for the finite parts of the remainder $\mathcal{R}_n$.

4.2 The MHV/Wilson loop duality

In a parallel development to the ABDK/BDS ansatz, Alday and Maldacena addressed the problem of calculating scattering amplitudes at strong coupling in $\mathcal{N} = 4$ super Yang-Mills using the AdS/CFT correspondence [15, 16]. Their remarkable result showed that the planar amplitude at strong coupling is calculated by a Wilson loop whose contour $\mathcal{C}_n$ is the n-edged polygon obtained by joining the lightlike momenta of the particles following the order induced by the colour structure of the planar amplitude. At strong coupling the calculation amounts to finding the minimal area of a surface ending on the contour $\mathcal{C}_n$ embedded at the boundary of a T-dual AdS_5 space [17]. Shortly after, it was realised that the very same Wilson loop evaluated at weak coupling reproduces all one-loop MHV amplitudes in $\mathcal{N} = 4$ super Yang-Mills [7, 8]. The conjectured relation between MHV amplitudes and Wilson loops found further strong support by explicit two loop calculations at four [9], five [10] and six points [62, 12, 99]. In particular, the absence of a non-trivial remainder function in the four- and five-point case was later explained in [10] from the Wilson loop perspective, where it was realised that the BDS ansatz is a solution to the anomalous Ward identity for the Wilson loop associated to the dual conformal symmetry [67].

A Wilson loop is the following non-trivial function of the gauge field A_μ defined

on a closed contour $\mathcal{C}$ in coordinate space

$$\mathcal{W}[\mathcal{C}] = \mathrm{Tr}\,\mathcal{P}\exp\left[ig\oint_{\mathcal{C}} dx^{\mu}A_{\mu}\right], \tag{4.8}$$

where $A_{\mu}(x) = A^{a}_{\mu}(x)t^{a}$ and t^{a} are the $SU(N)$ generators in the fundamental representation normalised as $\mathrm{tr}\left(t^{a}t^{b}\right) = \frac{1}{2}\delta^{ab}$. The operator $\mathcal{P}$ imposes path ordering of the generators t^{a}. Wilson loops are special because they give us a gauge invariant quantity for any loop $\mathcal{C}$ we can write down in coordinate space.

Calculating the expectation value of a Wilson loop at weak coupling, we can resort to perturbation theory, and expand the exponential in (4.8) in powers of the coupling constant g. For example, the first two terms in this expansion are

$$\langle 0|\mathcal{W}[\mathcal{C}]|0\rangle = 1 + \frac{1}{2}(ig)^{2}C_{F}C_{A}\oint_{C} dx^{\mu}\oint_{C} dy^{\nu}\langle 0|A_{\mu}(x)A_{\nu}(y)|0\rangle + \mathcal{O}(g^{4}), \tag{4.9}$$

where $C_{F} = (N^{2}-1)/(2N)$ is the Casimir of the fundamental representation of $SU(N)$ and $C_{A} = N$ is the adjoint Casimir. The $O(g^{1})$ term vanishes as it involves the expectation value of a single field. The expectation value $\langle 0|A_{\mu}(x)A_{\nu}(y)|0\rangle$ can also be expanded in g and at zeroth order it gives us the free gluon propagator $G_{\mu\nu}(x-y)$. In the expansion (4.9), we refer to the $g^{(2L)}$ term as the L-loop contribution to the Wilson loop.

As mentioned earlier, motivated by a calculation at strong coupling within String Theory, it has been observed that, on the weak coupling side, the n-point planar MHV amplitudes in $\mathcal{N}=4$ super Yang-Mills are equal to specific Wilson loops over a polygonal contour $\mathcal{C}_{n}$ with n lightlike sides, defined in dual momentum space. This duality at weak coupling is the main topic of this Chapter. More specifically, the helicity blind factor $\mathcal{M}_{n}$ we introduced in (4.1) defined in momentum space, appears to be dual to a Wilson loop living in dual momentum space, and over a polygonal contour constructed by connecting the dual coordinates x_{i}, $i = 1,\ldots,n$. The coordinates x_{i} are defined via (2.25) and the contour is the one shown in figure 2.2 after identifying $x_{n+1} \equiv x_{1}$. A sketch of the duality is given in Figure 4.1. The exact formulation of the MHV/Wilson loop duality involves the logarithms of the two quantities

$$\ln\mathcal{M}_{n} = \ln\langle\mathcal{W}[\mathcal{C}]\rangle + \mathcal{O}(1/N^{2}). \tag{4.10}$$

In (4.9) we expanded the Wilson loop in terms of the the coupling constant g. Alternatively, we can expand in powers of the 't Hooft coupling constant $a =$

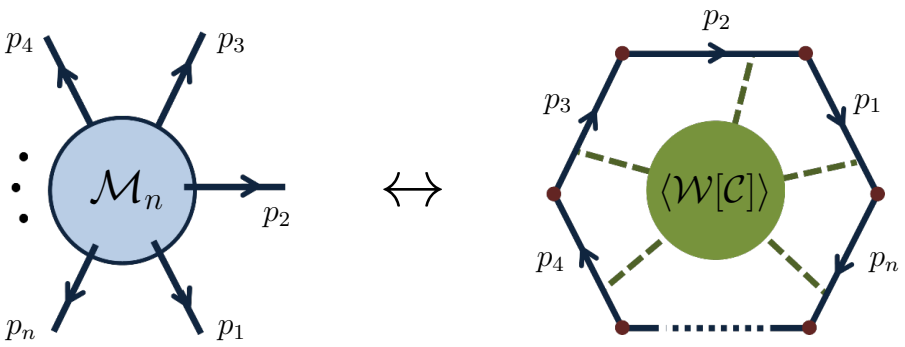

Figure 4.1: *The MHV amplitude/Wilson loop duality relates the logarithm of the helicity-blind function $\mathcal{M}_n$ of the MHV amplitudes (see (4.1)) to the logarithm of the expectation value of the Wilson loop $\langle \mathcal{W}[\mathcal{C}] \rangle$ over a specific polygonal contour C_n made out the momenta of the external particles.*

$g^2 N/(8\pi^2)$ as follows

$$\langle \mathcal{W}[\mathcal{C}] \rangle = 1 + \sum_{l=1}^{\infty} a^l \, W_n^{(l)}, \tag{4.11}$$

where $W_n^{(l)}$ is the l-loop contribution to the expectation value of the n-sided polygonal Wilson loop. The non-Abelian exponentiation theorem [100, 101] guarantees that we can write the Wilson loop in an exponentiated form

$$\langle \mathcal{W}[\mathcal{C}] \rangle = \exp \sum_{l=1}^{\infty} a^l w_n^{(l)}, \tag{4.12}$$

where $w_n^{(l)}$ is the l-loop contribution to the logarithm of the n-sided polygonal Wilson loop.

The $w_n^{(l)}$ are obtained from subsets of Feynman diagrams [100, 101] contributing to the $W_n^{(l)}$, and, in addition, the colour weights assigned to the diagrams in $w_n^{(l)}$ are, in general, different from the colour weights of corresponding diagrams in $W_n^{(l)}$. The general rule for finding the surviving diagrams and their coefficients, is to keep only parts with "maximal non-abelian colour factor". At two-loops this factor is equal to the Casimirs of the fundamental and the adjoint representations $C_F C_A$ [102]. For example, the ladder diagram, appearing on the left in Figure 4.2, has colour factor $\mathrm{tr}[t^a t^a t^b t^b] = d_F C_F^2$, and therefore does not contribute to the logarithm of the Wilson loop. The right diagram in Figure 4.2, corresponding to the cross diagram, has colour factor $\mathrm{tr}[t^a t^b t^a t^b] = d_F C_F (C_F - 1/2 C_A)$ where d_F is equal to the dimension of the representation, and therefore this diagram survives with a modified colour factor $-1/2 d_F C_F C_A$, corresponding to its maximally non-abelian part. For a recent

algorithm for computing the colour factor associated with any given diagram in the exponent we refer the reader to [103].

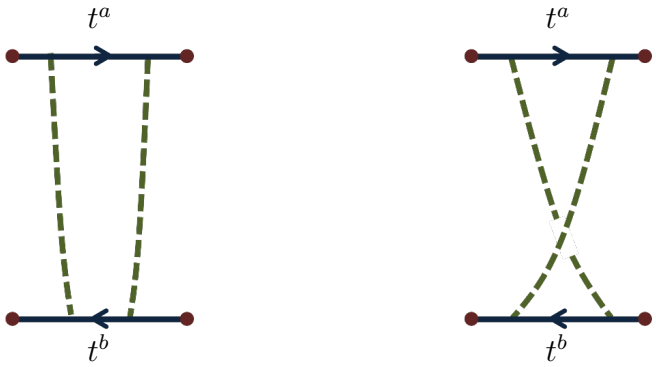

Figure 4.2: *Non-abelian exponentiation dictates that only maximally non-abelian parts of diagrams survive in the logarithm of the Wilson loop. For example, at two loops, the ladder diagram (left diagram) does not appear at all, while the cross diagram (right diagram) appears with a modified factor corresponding to its maximally non-abelian part.*

Expanding the exponential in (4.11) we get

$$\begin{aligned}\exp\sum_{l=1}^{\infty} a^l w_n^{(l)} &= 1 + \left(a w_n^{(1)} + a^2 w_n^{(2)} + \mathcal{O}(a^3)\right) + \frac{1}{2}\left(a w_n^{(1)} + \mathcal{O}(a^2)\right)^2 \\ &= 1 + a w_n^{(1)} + a^2\left[w_n^{(2)} + \frac{1}{2}(w_n^{(1)})^2\right] + \mathcal{O}(a^3),\end{aligned} \tag{4.13}$$

and equating the coefficients of each power of a between (4.12) and (4.13) we get

$$w_n^{(1)} = W_n^{(1)}, \qquad w_n^{(2)} = W_n^{(2)} - \frac{1}{2}(W_n^{(1)})^2. \tag{4.14}$$

Polygonal Wilson loops suffer from UV divergences due to the presence of the cusps, that are regulated by working in $D = 4 - 2\epsilon_{\rm UV}$, where $\epsilon_{\rm UV} > 0$. The ultraviolet $\epsilon_{\rm UV}$ we use in Wilson loops is related to the infrared dimensional regularisation parameter ϵ that we encounter in amplitude calculations, via $\epsilon_{\rm UV} = -\epsilon$. To facilitate the comparison with the corresponding quantities for amplitudes, in the following discussion about Wilson loops we express the results in terms of the infrared parameter ϵ.

4.3 The Wilson loop remainder function

As discussed in more detail in Section 4.5, the one-loop Wilson loop $w_n^{(1)}$ times the tree-level MHV amplitude is equal to the one-loop MHV amplitude, first calculated in [84] using the unitarity-based approach [85], up to a regularization-dependent factor. This implies that non-trivial remainder functions can only appear at two and higher loops. At two loops, which is our main focus in [14] and the current Chapter, and in a similar fashion to (4.6), we define the remainder function $\mathcal{R}_n^{\rm WL}$ for an n-sided Wilson loop as

$$w_n^{(2)}(\epsilon) = f_{\rm WL}^{(2)}(\epsilon) w_n^{(1)}(2\epsilon) + C_{\rm WL}^{(2)} + \mathcal{R}_n^{\rm WL} + E_n^{\rm WL}(\epsilon), \tag{4.15}$$

where

$$f_{\rm WL}^{(2)}(\epsilon) = f_0^{(2)} + f_{1,\rm WL}^{(2)}\epsilon + f_{2,\rm WL}^{(2)}\epsilon^2. \tag{4.16}$$

Note that $f_0^{(2)} = -\zeta_2$, which is the same as on the amplitude side, while $f_{1,\rm WL}^{(2)} = G_{\rm ik}^{(2)} = 7\zeta_3$ [104]. We expect a remainder function at every loop order l and the corresponding equations would be

$$w_n^{(l)}(\epsilon) = f_{\rm WL}^{(l)}(\epsilon) w_n^{(1)}(l\epsilon) + C_{\rm WL}^{(l)} + \mathcal{R}_{n,\rm WL}^{(l)} + E_{n,\rm WL}^{(l)}(\epsilon). \tag{4.17}$$

Similarly to the amplitude case, the remainder $\mathcal{R}_n^{\rm WL}$ is an ϵ-independent function, while we parametrise the ϵ-dependent quantity $E_n^{\rm WL}$ as

$$E_n^{\rm WL}(\epsilon) = \epsilon\, \mathcal{E}_n^{\rm WL} + \mathcal{O}(\epsilon^2). \tag{4.18}$$

In [105], the four- and five-edged Wilson loops were cast in the form (4.15) and the natural requirements

$$\mathcal{R}_4^{\rm WL} = \mathcal{R}_5^{\rm WL} = 0, \tag{4.19}$$

allowed for a complete determination of the coefficients $f_{2,\rm WL}^{(2)}$ and $C_{\rm WL}^{(2)}$. The $\mathcal{O}(\epsilon^0)$ and $\mathcal{O}(\epsilon)$ coefficients of $f_{\rm WL}^{(2)}(\epsilon)$ had been determined earlier in [9], while the two conditions (4.19) give us the remaining two unknowns, leading to the values [105]

$$f_{\rm WL}^{(2)}(\epsilon) = -\zeta_2 + 7\zeta_3\,\epsilon - 5\zeta_4\,\epsilon^2, \tag{4.20}$$

and

$$C_{\rm WL}^{(2)} = -\frac{1}{2}\zeta_2^2. \tag{4.21}$$

As noticed in [105], there is an intriguing agreement between the constant $C^{(2)}_{\rm WL}$ and the corresponding value (4.5) of the same quantity on the amplitude side.

What has been observed so far is a duality between Wilson loops and amplitudes up to finite terms. In turn this can be reinterpreted as an equality of the corresponding remainder functions

$$\mathcal{R}_n = \mathcal{R}_n^{\rm WL}. \tag{4.22}$$

A consequence of the precise determination of the constants $f^{(2)}_{2,\rm WL}$ and $C^{(2)}_{\rm WL}$ is that no additional constant term is allowed on the right hand side of (4.22). For the same reason, the Wilson loop remainder function must then have the same collinear limits as its amplitude counterpart, i.e.

$$\mathcal{R}_n^{\rm WL} \to \mathcal{R}_{n-1}^{\rm WL}, \tag{4.23}$$

with no extra constant on the right hand side of (4.23). An alternative interpretation of the duality in terms of certain ratios of amplitudes and Wilson loops has been given recently in [106].

Our main result in [14] and the current Chapter is that for $n = 4, 5$ the relation between amplitudes and Wilson loops continues to hold for terms of $\mathcal{O}(\epsilon^1)$. In particular we find

$$\mathcal{E}_4^{(2)} = \mathcal{E}_{4,\rm WL}^{(2)} - 3\zeta_5, \tag{4.24}$$

$$\mathcal{E}_5^{(2)} = \mathcal{E}_{5,\rm WL}^{(2)} - \frac{5}{2}\zeta_5. \tag{4.25}$$

Note that these results have been obtained (semi-)numerically with typical errors of 10^{-8} at $n = 4$ and 10^{-4} for $n = 5$. Details of the calculations are presented in the remaining of this Chapter. More precisely $\mathcal{E}_4^{(2)}$ is known analytically [107], while the analytic evaluation of $\mathcal{E}_{4,\rm WL}^{(2)}$ is discussed in appendix A of [14]. At five points all results are numerical and furthermore on the amplitude side we only considered the parity-even terms. It is an interesting open question whether the parity-odd terms cancel at $\mathcal{O}(\epsilon)$ as they do at $\mathcal{O}(\epsilon^0)$ [59].

4.4 MHV amplitudes

In this section we review results for the MHV amplitudes at one and two loops. These are necessary ingredients in making the comparison with the Wilson loop.

4.4.1 One-loop four- and five-point case

We begin by presenting the one-loop MHV amplitudes, for which analytic results exist to all orders in ϵ. Following in this Chapter the conventions of [57], the four-point amplitude is given by [108]

$$\mathcal{M}_4^{(1)} = -\frac{1}{2} st I_4^{(1)}, \tag{4.26}$$

where $s = (p_1 + p_2)^2$, $t = (p_2 + p_3)^2$ are the usual Mandelstam variables and $I_4^{(1)}$ is the massless scalar box integral, depicted in Figure 4.3, and given by

$$I_4^{(1)} = \frac{e^{\epsilon\gamma}}{i\pi^{D/2}} \int d^D p \frac{1}{p^2 (p - p_1)^2 (p - p_1 - p_2)^2 (p + p_4)^2}, \tag{4.27}$$

which we have written out in order to emphasize the normalization convention (followed throughout this Chapter) that each loop momentum integral carries an overall factor of $e^{\epsilon\gamma}/i\pi^{D/2}$. The integral may be evaluated explicitly (see for example [90]) in

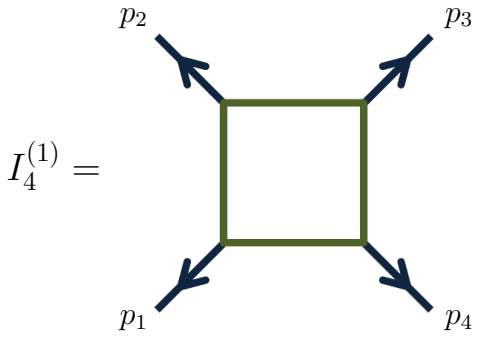

Figure 4.3: *The massless scalar box integral* $I_4^{(1)}$.

terms of the ordinary hypergeometric function ${}_2\mathrm{F}_1$, leading to the exact expression

$$\mathcal{M}_4^{(1)} = -\frac{e^{\epsilon\gamma}}{\epsilon^2} \frac{\Gamma(1+\epsilon)\Gamma^2(1-\epsilon)}{\Gamma(1-2\epsilon)} \left[(-s)^{-\epsilon} {}_2\mathrm{F}_1(1, -\epsilon, 1-\epsilon, 1+s/t) + (s \leftrightarrow t) \right], \tag{4.28}$$

valid to all orders in ϵ. We will always be studying the amplitude/Wilson loop duality in the fully Euclidean regime where all momentum invariants such as s and t take negative values. The formula (4.28) applies in this regime as long as we are careful to navigate branch cuts according to the rule

$$(-z)^{-\epsilon} {}_2\mathrm{F}_1(-\epsilon, -\epsilon, 1-\epsilon, 1+z) := \lim_{\varepsilon \to 0} \mathrm{Re} \left[\frac{{}_2\mathrm{F}_1(-\epsilon, -\epsilon, 1-\epsilon, 1+z+i\varepsilon)}{(-z+i\varepsilon)^{\epsilon}} \right], \tag{4.29}$$

when $z > 0$.

Five-point loop amplitudes $\mathcal{M}_5^{(L)}$ contain both parity-even and parity-odd contributions after dividing by the tree amplitude as in (4.1).

The parity-even part of the one-loop five-point amplitude is given by [109]

$$\mathcal{M}_{5+}^{(1)} = -\frac{1}{4}\sum_{\text{cyclic}} s_{34}s_{45}I_5^{(1)}, \tag{4.30}$$

where the sum runs over the five cyclic permutations of the external momenta p_i, and the integral $I_5^{(1)}$ is depicted in Figure 4.4. This integral can also be explicitly

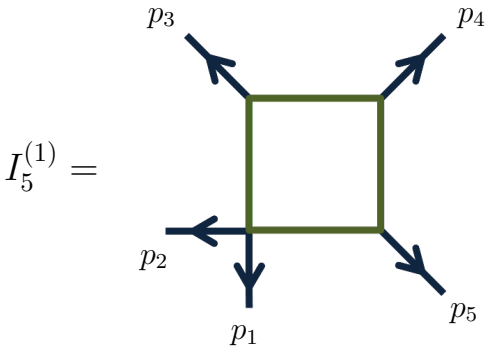

Figure 4.4: *The one-loop scalar box integral $I_5^{(1)}$ encountered at five points.*

evaluated (see for example [90]), leading to the all-orders in ϵ result

$$\begin{aligned}\mathcal{M}_{5+}^{(1)} = &-\frac{e^{\epsilon\gamma}}{\epsilon^2}\frac{\Gamma(1+\epsilon)\Gamma^2(1-\epsilon)}{\Gamma(1-2\epsilon)}\frac{1}{2}\\ &\times\sum_{\text{cyclic}}\left[\left(-\frac{s_{12}-s_{45}}{s_{34}s_{45}}\right)^{\epsilon}{}_2\mathrm{F}_1(-\epsilon,-\epsilon,1-\epsilon,1-\frac{s_{34}}{s_{12}-s_{45}})\right.\\ &\quad+\left(-\frac{s_{12}-s_{34}}{s_{34}s_{45}}\right)^{\epsilon}{}_2\mathrm{F}_1(-\epsilon,-\epsilon,1-\epsilon,1-\frac{s_{45}}{s_{12}-s_{34}})\\ &\left.-\left(-\frac{(s_{12}-s_{34})(s_{12}-s_{45})}{s_{12}s_{34}s_{45}}\right)^{\epsilon}{}_2\mathrm{F}_1(-\epsilon,-\epsilon,1-\epsilon,1-\frac{s_{34}s_{45}}{(s_{12}-s_{34})(s_{12}-s_{45})})\right],\end{aligned} \tag{4.31}$$

again keeping in mind (4.29).

4.4.2 Two-loop four- and five-point case

The two-loop four-point amplitude is given by [110]

$$\mathcal{M}_4^{(2)} = \frac{1}{4}s^2tI_4^{(2)} + (s \leftrightarrow t), \tag{4.32}$$

where the double box integral $I_4^{(2)}$ is depicted in Figure 4.5, and it may be evaluated analytically through $\mathcal{O}(\epsilon^2)$ using results from [107] (no all-orders in ϵ expression for the double box integral is known), from which we find

$$\begin{aligned}\mathcal{E}_4 = {} & 5\,\mathrm{Li}_5(-x) - 4L\,\mathrm{Li}_4(-x) + \frac{1}{2}(3L^2+\pi^2)\,\mathrm{Li}_3(-x) - \frac{L}{3}(L^2+\pi^2)\,\mathrm{Li}_2(-x) \\ & - \frac{1}{24}(L^2+\pi^2)^2\log(1+x) + \frac{2}{45}\pi^4 L - \frac{39}{2}\zeta_5 + \frac{23}{12}\pi^2\zeta_3,\end{aligned} \tag{4.33}$$

where $x = t/s$ and $L = \log x$. In order to be able to present the amplitude remainder (4.33) in this form, we have pulled out a factor of $(st)^{-L\epsilon/2}$ from each loop amplitude $\mathcal{M}_4^{(L)}$. This renders the amplitudes, and hence the ABDK remainder

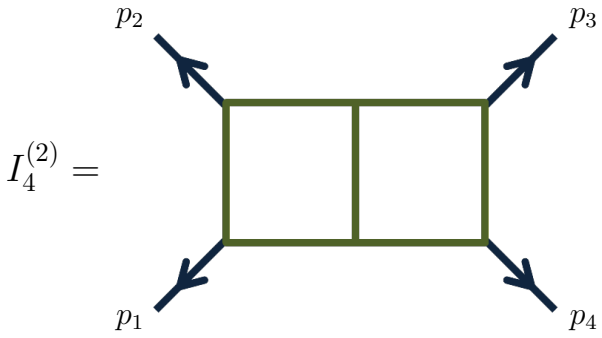

Figure 4.5: *Double box integral $I_4^{(2)}$ at four points.*

$E_4(\epsilon)$, dimensionless functions of the single variable x. We perform this step in the four-point case only, where we are able to present analytic results for the amplitude and Wilson loop remainders.

The parity-even part of the two-loop five-point amplitude involves the two integrals shown in Figure 4.6, in terms of which the former is written as [111, 58, 59]

$$\mathcal{M}_{5+}^{(2)} = \frac{1}{8}\sum_{\text{cyclic}}\left(s_{34}s_{45}^2 I^{(2)a} + (p_i \to p_{6-i})\right) + s_{12}s_{34}s_{45}I^{(2)d}. \tag{4.34}$$

To evaluate this amplitude to $\mathcal{O}(\epsilon)$ we resort to a numerical calculation using Mellin-Barnes parameterizations of the integrals (which may be found for example in [58]), which we then expand through $\mathcal{O}(\epsilon)$, simplify, and numerically integrate with the help of the `MB`, `MBresolve`, and `barnesroutines` programs [112, 113]. In this manner we have determined the $\mathcal{O}(\epsilon)$ contribution $\mathcal{E}_5^{(2)}$ to the five-point ABDK relation numerically at a variety of kinematic points. The results are displayed in Tables 4.2 and 4.4. We present the Mellin-Barnes method in Section 4.9, while in Section 4.10 we discuss its implementation for the Wilson loop integrals.

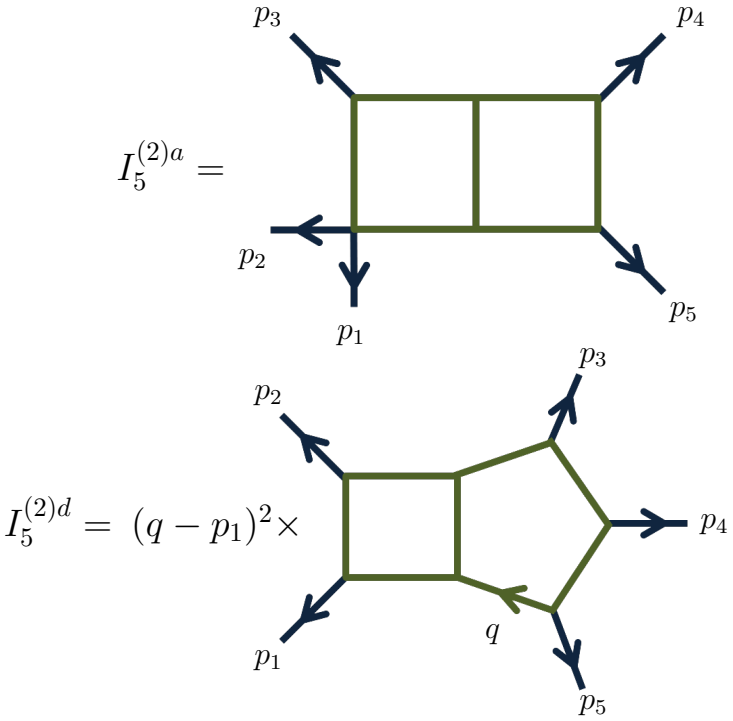

Figure 4.6: *Integrals appearing in the amplitude* $\mathcal{M}_{5+}^{(2)}$. *Note that* $I_5^{(2)d}$ *contains the indicated scalar numerator factor involving* q, *one of the loop momenta.*

4.5 Wilson loops at one loop

As a warmup we will present the calculation of the one-loop polygonal lightlike Wilson loop. This was found in [8] for any number of edges and to all orders in the dimensional regularisation parameter ϵ. Our goal is to calculate the g^2 term in the expansion (4.9) of the Wilson loop evaluated on the lightlike contour shown on the right-hand side of Figure 4.1. The general diagram involves a single gluon propagator with its two endpoints running on the contour $\mathcal{C}_n$ in a way preserving their ordering, as shown on Figure 4.7. We use a real parameter τ to parametrise the points $x^\mu(\tau)$ of the contour $\mathcal{C}_n$. We rewrite the the Wilson loop (4.8) as

$$\mathcal{W}[\mathcal{C}] = \mathrm{Tr}\,\mathcal{P}\exp\left[ig\oint_{\mathcal{C}} d\tau\, A_\mu(x^\mu(\tau))\,\dot{x}^\mu(\tau)\right]. \tag{4.35}$$

Employing Feynman gauge and working in $D = 4 - 2\epsilon_{\mathrm{UV}}$ dimensions, where the ultraviolet dimensional regularisation parameter $\epsilon_{\mathrm{UV}} > 0$, the gluon propagator in

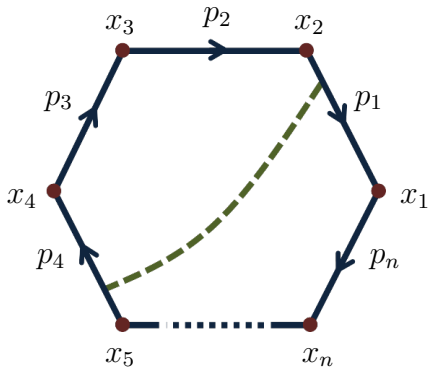

Figure 4.7: *General diagram contributing to the one-loop correction to the expectation value of the Wilson loop. The endpoints of the gluon propagator run on the lightlike polygonal contour in a way preserving their ordering.*

dual momentum space is

$$\begin{aligned} G_{\mu\nu}(z) &= -\frac{\pi^{2-\frac{D}{2}}}{4\pi^2}\Gamma\left(\frac{D}{2}-1\right)\frac{g_{\mu\nu}}{(-z^2+i\varepsilon)^{\frac{D}{2}-1}} \\ &= -\frac{\pi^{\epsilon_{\mathrm{UV}}}}{4\pi^2}\Gamma\left(1-\epsilon_{\mathrm{UV}}\right)\frac{g_{\mu\nu}}{(-z^2+i\varepsilon)^{1-\epsilon_{\mathrm{UV}}}}. \end{aligned} \tag{4.36}$$

We distinguish three different classes of diagrams. The first class is the one where both endpoints of the propagator are attached to the the same lightlike segment p_i as shown in figure 4.8. Using parameters $\tau_1, \tau_2 \in [0,1]$ we rewrite the positions of

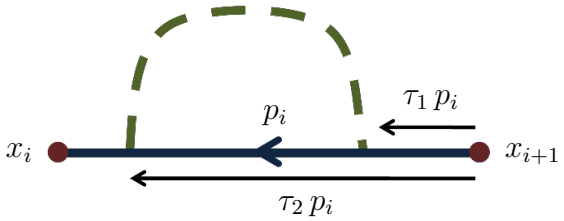

Figure 4.8: *Diagrams where the gluon propagator is attached to a single lightlike segment give a vanishing contribution to the one-loop Wilson loop.*

the endpoints with respect to the cusp x_{i+1}, and the double integral for this diagram gives

$$D_1(p_i) = -\frac{\Gamma(1-\epsilon_{\mathrm{UV}})}{4\pi^{2-\epsilon_{\mathrm{UV}}}}\int_0^1 d\tau_1 \int_0^1 d\tau_2 \frac{p_i^2}{\left[-p_i^2(\tau_2-\tau_1)^2\right]^{1-\epsilon_{\mathrm{UV}}}} = 0, \tag{4.37}$$

which vanishes because $p_i^2 = 0$ and $\epsilon_{\mathrm{UV}} > 0$.

The second class of diagrams is the ones where the gluon propagator is stretching between two adjacent segments p_i and p_{i+1}, as depicted in Figure 4.9. This diagram

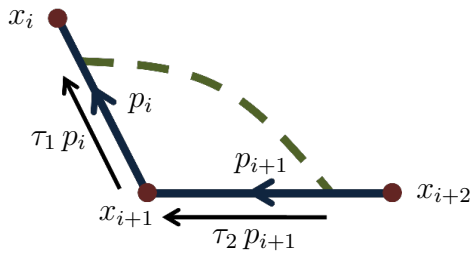

Figure 4.9: *Cusp diagram contributing to the one-loop Wilson loop. Diagrams of this kind are ultraviolet divergent in dual momentum space, while they match the infrared divergent parts of the amplitude in momentum space.*

is a function of the only momentum invariant $s_{i,i+1} = 2p_i \cdot p_{i+1}$. We are again reparametrising the integral into a double integral over $\tau_1, \tau_2 \in [0,1]$ as follows

$$\begin{aligned} D_2(s_{i,i+1}) &= -\frac{\Gamma(1-\epsilon_{\text{UV}})}{4\pi^{2-\epsilon_{\text{UV}}}} \int_0^1 d\tau_1 \int_0^1 d\tau_2 \, \frac{p_i \cdot p_{i+1}}{\left(-\left[p_i\tau_1 + p_{i+1}\tau_2\right]^2\right)^{1-\epsilon_{\text{UV}}}} \\ &= -\frac{\Gamma(1-\epsilon_{\text{UV}})}{4\pi^{2-\epsilon_{\text{UV}}}} \frac{1}{2} \left[-\frac{(-s_{i,i+1})^{\epsilon_{\text{UV}}}}{\epsilon_{\text{UV}}^2}\right]. \end{aligned} \tag{4.38}$$

The last class consists of diagrams where the gluon propagator stretches between non-adjacent lightlike segments p_i and p_j separated by segments with total momentum P, as depicted in Figure 4.10. The integral for this diagram is given by

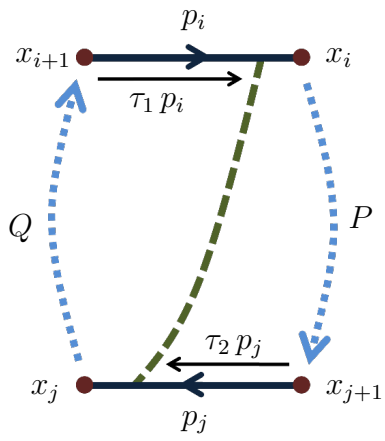

Figure 4.10: *Diagrams where the gluon propagator stretches between non-adjacent lightlike segments give finite contributions to the Wilson loop.*

$$D_3(s,t,u) = -\frac{\Gamma(1-\epsilon_{\rm UV})}{4\pi^{2-\epsilon_{\rm UV}}} \int_0^1 d\tau_1 \int_0^1 d\tau_2 \, \frac{p_i \cdot p_j}{\left(-\left[p_i(1-\tau_1) + P + p_j\tau_2\right]^2\right)^{1-\epsilon_{\rm UV}}}, \quad (4.39)$$

which should be a function of the invariants $s = (p_i + P)^2$, $t = (P + q)^2$ and $u = (p_i + p_j)^2 = 2p_i \cdot p_j$. Due to momentum conservation $p_i + P + p_j + Q = 0$ and $s+t+u = P^2+Q^2$. This integral is finite in four dimensions and its contribution to the Wilson loop can be found to all orders in ϵ and is (up to an ϵ-dependent factor) precisely equal to the finite part of a two-mass easy or one-mass box function [8].

The general one-loop MHV amplitude is made out of two-mass-easy box functions according to (4.2). The relation between the Wilson loop diagram and the corresponding 2me box function is [8]

$$F^{\rm 2me}(p,P,q,Q)\Big|_{\rm finite} = e^{\epsilon\gamma}\frac{\Gamma(1+\epsilon)\Gamma^2(1-\epsilon)}{\Gamma(1-2\epsilon)} \times \mathcal{F}_\epsilon(s,t,P^2,Q^2), \quad (4.40)$$

where

$$\mathcal{F}_\epsilon(s,t,P^2,Q^2) = \int_0^1 d\tau_1\, d\tau_2 \, \frac{u/2}{\left\{-\left[P^2 + (s-P^2)\tau_1 + (t-P^2)\tau_2 + u\tau_1\tau_2\right] - i\varepsilon\right\}^{1+\epsilon}}, \quad (4.41)$$

and $s = (p + P)^2$, $t = (P + q)^2$ and $u = P^2 + Q^2 - s - t$. In Appendix B, we present two different forms for the function $\mathcal{F}_\epsilon$. Notice that we have included an infinitesimal negative imaginary part $-i\varepsilon$ in the denominator which dictates the analytic properties of the integral. This has the opposite sign to the one expected from a propagator term in a Wilson loop in configuration space. On the other hand it has the correct sign for the present application, namely for the duality with amplitudes [114]. One simple way to deal with this is simply to add an identical positive imaginary part to all kinematic invariants

$$s \to s + i\varepsilon, \quad t \to t + i\varepsilon, \quad P^2 \to P^2 + i\varepsilon, \quad Q^2 \to Q^2 + i\varepsilon. \quad (4.42)$$

The general n-point one loop amplitude is given by the sum over precisely these two-mass easy and one-mass box functions (in the case P or Q is massless) [84] to (ϵ^0). Thus the Wilson loop is equal to the amplitude at one loop for any n up to finite order in ϵ only (and up to a kinematic independent factor).

However, at four and five points a much stronger statement can be made. The four-point amplitude and the parity-even part of the five-point amplitude are both given by the sum over zero- and one-mass boxes to all orders in ϵ. Thus the Wilson loop correctly reproduces these one-loop amplitudes to all orders in ϵ. Using the

results in appendix B of [14] we find that the four-point Wilson loop (in a form which is manifestly real in the Euclidean regime $s,t<0$) is given by

$$\begin{aligned} W_4^{(1)} &= \Gamma(1+\epsilon)e^{\epsilon\gamma}\left\{-\frac{1}{\epsilon^2}\left[(-s)^{-\epsilon}+(-t)^{-\epsilon}\right]+\mathcal{F}_\epsilon(s,t,0,0)+\mathcal{F}_\epsilon(t,s,0,0)\right\} \\ &= \Gamma(1+\epsilon)e^{\epsilon\gamma}\left\{-\frac{1}{\epsilon^2}\left[(-s)^{-\epsilon}+(-t)^{-\epsilon}\right]\right. \\ &\qquad +\frac{1}{\epsilon^2}\left(\frac{u}{st}\right)^{\epsilon}\left[\left(\frac{t}{s}\right)^{\epsilon}{}_2\mathrm{F}_1(\epsilon,\epsilon;1+\epsilon;-t/s)\right. \\ &\qquad\qquad \left.\left.+\left(\frac{s}{t}\right)^{\epsilon}{}_2\mathrm{F}_1(\epsilon,\epsilon;1+\epsilon;-s/t)-2\pi\epsilon\cot(\epsilon\pi)\right]\right\}. \end{aligned} \tag{4.43}$$

The generic form of the function $\mathcal{F}_\epsilon$ is given in (B.1) or equivalently in (B.4).

For the five-point amplitude we display a new form which has a simple analytic continuation in all kinematical regimes. It is given in terms of ${}_3\mathrm{F}_2$ hypergeometric functions and is derived in detail in Appendix B of [14]

$$\begin{aligned} W_5^{(1)} &= \sum_{i=1}^{5}\Gamma(1+\epsilon)e^{\epsilon\gamma}\left[-\frac{1}{2\epsilon^2}(-s_{i,i+1})^{-\epsilon}+\mathcal{F}_\epsilon(s_{i,i+1},s_{i+1,i+2},s_{i+3,i+4},0)\right] \\ &= \sum_{i=1}^{5}\Gamma(1+\epsilon)e^{\epsilon\gamma}\left\{-\frac{1}{2\epsilon^2}(-s_{i,i+1})^{-\epsilon}\right. \\ &\qquad -\frac{1}{2}\left(\frac{s_{i+3,i+4}-s_{i,i+1}-s_{i+1,i+2}}{s_{i,i+1}s_{i+1,i+2}}\right)^{\epsilon} \\ &\qquad \times\left[\tfrac{s_{i+3,i+4}-s_{i,i+1}}{s_{i+1,i+2}}\,{}_3\mathrm{F}_2\left(1,1,1+\epsilon;2,2;\tfrac{s_{i+3,i+4}-s_{i,i+1}}{s_{i+1,i+2}}\right)\right. \\ &\qquad\quad +\tfrac{s_{i+3,i+4}-s_{i+1,i+2}}{s_{i,i+1}}\,{}_3\mathrm{F}_2\left(1,1,1+\epsilon;2,2;\tfrac{s_{i+3,i+4}-s_{i+1,i+2}}{s_{i,i+1}}\right)+\frac{H_{-\epsilon}}{\epsilon} \\ &\qquad\quad -\tfrac{(s_{i+3,i+4}-s_{i,i+1})(s_{i+3,i+4}-s_{i+1,i+2})}{s_{i,i+1}s_{i+1,i+2}} \\ &\qquad\qquad \left.\left.\times\,{}_3\mathrm{F}_2\left(1,1,1+\epsilon;2,2;\tfrac{(s_{i+3,i+4}-s_{i,i+1})(s_{i+3,i+4}-s_{i+1,i+2})}{s_{i,i+1}s_{i+1,i+2}}\right)\right]\right\}, \end{aligned} \tag{4.44}$$

where H_n is the n^{th}-harmonic number. Using hypergeometric identities one can show that (up to the prefactor) the four- and five-sided Wilson loops, (4.43) and (4.44), are equal to the four-point and the (parity-even part of the) five-point amplitudes of (4.28) and (4.31).

The precise relation between the Wilson loop and the amplitude is

$$W_4^{(1)}=\frac{\Gamma(1-2\epsilon)}{\Gamma^2(1-\epsilon)}\mathcal{M}_4^{(1)}, \qquad\qquad W_5^{(1)}=\frac{\Gamma(1-2\epsilon)}{\Gamma^2(1-\epsilon)}\mathcal{M}_{5+}^{(1)}, \tag{4.45}$$

where $\mathcal{M}_4^{(1)}$ is the one-loop four-point amplitude and $\mathcal{M}_{5+}^{(1)}$ is the parity-even part

of the five-point amplitude.

4.6 Dual conformal symmetry

Having demonstrated the duality between MHV amplitudes and polygonal lightlike Wilson loops at one-loop, we move on to discuss the 'dual conformal symmetry', a symmetry shared by the two objects appearing on the duality. This is a symmetry under the conformal group acting in the dual momentum space x defined in (2.25). A lightlike Wilson loop is manifestly invariant under dual conformal transformations in four dimensions, as the conformal group maps null vectors to null vectors. However, due to the presence of ultraviolet divergences, we are forced to perform dimensional regularisation and work in $D = 4 - 2\epsilon_{\rm UV}$ dimensions and the invariance is broken.

The amplitude and the Wilson loop contain divergences in the infrared and ultraviolet respectively. We write

$$\ln \mathcal{M}_n = \ln Z_n + \ln F_n + \mathcal{O}(\epsilon), \tag{4.46}$$

$$\ln W_n = \ln Z_n^{(\rm WL)} + \ln F_n^{(\rm WL)} + \mathcal{O}(\epsilon_{\rm UV}), \tag{4.47}$$

where the Z terms contain all the poles in the dimensional regulators $\epsilon \equiv \epsilon_{\rm IR}$ and $\epsilon_{\rm UV}$, and the F terms contain the finite parts as $\epsilon \to 0$. The original content of the conjectured MHV amplitude/Wilson loop duality was the matching of the finite parts

$$\ln F_n = \ln F_n^{(\rm WL)} + \text{const.} \tag{4.48}$$

In the following sections we will present results suggesting that the duality holds even beyond the finite terms, i.e. at $\mathcal{O}(\epsilon)$.

Returning to the topic of dual conformal symmetry, the generators of the $SO(2,4)$ conformal transformations are: rotations $\mathbb{M}^{\mu\nu}$, dilatations $\mathbb{D}$, translations $\mathbb{P}^\mu$ and conformal boosts $\mathbb{K}^\mu$. These transformations act on fundamental (gauge, gaugino, scalars) fields $\phi_I(x)$ with conformal weight d_ϕ and Lorentz indices I, while their generators are [10]

$$\begin{aligned}
\mathbb{M}^{\mu\nu}\phi_I &= (x^\mu\partial^\nu - x^\nu\partial^\mu)\phi_I + (m^{\mu\nu})_I{}^J\phi_J, \\
\mathbb{D}\,\phi_I &= x\cdot\partial\,\phi_I + d_\phi\,\phi_I, && (4.49)\\
\mathbb{P}^\mu\phi_I &= \partial^\mu\,\phi_I, && (4.50)\\
\mathbb{K}^\mu\phi_I &= \left(2x^\mu x\cdot\partial - x^2\partial^\mu\right)\phi_I + 2x^\mu\,d_\phi\,\phi_I + 2x_\nu(m^{\mu\nu})_I{}^J\phi_J,
\end{aligned}$$

where $m^{\mu\nu}$ is the generator of spin rotations, e.g., $m^{\mu\nu} = 0$ for a scalar field and $(m^{\mu\nu})_\lambda{}^\rho = g^{\nu\rho}\delta^\mu_\lambda - g^{\mu\rho}\delta^\nu_\lambda$ for a gauge field.

In dimensionally regularised $\mathcal{N} = 4$ super Yang-Mills, the Wilson loop $\langle W_n \rangle$ is given by the following functional integral

$$\langle W_n \rangle = \int \mathcal{D}A\, \mathcal{D}\lambda\, \mathcal{D}\phi\; e^{iS_\epsilon[A,\,\lambda,\,\phi]}\, \mathrm{Tr}\left[\mathcal{P}\mathrm{exp}\left(i \oint_{\mathcal{C}_n} dx \cdot A(x)\right)\right], \tag{4.51}$$

where the integration goes over gauge fields A, gauginos λ, and scalars ϕ. The action is given by

$$S_\epsilon = \frac{1}{g^2\mu^{2\epsilon}} \int d^D x\; \mathcal{L}(x), \tag{4.52}$$

and the Lagrangian is schematically

$$\mathcal{L} = \mathrm{Tr}\left[-\frac{1}{2}F^2_{\mu\nu}\right] + \text{gaugino} + \text{scalars} + \text{gauge fixing} + \text{ghosts}. \tag{4.53}$$

In (4.52), μ is the normalisation scale and all fields are redefined in a way such that the coupling constant g is not present inside the Lagrangian $\mathcal{L}(x)$. This way, the canonical dimension of the gauge fields $A^\mu(x)$ is preserved, and therefore, the conformal invariance of the path-ordered exponential entering the functional integral in (4.51) is also preserved. However, since we are working in D rather than four dimensions, due to the presence of the integration measure $\int d^D x$ in (4.52), the action S_ϵ is not invariant under dilatations and conformal boosts, which yields an anomaly in the the Ward identities. The conformal Ward identities can be derived following standard methods [115, 116, 117, 118, 119].

The action has a non-vanishing variation under dilatations [10]

$$\delta_{\mathbb{D}} S_\epsilon = -\frac{2\epsilon}{g^2\mu^{2\epsilon}} \int d^D x\; \mathcal{L}(x). \tag{4.54}$$

As a result, the action of the dilatations generator on $\langle W_n \rangle$, as defined in (4.51), yields an anomalous term given by

$$\mathbb{D}\,\langle W_n \rangle = \sum_{i=1}^{n} (x_i \cdot \partial_i)\;\langle W_n \rangle = -\frac{2i\epsilon}{g^2\mu^{2\epsilon}} \int d^D x\; \langle \mathcal{L}(x) W_n \rangle. \tag{4.55}$$

Similarly, the anomalous term in the action of the special conformal generator is

$$\mathbb{K}^\nu \langle W_n \rangle = \sum_{i=1}^{n} (2x_i^\nu\, x_i \cdot \partial_i - x_i^2 \partial_i^\nu)\langle W_n \rangle = -\frac{4i\epsilon}{g^2\mu^{2\epsilon}} \int d^D x\; x^\nu\; \langle \mathcal{L}(x) W_n \rangle. \tag{4.56}$$

In terms of the logarithm of the Wilson loop, (4.55) and (4.56) give

$$\mathbb{D}\ln\langle W_n\rangle = -\frac{2i\epsilon}{g^2\mu^{2\epsilon}}\int d^D x\ \frac{\langle\mathcal{L}(x)W_n\rangle}{\langle W_n\rangle} \tag{4.57}$$

$$\mathbb{K}^\nu\ln\langle W_n\rangle = -\frac{4i\epsilon}{g^2\mu^{2\epsilon}}\int d^D x\ x^\nu\ \frac{\langle\mathcal{L}(x)W_n\rangle}{\langle W_n\rangle}. \tag{4.58}$$

These anomalies formally vanish as $\epsilon\to 0$, but when inserted in loops, they survive because of divergent terms with powers of $1/\epsilon$.

In the limit $\epsilon\to 0$, the special conformal Ward identity takes the form [9]

$$\sum_{i=1}^{n}\left(2x_i^\nu\ x_i\cdot\partial_i - x_i^2\partial_i^\nu\right)\ln F_n = \frac{1}{2}\Gamma_{\text{cusp}}(a)\sum_{i=1}^{n}\ln\frac{x_{i,i+2}^2}{x_{i-1,i+1}^2}\ x_{i,i+1}^\nu, \tag{4.59}$$

where $\Gamma_{\text{cusp}}^{(l)}$ are the expansion coefficients of the cusp anomalous dimension

$$\Gamma_{\text{cusp}}(a) = \sum_{l\geq 1} a^l\,\Gamma_{\text{cusp}}^{(l)} = 2a - \frac{\pi^2}{3}a^2 + \mathcal{O}(a^3). \tag{4.60}$$

The conformal Ward identity (4.59) restricts the form of finite part of the Wilson loop W_n. For $n=4,5$, (4.59) has a unique solution up to an additive constant [10]

$$\ln F_4 = \frac{1}{4}\Gamma_{\text{cusp}}(a)\ln^2\left(\frac{x_{13}^2}{x_{24}^2}\right) + \text{const}, \tag{4.61}$$

$$\ln F_5 = -\frac{1}{8}\Gamma_{\text{cusp}}(a)\sum_{i=1}^{5}\ln\left(\frac{x_{i,i+2}^2}{x_{i,i+3}^2}\right)\ln\left(\frac{x_{i+1,i+3}^2}{x_{i+2,i+4}^2}\right) + \text{const}. \tag{4.62}$$

This can be easily verified by making use of the identity $\mathbb{K}^\mu x_{ij}^2 = 2(x_i^\mu + x_j^\mu)x_{ij}^2$. The solutions (4.61) and (4.62) give exactly the form of the BDS ansatz [107] for the helicity-blind part $\mathcal{M}_n$ of the MHV amplitude, discussed in Section 4.1.

At four and five points, one cannot build any conformal invariants out of the x_i's that are lightlike separated $x_{i,i+1}^2 = 0$, and as a result, the form of F_4 and F_5 are fixed up to an additive constant. For $n>5$ one can build conformal cross-ratios that have the form

$$\frac{x_{ij}^2 x_{kl}^2}{x_{ik}^2 x_{jl}^2}. \tag{4.63}$$

For example, at six points there are three cross-ratios

$$u_1 = \frac{x_{13}^2 x_{46}^2}{x_{14}^2 x_{36}^2}, \qquad u_2 = \frac{x_{24}^2 x_{15}^2}{x_{25}^2 x_{14}^2}, \qquad u_3 = \frac{x_{35}^2 x_{26}^2}{x_{36}^2 x_{25}^2}. \tag{4.64}$$

The general solution of the Ward identity for $n > 5$ will contain an arbitrary function of the conformal cross-ratios.

Superamplitudes are invariant under a superconformal symmetry acting in dual momentum space termed 'dual superconformal symmetry' [68]. This symmetry has been explained from the string theory point of view [120, 121] using a T-duality of the superstring theory on $AdS_5 \times S_5$ which involves a bosonic T-duality [17] together with a new fermionic T-duality. The T-duality exchanges the original with the dual superconformal symmetries.

In order study the dual superconformal symmetry, we express any amplitude in terms of the dual momenta x_i introduced in (2.25) and their supersymmetric partners $\theta_i^{A\alpha}$ defined in a similar fashion

$$\eta_i^A \, \lambda_i^\alpha = \theta_i^{A\alpha} - \theta_{i+1}^{A\alpha}. \tag{4.65}$$

Special conformal transformations can be obtained by an inversion followed by a translation, and a further inversion. Combining inversions with supersymmetry transformations, one generates all the superconformal transformations. At tree level, the dual supersymmetries are either manifest or they are related to ordinary special superconformal symmetries [68], and therefore it suffices to show invariance under dual inversions. Under inversions, the dual coordinates transform as follows [68]

$$x_{i,\alpha\dot\beta} \to \frac{x_{i,\beta\dot\alpha}}{x_i^2}, \qquad \theta_i^{A\alpha} \to \left(x_i^{-1}\right)^{\dot\alpha\beta} \theta_{i,\beta}^A. \tag{4.66}$$

It is easy to show that the MHV superamplitude transforms covariantly under inversions

$$A_{\rm MHV}(1,2,\ldots,n) \to A_{\rm MHV}(1,2,\ldots,n) \prod_{k=1}^{n} x_k^2. \tag{4.67}$$

Using supersymmetric BCFW recursion it has been shown that all tree-level superamplitudes transform in the same fashion [46].

4.7 Wilson loops at two loops

In this section, we present all the integrals making up the logarithm of the n-sided Wilson loop at two loops [105], in a form appropriate for numeric evaluation in `MATHEMATICA` using the package `MB` [112]. Notice that all the integrands are rewritten as functions of the momentum invariants only, i.e. squares of sums of consecutive momenta. Moreover, via appropriate changes of variables, all integrations are to be

performed on the interval $[0,1]$. For each of these functions, we list all symmetries under permutations of its arguments. Using these symmetries, allows us to reduce the actual number of diagrams that need to be evaluated.

We remind the reader that, in order to regularise the UV divergences of Wilson loops, we work in $D = 4 - 2\epsilon_{\rm UV}$ dimensions, where $\epsilon_{\rm UV} > 0$. The following diagrams are written in terms of the ultraviolet regularisation parameter $\epsilon_{\rm UV}$. To facilitate the comparison between Wilson loops and scattering amplitudes, the numeric results we present later on have been expressed in terms of the infrared regularisation parameter $\epsilon < 0$ used in scattering amplitudes. The two parameters are related simply by $\epsilon_{\rm UV} = -\epsilon$.

The complete two-loop contribution to the logarithm of the n-sided polygonal Wilson loop is given by [105]

$$
\begin{aligned}
w_n^{(2)} = \mathcal{C} \Bigg\{ & \sum_{1\le i<j<k\le n} \Big[f_H(p_i,p_j,p_k;Q_{jk},Q_{ki},Q_{ij}) + f_C(p_i,p_j,p_k;Q_{jk},Q_{ki},Q_{ij}) \\
& \qquad + f_C(p_j,p_k,p_i;Q_{ki},Q_{ij},Q_{jk}) + f_C(p_k,p_i,p_j;Q_{ij},Q_{jk},Q_{ki}) \Big] \\
& + \sum_{1\le i<j\le n} \Big[f_X(p_i,p_j;Q_{ji},Q_{ij}) + f_Y(p_i,p_j;Q_{ji},Q_{ij}) + f_Y(p_j,p_i;Q_{ij},Q_{ji}) \Big] \\
& + \sum_{1\le i<k<j<l\le n} (-1/2) f_P(p_i,p_j;Q_{ji},Q_{ij}) f_P(p_k,p_l;Q_{lk},Q_{kl}) \Bigg\} . \qquad (4.68)
\end{aligned}
$$

This expression involves five different classes of diagrams that we denote by f_H,f_C,f_X,f_Y and f_P, and we present in detail in the following sections. The summations are such that, for each diagram, and preserving the ordering of the external momenta, each non-equivalent permutation of the arguments appears only once.

4.7.1 Hard diagram

The first integral corresponds to the hard diagram $f_H(p_1,p_2,p_3;Q_1,Q_2,Q_3)$ that contains three gluon propagators, that meet at a three-point vertex, and they are attached to three different lightlike segments. These segments correspond to the momenta p_1, p_2 and p_3 and are separated by three sums of momenta Q_1, Q_2 and Q_3, as shown in Figure 4.11. Depending on the number of lightlike segments between each pair of p's, the corresponding Q can be zero, massless or even massive. The integral for the hard diagram in its general form is given in Appendix B of [105].

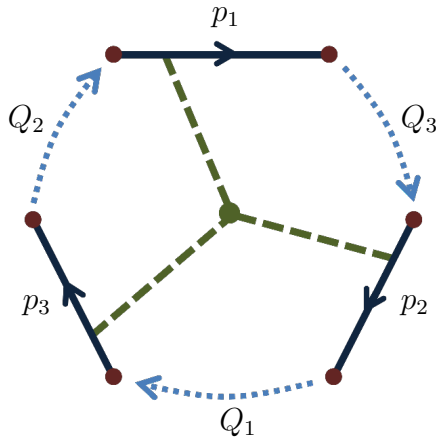

Figure 4.11: *The hard diagram* $f_H(p_1, p_2, p_3; Q_1, Q_2, Q_3)$.

We rewrite it as

$$f_H(p_1, p_2, p_3; Q_1, Q_2, Q_3) = \frac{1}{8}\frac{\Gamma(2-2\epsilon_{\rm UV})}{\Gamma(1-\epsilon_{\rm UV})^2}\int_0^1 (\prod_{i=1}^3 d\tau_i)\int_0^1 (\prod_{i=1}^3 d\alpha_i)\,\delta(1-\sum_{i=1}^3\alpha_i)(\alpha_1\alpha_2\alpha_3)^{-\epsilon_{\rm UV}}\frac{\mathcal{N}}{\mathcal{D}^{2-2\epsilon_{\rm UV}}}. \tag{4.69}$$

The numerator and denominator, written as functions of the momentum invariants, are given by

$$\begin{aligned}\mathcal{D} = -\alpha_1\alpha_2\big[&(p_1+Q_3+p_2)^2(1-\tau_1)\tau_2 + (p_1+Q_3)^2(1-\tau_1)(1-\tau_2)\\ &+(Q_3+p_2)^2\tau_1\tau_2 + Q_3^2\tau_1(1-\tau_2)\big] + \text{cyclic}(1,2,3),\end{aligned} \tag{4.70}$$

and

$$\begin{aligned}\mathcal{N} = &\,2\left[2(p_1p_2)(p_3Q_3) - (p_2p_3)(p_1Q_3) - (p_1p_3)(p_2Q_3)\right]\alpha_1\alpha_2\\ &+2(p_1p_2)(p_3p_1)\left[\alpha_1\alpha_2(1-\tau_1) + \alpha_3\alpha_1\tau_1\right] + \text{cyclic}(1,2,3),\end{aligned} \tag{4.71}$$

where

$$\begin{aligned}2p_ip_{i+1} &= -(p_i+Q_{i+2})^2 + Q_{i+2}^2 - (Q_{i+2}+p_{i+1})^2 + (Q_i+p_{i+2}+Q_{i+1})^2,\\ 2p_iQ_i &= -(p_i+Q_{i+2}+p_{i+1})^2 + (Q_{i+2}+p_{i+1})^2\\ &\quad - (p_{i+2}+Q_{i+1}+p_i)^2 + (p_{i+2}+Q_{i+1})^2,\\ 2p_iQ_j &= (p_i+Q_j)^2 - Q_j^2,\end{aligned} \tag{4.72}$$

and in (4.70) and (4.71), we are summing over cyclic permutations of the set of indices $\{1, 2, 3\}$. We get rid of the delta function in (4.69) by setting $\alpha_1 \to 1 - \zeta$, $\alpha_2 \to \zeta\rho$ and $\alpha_3 \to \zeta(1 - \rho)$, while we pick up a Jacobian of ζ. Finally, we are left with an integral over the τ_i's, ζ and ρ in the interval $[0, 1]$.

The hard diagram is symmetric under cyclic permutations of its arguments and reflections

$$f_H(p_1, p_2, p_3; Q_1, Q_2, Q_3) = f_H(p_3, p_1, p_2; Q_3, Q_1, Q_2), \tag{4.73}$$

$$f_H(p_1, p_2, p_3; Q_1, Q_2, Q_3) = f_H(p_3, p_2, p_1; Q_3, Q_2, Q_1). \tag{4.74}$$

4.7.2 Curtain diagram

The next diagram we encounter is the curtain diagram $f_C(p_1, p_2, p_3; Q_1, Q_2, Q_3)$, where two gluon propagators stretch between two pairs of lightlike segments that share one side, as shown in Figure 4.12. As three lightlike sides in this diagram, the

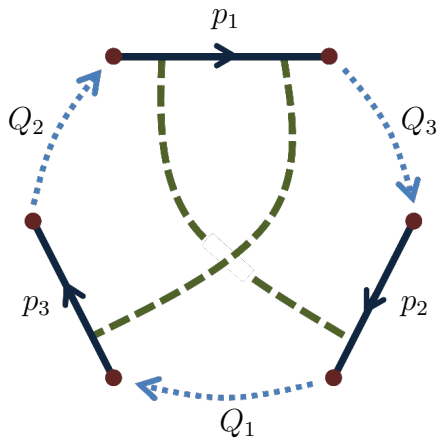

Figure 4.12: *The curtain diagram* $f_C(p_1, p_2, p_3; Q_1, Q_2, Q_3)$.

labelling is identical to the hard diagram case. However, the curtain diagram is less symmetric and the first of the arguments, namely p_1 labels the common side. The integrations for the two endpoints on the common side are such that the ordering of these endpoints is preserved. This integral is given in Appendix C of [105]. After trading σ_1 for ρ via $\sigma_1 \to \tau_1\rho$, we convert this integral to one where all integrations are in the interval $[0, 1]$. We have

$$f_C(p_1, p_2, p_3; Q_1, Q_2, Q_3) = -\frac{1}{2}\int_0^1 \left(\prod_1^3 d\tau_i\right) \int_0^1 d\rho\, \tau_1\, \mathcal{N}\, \frac{1}{(\mathcal{D}_1)^{1-\epsilon_{\rm UV}}}\, \frac{1}{(\mathcal{D}_2)^{1-\epsilon_{\rm UV}}}, \tag{4.75}$$

where the factor τ_1 is just the Jacobian from the change of variables. The numerator written in terms of momenta invariants is

$$\begin{aligned}\mathcal{N} = \frac{1}{4}\Big(&- (p_1+Q_3)^2 + Q_3^2 - (Q_3+p_2)^2 + (Q_1+p_3+Q_2)^2\Big)\\ &\times\Big(- (p_3+Q_2)^2 + Q_2^2 - (Q_2+p_1)^2 + (Q_3+p_2+Q_1)^2\Big)\,,\end{aligned} \tag{4.76}$$

while the two terms appearing on the denominator are

$$\begin{aligned}\mathcal{D}_1 = &-(p_1+Q_3+p_2)^2(1-\tau_1)\tau_2 - (p_1+Q_3+p_2)^2\tau_1(1-\rho)\tau_2\\ &- (p_1+Q_3)^2(1-\tau_1)(1-\tau_2) - (p_1+Q_3)^2\tau_1(1-\rho)(1-\tau_2)\\ &- (Q_3+p_2)^2\tau_1\rho\tau_2 - Q_3^2\tau_1\rho(1-\tau_2),\end{aligned} \tag{4.77}$$

$$\begin{aligned}\mathcal{D}_2 = &-(p_3+Q_2+p_1)^2\tau_1\tau_3 - (Q_2+p_1)^2\tau_1(1-\tau_3)\\ &- (p_3+Q_2)^2(1-\tau_1)\tau_3 - Q_2^2(1-\tau_1)(1-\tau_3).\end{aligned} \tag{4.78}$$

The curtain diagram is symmetric under a simultaneous exchange of labels $2 \leftrightarrow 3$ on both the p's and the Q's

$$f_C(p_1,p_2,p_3;Q_1,Q_2,Q_3) = f_C(p_1,p_3,p_2;Q_1,Q_3,Q_2). \tag{4.79}$$

4.7.3 Cross diagram

In the cross diagram $f_X(p_1,p_2;Q_1,Q_2)$, two lightlike segments are involved and two gluon propagators strech between them as shown in Figure 4.13. The two segments

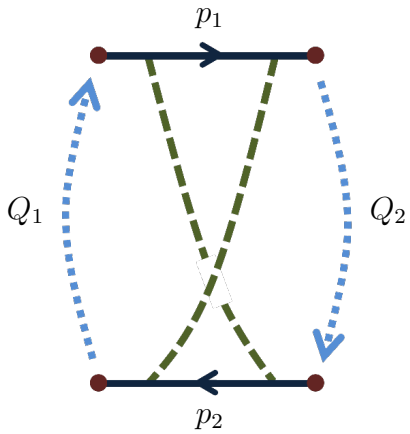

Figure 4.13: *The cross diagram* $f_X(p_1,p_2;Q_1,Q_2)$.

correspond to the momenta p_1 and p_2 and they are separated by the sum of momenta

Q_1 and Q_2 that can be zero, massless or massive. Similarly to the curtain diagram case, the endpoints on both segments are ordered. The integral for this diagram is given in Appendix D of [105]. We perform the changes of variables $\tau_1 \to \sigma_1\rho_1$ and $\sigma_2 \to \tau_2\rho_2$, generating the Jacobian $\sigma_1\tau_2$, and arriving at the following expression for cross integral

$$f_X(p_1,p_2;Q_1,Q_2) = -\frac{1}{2}\int_0^1 d\sigma_1 \int_0^1 d\tau_2 \int_0^1 d\rho_1 d\rho_2\, \sigma_1\tau_2\, \mathcal{N}\, \frac{1}{(\mathcal{D}_1)^{1-\epsilon_{\rm UV}}}\, \frac{1}{(\mathcal{D}_2)^{1-\epsilon_{\rm UV}}}. \tag{4.80}$$

The numerator written in terms of momenta invariants is

$$\mathcal{N} = \frac{1}{4}\Big(-(Q_1+p_1)^2 + Q_1^2 - (p_1+Q_2)^2 + Q_2^2\Big)^2, \tag{4.81}$$

while the two terms appearing on the denominator are

$$\begin{aligned}\mathcal{D}_1 = &-(Q_1+p_1)^2(1-\sigma_1)\tau_2\rho_2 - (p_1+Q_2)^2\sigma_1(1-\tau_2) - (p_1+Q_2)^2\sigma_1\tau_2(1-\rho_2)\\ &- Q_1^2\sigma_1\tau_2\rho_2 - Q_2^2(1-\sigma_1)(1-\tau_2) - Q_2^2(1-\sigma_1)\tau_2(1-\rho_2),\end{aligned} \tag{4.82}$$

$$\begin{aligned}\mathcal{D}_2 = &-(Q_1+p_1)^2(1-\sigma_1)\tau_2 - (Q_1+p_1)^2\sigma_1(1-\rho_1)\tau_2 - (p_1+Q_2)^2\sigma_1\rho_1(1-\tau_2)\\ &- Q_1^2\sigma_1\rho_1\tau_2 - Q_2^2(1-\sigma_1)(1-\tau_2) - Q_2^2\sigma_1(1-\rho_1)(1-\tau_2).\end{aligned} \tag{4.83}$$

The cross diagram is symmetric under the exchange of $p_1 \leftrightarrow p_2$ or $Q_1 \leftrightarrow Q_2$

$$f_X(p_1,p_2;Q_1,Q_2) = f_X(p_2,p_1;Q_1,Q_2), \tag{4.84}$$

$$f_X(p_1,p_2;Q_1,Q_2) = f_X(p_1,p_2;Q_2,Q_1). \tag{4.85}$$

4.7.4 Y and self-energy diagram

The next diagram we encounter is the Y diagram, which is similar to the hard diagram presented in Section 4.7.1, with the only difference that two propagators are attached to the same segment as shown in the first diagram of Figure 4.14. Part of this integral is exactly cancelled by half of the second diagram on Figure 4.14, which corresponds to the one-loop self-energy correction to the gluon propagator (see Appendix E of [105]). What we are left with is what we will refer to as the Y diagram $f_Y(p_1,p_2;Q_1,Q_2)$. The other half of the self-energy diagram cancels the corresponding term in the upside-down Y diagram $f_Y(p_2,p_1;Q_2,Q_1)$. The integral

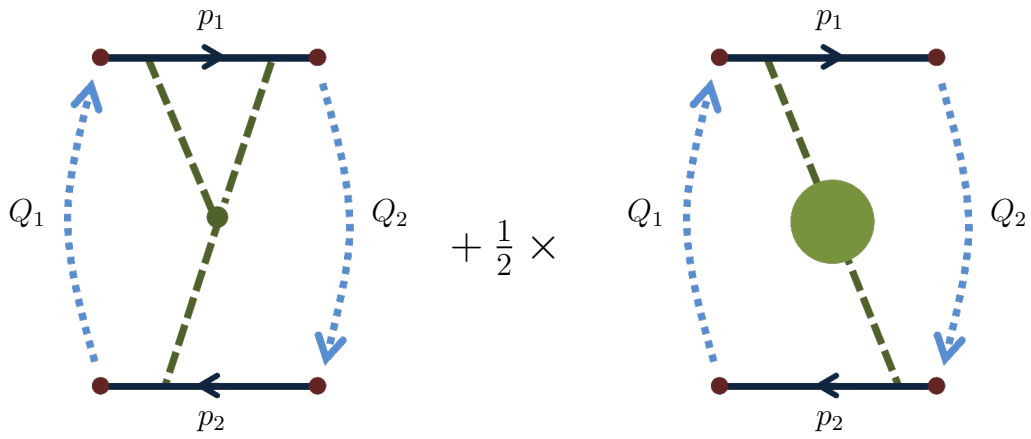

Figure 4.14: *The Y diagram and half self-energy diagram packaged together into* $f_Y(p_1, p_2; Q_1, Q_2)$.

for the curtain diagram contains two terms and it reads

$$f_Y(p_1,p_2;Q_1,Q_2) = \frac{1}{8\epsilon_{\rm UV}}\frac{\Gamma(1-2\epsilon_{\rm UV})}{\Gamma(1-\epsilon_{\rm UV})^2}\int_0^1 d\sigma\int_0^1 d\tau_1\int_0^1 d\tau_2 \\ \times(-\sigma^{-\epsilon_{\rm UV}})(1-\sigma)^{-\epsilon_{\rm UV}}\,\mathcal{N}\left(\frac{1}{(\mathcal{D}_1)^{1-2\epsilon_{\rm UV}}}+\frac{1}{(\mathcal{D}_2)^{1-2\epsilon_{\rm UV}}}\right). \tag{4.86}$$

The common numerator written in terms of the momenta invariants is

$$\mathcal{N} = \frac{1}{2}\Big(-(Q_1+p_1)^2+Q_1^2-(p_1+Q_2)^2+Q_2^2\Big), \tag{4.87}$$

while the two denominator terms are

$$\mathcal{D}_1 = -(Q_1+p_1)^2\sigma\tau_1(1-\tau_2)-(p_2+Q_1)^2(1-\sigma)\tau_2-(p_2+Q_1)^2\sigma(1-\tau_1)\tau_2 \\ -Q_1^2(1-\sigma)(1-\tau_2)-Q_1^2\sigma](1-\tau_1)(1-\tau_2)-Q_2^2\sigma\tau_1\tau_2, \tag{4.88}$$

$$\mathcal{D}_2 = -(p_1+Q_2)^2\sigma\tau_1(1-\tau_2)-(Q_2+p_2)^2(1-\sigma)\tau_2-(Q_2+p_2)^2\sigma(1-\tau_1)\tau_2 \\ -Q_2^2(1-\sigma])(1-\tau_2)-Q_2^2\sigma(1-\tau_1)(1-\tau_2)-Q_1^2\sigma\tau_1\tau_2. \tag{4.89}$$

As there are two propagators attached to the segment p_1, while only one to the segment p_2, the Y diagram is not symmetric under $p_1 \leftrightarrow p_2$, but only under $Q_1 \leftrightarrow Q_2$

$$f_Y(p_1,p_2;Q_1,Q_2) = f_Y(p_1,p_2;Q_2,Q_1). \tag{4.90}$$

4.7.5 Factorised cross diagram

Finally, the factorised cross diagram involves four different lightlike segments, that are connected in pairs by two gluon propagators as shown in Figure 4.15. The

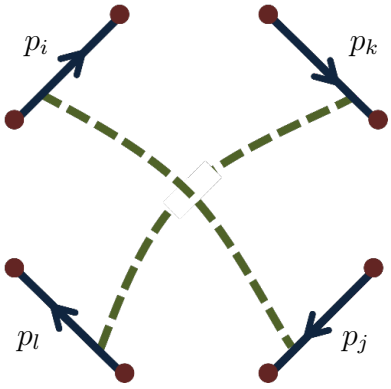

Figure 4.15: *The factorised cross diagram.*

first propagator stretches between the segments p_i and p_j that are separated by the sum of momenta Q_{ij} and Q_{ji}, while the second one stretches between p_k and p_l separated by Q_{kl} and Q_{lk}. This contribution is given by $-1/2$ times the product of two one-loop diagrams

$$-\frac{1}{2} f_P(p_i, p_j; Q_{ji}, Q_{ij}) f_P(p_k, p_l; Q_{lk}, Q_{kl}). \tag{4.91}$$

The one-loop integral f_P is given by

$$f_P(p, q; P, Q) = \int_0^1 d\tau_1 d\tau_2 \frac{\mathcal{N}}{\mathcal{D}^{1-\epsilon_{\rm UV}}}. \tag{4.92}$$

The numerator and denominator in the integrand of (4.92), written in terms of momenta invariants, are given by

$$\mathcal{N} = \frac{1}{2}\left(P^2 + Q^2 - (p+P)^2 - (P+q)^2,\right), \tag{4.93}$$

and

$$\mathcal{D} = -P^2(1-\tau_1)(1-\tau_2) - (p+P)^2\tau_1(1-\tau_2) - (P+q)^2\tau_2(1-\tau_1) - Q^2\tau_1\tau_2. \tag{4.94}$$

Similarly to the cross diagram, f_P is symmetric under the exchange of $p_1 \leftrightarrow p_2$ or $Q_1 \leftrightarrow Q_2$

$$\begin{aligned} f_P(p_1,p_2;Q_1,Q_2) &= f_P(p_2,p_1;Q_1,Q_2), \\ f_P(p_1,p_2;Q_1,Q_2) &= f_P(p_1,p_2;Q_2,Q_1). \end{aligned} \tag{4.95}$$

4.8 Four- and five-sided Wilson loop at $\mathcal{O}(\epsilon)$

The computation of the four-point two-loop Wilson loop up to (ϵ^0) was first performed in [9]. In appendix A of [14] we give expressions for all the contributing diagrams to all orders in ϵ in all cases except for the hard diagram, which we give up to and including terms of $\mathcal{O}(\epsilon)$. Summing up the contributions from all these diagrams we obtain the result for the two-loop four-point Wilson loop to $\mathcal{O}(\epsilon)$. This is displayed in (4.96).

Our final result for the four-point Wilson loop at two loops expanded up to and including terms of $\mathcal{O}(\epsilon)$ is

$$w_4^{(2)} = \mathcal{C} \times \left[(-s)^{-2\epsilon} + (-t)^{-2\epsilon}\right] \times \left[\frac{w_2}{\epsilon^2} + \frac{w_1}{\epsilon} + w_0 + w_{-1}\epsilon + \mathcal{O}(\epsilon^2)\right], \tag{4.96}$$

where

$$w_2 = \frac{\pi^2}{48}, \tag{4.97}$$

$$w_1 = -\frac{7\zeta_3}{8}, \tag{4.98}$$

$$w_0 = -\frac{\pi^2}{48}\left(\log^2 x + \pi^2\right) + \frac{\pi^4}{144} = -\frac{\pi^2}{48}\left(\log^2 x + \frac{2}{3}\pi^2\right), \tag{4.99}$$

$$\begin{aligned} w_{-1} = -\frac{1}{1440}\Big[&-46\pi^4 \log x - 10\pi^2 \log^3 x + 75\pi^4 \log(1+x) + 90\pi^2 \log^2 x \log(1+x) \\ &+ 15\log^4 x \log(1+x) + 240\pi^2 \log x\, \mathrm{Li}_2(-x) + 120 \log^3 x\, \mathrm{Li}_2(-x) \\ &- 300\pi^2 \mathrm{Li}_3(-x) - 540 \log^2 x\, \mathrm{Li}_3(-x) + 1440 \log x\, \mathrm{Li}_4(-x) \\ &- 1800 \mathrm{Li}_5(-x) - 1560\pi^2\zeta_3 - 1260 \log^2 x\, \zeta_3 + 5940\zeta_5\Big], \end{aligned} \tag{4.100}$$

and

$$\mathcal{C} := 2\left[\Gamma(1+\epsilon)e^{\gamma\epsilon}\right]^2 = 2\left(1 + \zeta_2\epsilon^2 - \frac{2}{3}\zeta_3\epsilon^3\right) + \mathcal{O}(\epsilon^4). \tag{4.101}$$

We recall that $x = t/s$.

We would like to point out the simplicity of our result (4.96). Specifically, (4.97)-

(4.100) are expressed only in terms of standard polylogarithms. Harmonic polylogarithms and Nielsen polylogarithms are present in the expressions of separate Wilson loop diagrams, as can be seen in appendix A of [14], but cancel after summing all contributions.

Using the result (4.96) and the one-loop expression for the Wilson loop, one can work out the expression for the remainder function at $\mathcal{O}(\epsilon)$, as defined in (4.15) and (4.18). Our result is

$$\begin{aligned}\mathcal{E}^{(2)}_{4,\mathrm{WL}} = \frac{1}{360}\Big[&16\pi^4\log x - 15\pi^4\log(1+x) - 30\pi^2\log^2 x\log(1+x)\\ &- 15\log^4 x\log(1+x) - 120\pi^2\log x\mathrm{Li}_2(-x) - 120\log^3(x)\mathrm{Li}_2(-x)\\ &+ 180\pi^2\mathrm{Li}_3(-x) + 540\log^2 x\mathrm{Li}_3(-x) - 1440\log(x)\mathrm{Li}_4(-x)\\ &+ 1800\mathrm{Li}_5(-x) + 690\pi^2\zeta_3 - 5940\zeta_5\Big]. \end{aligned} \tag{4.102}$$

Remarkably, (4.102) does not contain any harmonic polylogarithms. We will compare the Wilson loop remainder (4.102) to the corresponding amplitude remainder (4.33) in Section 4.11.1. Similarly to what was done for the amplitude remainder (4.33), in arriving at (4.102) we have pulled out a factor of $(st)^{-\epsilon/2}$ per loop in order to obtain a result which depends only on the ratio $x := t/s$.

The five-point two-loop Wilson loop was calculated up to $\mathcal{O}(\epsilon^0)$ in [10]. In order to obtain results at one order higher in ϵ we have proceeded by using numerical methods. In particular we have used Mellin-Barnes techniques to evaluate and expand all the two-loop integrals, as described in more detail in Sections 4.9 and 4.10.

4.9 Mellin-Barnes method

At the heart of the Mellin-Barnes (MB) method lies the Mellin-Barnes representation, which allows us to replace a sum of two terms raised to some power by the product of these terms raised to some powers. One achieves this factorisation at the cost of introducing a Mellin integration over a complex parameter z. More specifically, the MB representation reads

$$\frac{1}{(X+Y)^\lambda} = \frac{1}{2\pi i}\frac{1}{\Gamma(\lambda)}\int_{-i\infty}^{+i\infty} dz\, \frac{X^z}{Y^{\lambda+z}}\Gamma(-z)\Gamma(\lambda+z), \tag{4.103}$$

where the contour of integration is such that the $\Gamma(\cdots + z)$ poles are to the left of the contour and the $\Gamma(\cdots - z)$ poles are to the right. A possible contour in the

case $\lambda = -1/2 - i/2$ is shown in Figure 4.16. By applying the same formula several

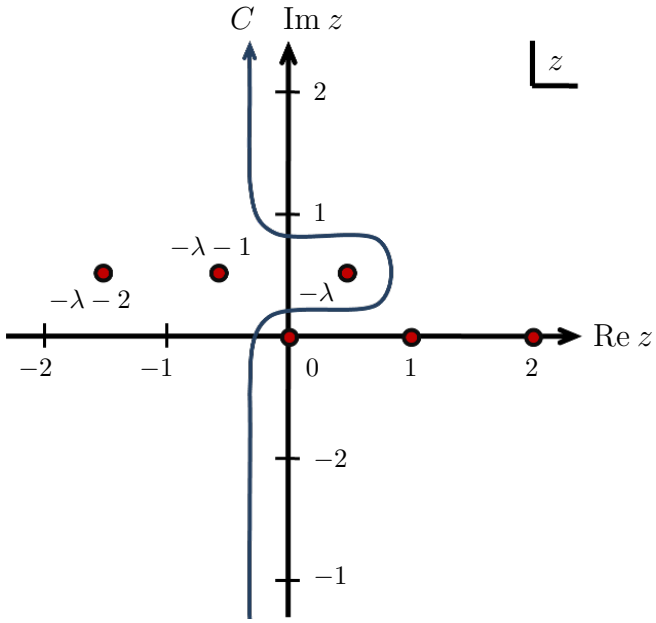

Figure 4.16: *Possible integration contour for the Mellin integration in (4.103) for* $\lambda = -1/2 - i/2$.

times, we can easily generalise (4.103) to the case with m terms in the denominator

$$\frac{1}{(\sum_{s=1}^{m} X_s)^{\lambda}} = \frac{1}{(2\pi i)^{m-1}} \frac{1}{\Gamma(\lambda)} \left(\prod_{s=1}^{m-1} \int_{-i\infty}^{+i\infty} dz_s \right) \frac{\prod_{s=1}^{m-1} X_s^{z_s} \Gamma(-z_s)}{X_m^{\lambda + \sum_{s=1}^{m-1} z_s} \Gamma(\lambda + \sum_{s=1}^{m-1} z_s)}, \tag{4.104}$$

which introduces $(m-1)$ MB integration variables z_s.

Integrals for Feynman diagrams (see for example all the integrals for the two-loop Wilson loop presented in detail in Section 4.7) involve integrations over parameters τ_i. One proceeds by obtaining an MB representation for the integrand of each Feynman integral using (4.104). This introduces Mellin integrations over Mellin parameters z_s on top of those over the τ_i's. As one can see from (4.104), we achieve the factorisation of the integrand into a product of all the terms, that originally appeared in the sum on its denominator, raised to powers involving the parameters z_s and the dimensional regularisation parameter ϵ.

We first perform the integrations over the τ_i's, that can be easily done by means of the simple substitution

$$\int_0^1 d\tau \, \tau^{\alpha} (1-\tau)^{\beta} = \frac{\Gamma(\alpha+1)\Gamma(\beta+1)}{\Gamma(\alpha+\beta+2)} \, . \tag{4.105}$$

At this point, we are left with an integrand that is an analytic function containing powers of the momentum invariants $(-s_{ij})^{f(\{z_s\},\epsilon)}$ and Gamma functions $\Gamma(g(\{z_s\},\epsilon))$, where f and g are linear combinations of the z_s's and ϵ.

The next step is to pick the appropriate contours of integration. One resolves any singularities in ϵ by means of shifting contours and taking residues, so that the integrand can be Laurent expanded in the dimensional regularisation parameter ϵ, giving us one integral at each order in ϵ, up to the desired order.

The very last step is to perform the Mellin integrations over the parameters z_s. In some cases, one can perform some of them explicitly, by means of the first and the second Barnes lemma and their corollaries. The first Barnes lemma reads

$$\frac{1}{2\pi i}\int_{-i\infty}^{+i\infty} dz\,\Gamma(\lambda_1+z)\Gamma(\lambda_2+z)\Gamma(\lambda_3-z)\Gamma(\lambda_4-z) = \frac{\Gamma(\lambda_1+\lambda_3)\Gamma(\lambda_1+\lambda_4)\Gamma(\lambda_2+\lambda_3)\Gamma(\lambda_2+\lambda_4)}{\Gamma(\lambda_1+\lambda_2+\lambda_3+\lambda_4)}, \tag{4.106}$$

while the second Barnes lemma reads

$$\frac{1}{2\pi i}\int_{-i\infty}^{+i\infty} dz\,\frac{\Gamma(\lambda_1+z)\Gamma(\lambda_2+z)\Gamma(\lambda_3+z)\Gamma(\lambda_4-z)\Gamma(\lambda_5-z)}{\Gamma(\lambda_6+z)} = \frac{\Gamma(\lambda_1+\lambda_4)\Gamma(\lambda_2+\lambda_4)\Gamma(\lambda_3+\lambda_4)\Gamma(\lambda_1+\lambda_5)\Gamma(\lambda_2+\lambda_5)\Gamma(\lambda_3+\lambda_5)}{\Gamma(\lambda_1+\lambda_2+\lambda_4+\lambda_5)\Gamma(\lambda_1+\lambda_2+\lambda_4+\lambda_5)\Gamma(\lambda_2+\lambda_3+\lambda_4+\lambda_5)}. \tag{4.107}$$

A list of corollaries of the two Barnes lemmas can be found in Appendix D of [122]. If at this point there are still Mellin integrations left to be performed, one resorts to numeric integration to obtain numeric results at specific kinematic points as we describe in more detail in the following section.

For a more extensive discussion of the Mellin-Barnes method with examples we refer the reader to [122].

4.10 Implementation of Mellin-Barnes method

The two-loop four and five-point Wilson loops and five-point amplitude have been numerically evaluated by means of the Mellin-Barnes (MB) method using the `MB` package [112] in `MATHEMATICA`.

In the Wilson loop case, we have constructed a completely automated computer algorithm, that, for specific n, calculates all the needed diagrams according to (4.68), carrying out all the necessary operations to finally give us specific values for the complete Wilson loop at specific kinematic points. All the integrals for the different

Diagram	$n=4$	$n=5$	$n=6$
f_H	3	6	8
f_C	2	6	7
f_X	4	8	10
f_Y	2	4	5
$f_P\, f_P$	2	4	6

Table 4.1: *Maximum number of Mellin integrations encountered in each class of diagrams in the n-sided two-loop Wilson loop for* $n = 4, 5, 6$.

diagrams have been coded in a generic form as presented in Sections 4.7.1 – 4.7.5. In Table 4.1, we list the maximum number of Mellin integrations one encounters in each class of diagrams for $n = 4, 5, 6$; this number is equal to $m - 1$, where m is the number of non-vanishing terms in the denominator of each integral. Whether a term vanishes or not depends on whether the arguments Q_i's are zero, massless or massive.

In the first steps of our algorithm, and for a given n, we obtain MB representations for all the integrals needed via (4.104) and then perform the Feynman integrations via the substitution (4.105). Then, we use various `MATHEMATICA` packages to perform a series of operations in an automated way to finally obtain a numerical expression at specific kinematic points.

We will briefly summarise these steps followed, while for more details we refer the reader to the references documenting these packages and references therein. Using the `MBresolve` package [113], we pick appropriate contours and resolve the singularity structure of the integrand in ϵ. The latter involves taking residues and shifting contours, and is essential in order to be able to Laurent expand the integrand in ϵ. Using the `barnesroutines` package [112, 113], we apply the Barnes lemmas, which in general generate more integrals but decrease their dimensionality, leading to higher precision results. Finally, using the `MB` package [112] we numerically integrate at specific Euclidean kinematic points to obtain a numerical expression. While all manipulations of the integrals and the expansion in ϵ are performed in `MATHEMATICA`, the actual numerical integration for each term is performed using the `CUBA` routines [123] for multidimensional numerical integration in `FORTRAN`.

The high number of diagrams, and number of integrals for each diagram, makes the task of running the `FORTRAN` integrations ideal for parallel computing. In order to obtain high precision results in a reasonable amount of time, the task of evaluating the `FORTRAN` files, was shifted, at an early stage of the project, from a single computer, to a cluster of computers with 32 CPU units in Brown University,

and finally to the Queen Mary, University of London High Throughput Computing Facility, a cluster of 1.5K CPU units.

Within the `MB` package, integrations of dimensionality up to four are by default performed using the deterministic `CUBA` routine `Cuhre`, that samples over an optimal grid of points depending on the way the integrand varies. For higher dimensional integrals, the `CUBA` routine `Vegas` is used, that performs Monte-Carlo integration over a random sample of points. `Vegas` gives faster results but we have noticed that this routine fails to deliver high precision results for the specific integrals we want to calculate. For this reason, and since parallel computing gives us enough computer power, or equivalently, enough computer time, we have used the `Cuhre` routine for all the integrals, involving up to 8 Mellin integrations in the case of the cross diagram for $n = 5$.

In Sections 4.7.1 – 4.7.5, we have also listed the symmetries of each diagram. Using these symmetries, and given a result for a diagram d for kinematics K, all the equivalent diagrams $Eq(d)$ will give the same result for the same kinematics K. We can rotate the labels of the momenta in all these diagrams sending $i- > i+r$ (where $r = 1, \ldots, n-1$), to obtain more diagrams $Rot(d, r)$ with the same result, but this time the diagrams are evaluated at the kinematic point $Rot(Kin, r)$, obtained by applying the same rotation to the kinematics K. If the kinematics are symmetric under this rotation $Rot(K, r) = K$, for example the kinematics $(s_{12} \leftarrow -1, s_{23} \leftarrow -1, s_{34} \leftarrow -1, s_{45} \leftarrow -1, s_{51} \leftarrow -1)$ in the $n = 5$ case, multiple diagrams that need to be evaluated will be found to be equivalent, reducing the number of them that actually needs to be calculated. Moreover, when parallely processing the `FORTRAN` files, we have discovered that several files were identical. We have implemented an algorithm that identifies and groups identical files, so that only a single one of them is run from each group, saving a considerable amount of computer time.

We have chosen to evaluate the two loop Wilson loop at different kinematic points as it appears in (4.68) without the prefactor $\mathcal{C}$. For each diagram, the `CUBA` routines give us its numeric value, together with its estimated error. It is straightforward to find the total error, as the complete Wilson loop is just a sum of diagrams. If, for example, we chose to evaluate up to $\mathcal{O}(\epsilon^0)$, we will obtain a numeric result that has the form

$$x = \frac{x_{-2} \pm \delta x_{-2}}{\epsilon^2} + \frac{x_{-1} \pm \delta x_{-1}}{\epsilon} + (x_0 \pm \delta x_0) + \mathcal{O}(\epsilon^0). \tag{4.108}$$

We can easily normalise this result at the very end with any factor $\mathcal{C}$. The mean

value of the normalised result is found by multiplying by the expansion of this factor

$$\mathcal{C} = \mathcal{C}_0 + \mathcal{C}_1\,\epsilon + \mathcal{C}_2\,\epsilon^2 + \mathcal{O}(\epsilon^3), \tag{4.109}$$

and collecting the terms for each power. However, the new error is less trivial to find and it is given by

$$\begin{aligned}\delta(\mathcal{C}\,x) = \frac{\mathcal{C}_0\,\delta x_{-2}}{\epsilon^2} + \frac{\sqrt{(\mathcal{C}_0\,\delta x_{-1})^2 + (\mathcal{C}_1\,\delta x_{-2})^2}}{\epsilon} \\ + \sqrt{(\mathcal{C}_0\,\delta x_0)^2 + (\mathcal{C}_1\,\delta x_{-1})^2 + (\mathcal{C}_2\,\delta x_{-2})^2}.\end{aligned} \tag{4.110}$$

4.11 Results: comparison of the remainder functions at $\mathcal{O}(\epsilon)$

In this section we present the results of the comparison of the amplitude and Wilson loop remainder functions at $\mathcal{O}(\epsilon)$.

4.11.1 Four-point amplitude and Wilson loop remainders

The remainder functions for the four-point amplitude and Wilson loops are given in (4.33) and (4.102) respectively. From these relations, it follows that the difference of remainders is the following constant x-independent term

$$\mathcal{E}_4^{(2)} = \mathcal{E}_{4,\mathrm{WL}}^{(2)} - 3\zeta_5, \tag{4.111}$$

as anticipated in (4.24).

We would like to stress that this is a highly nontrivial result since there is no reason a priori to expect that the four-point remainder on the amplitude and Wilson loop side, (4.33) and (4.102) respectively, agree (up to a constant shift). For example, anomalous dual conformal invariance is known to determine the form of the four- and five-point Wilson loop only up to $\mathcal{O}(\epsilon^0)$ terms [10], but does not constrain terms which vanish as $\epsilon \to 0$. The expressions we derived for the amplitude and Wilson loop four-point remainders at $\mathcal{O}(\epsilon)$ are also pleasingly simple, in that they only contain standard polylogarithms.

#	$(s_{12}, s_{23}, s_{34}, s_{45}, s_{51})$	$\mathcal{E}_5^{(2)}$	$\mathcal{E}_{5,\mathrm{WL}}^{(2)}$
1	$(-1,-1,-1,-1,-1)$	-8.4655 ± 0.0049	-5.87034 ± 0.00044
2	$(-1,-1,-2,-1,-1)$	-8.2350 ± 0.0024	-5.64560 ± 0.00063
3	$(-1,-2,-2,-1,-1)$	-7.7697 ± 0.0026	-5.17647 ± 0.00076
4	$(-1,-2,-3,-4,-5)$	-6.2304 ± 0.0031	-3.6409 ± 0.0011
5	$(-1,-1,-3,-1,-1)$	-8.2525 ± 0.0027	-5.65919 ± 0.00097
6	$(-1,-2,-1,-2,-1)$	-8.1417 ± 0.0023	-5.54972 ± 0.00058
7	$(-1,-3,-3,-1,-1)$	-7.6677 ± 0.0034	-5.0784 ± 0.0013
8	$(-1,-2,-3,-2,-1)$	-6.8995 ± 0.0029	-4.31395 ± 0.00093
9	$(-1,-3,-2,-5,-4)$	-6.9977 ± 0.0031	-4.40806 ± 0.00099
10	$(-1,-3,-1,-3,-1)$	-8.2759 ± 0.0025	-5.69086 ± 0.00085
11	$(-1,-4,-8,-16,-32)$	-8.7745 ± 0.0078	-6.1825 ± 0.0051
12	$(-1,-8,-4,-32,-16)$	-11.9855 ± 0.0080	-9.3855 ± 0.0051
13	$(-1,-10,-100,-10,-1)$	-2.914 ± 0.022	-0.300 ± 0.010
14	$(-1,-100,-10,-100,-1)$	-3.237 ± 0.011	-0.6648 ± 0.0028
15	$(-1,-1,-100,-1,-1)$	-12.686 ± 0.014	-10.108 ± 0.010
16	$(-1,-100,-1,-100,-1)$	-14.7067 ± 0.0077	-12.1136 ± 0.0071
17	$(-1,-100,-100,-1,-1)$	-182.32 ± 0.11	-179.722 ± 0.039
18	$(-1,-100,-10,-100,-10)$	-6.3102 ± 0.0062	-3.7281 ± 0.0013
19	$\left(-1,-\frac{1}{4},-\frac{1}{9},-\frac{1}{16},-\frac{1}{25}\right)$	-19.0031 ± 0.0077	-16.4136 ± 0.0021
20	$\left(-1,-\frac{1}{9},-\frac{1}{4},-\frac{1}{25},-\frac{1}{16}\right)$	-15.1839 ± 0.0046	-12.5995 ± 0.0016
21	$\left(-1,-1,-\frac{1}{4},-1,-1\right)$	-9.7628 ± 0.0028	-7.17588 ± 0.00079
22	$\left(-1,-\frac{1}{4},-\frac{1}{4},-1,-1\right)$	-9.5072 ± 0.0036	-6.9186 ± 0.0014
23	$\left(-1,-\frac{1}{4},-1,-\frac{1}{4},-1\right)$	-12.6308 ± 0.0031	-10.04241 ± 0.00083
24	$\left(-1,-\frac{1}{4},-\frac{1}{9},-\frac{1}{4},-1\right)$	-11.0200 ± 0.0056	-8.4281 ± 0.0030
25	$\left(-1,-\frac{1}{9},-\frac{1}{4},-\frac{1}{9},-1\right)$	-19.1966 ± 0.0070	-16.6095 ± 0.0043

Table 4.2: *Values of the $\mathcal{O}(\epsilon)$ five-point remainder for the amplitudes ($\mathcal{E}_5^{(2)}$) and Wilson loop ($\mathcal{E}_{5,WL}^{(2)}$) at different kinematic points.*

4.11.2 Five-point amplitude and Wilson loop remainders

We have numerically evaluated both the five-point two-loop amplitude and Wilson loop up to $\mathcal{O}(\epsilon)$ at 25 Euclidean kinematic points, i.e. points in the subspace of the kinematic invariants with all $s_{ij} < 0$. The choice of these points and the values of the remainder functions $\mathcal{E}_5^{(2)}$, $\mathcal{E}_{5,\mathrm{WL}}^{(2)}$ at (ϵ) together with the errors reported by the CUBA numerical integration library [123] appear in Table 4.2, while in Figures 4.17 we plot both remainders for all kinematic points. From these figures, it is apparent that the two remainders vary in a way such that the distance between them is constant.

We have calculated the difference between the amplitude and Wilson loop re-

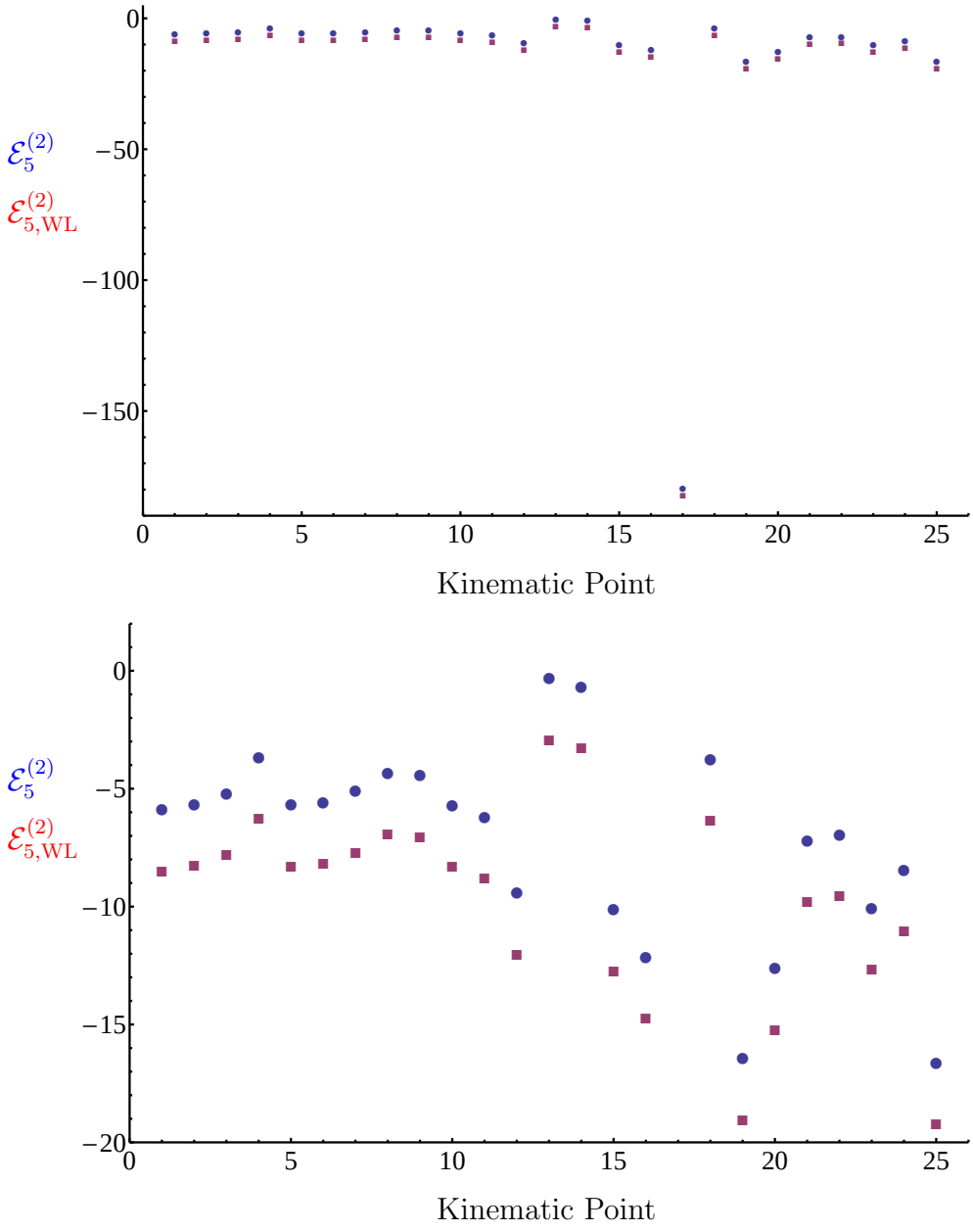

Figure 4.17: *Remainder functions at $\mathcal{O}(\epsilon)$ for the amplitude (circle) and the Wilson loop (square). The exact values together with their errors appear in Table 4.2. In the bottom Figure we have eliminated the point corresponding to kinematics* 17 *and zoomed in an area showing all the remaining points.*

mainders, see Table 4.3 and Figure 4.3. Remarkably, this difference also appears to be constant within our numerical precision as in the four-point case, and hence we conjecture that

$$\mathcal{E}_5^{(2)} = \mathcal{E}_{5,\mathrm{WL}}^{(2)} - \frac{5}{2}\zeta_5. \tag{4.112}$$

It is also intriguing that the constant difference is fit very well by a simple rational multiple of ζ_5, rather than a linear combination of ζ_5 and $\zeta_2\zeta_3$ as would have been allowed more generally by transcendentality.

A number is transcendental when it is not algebraic. An algebraic number is a complex number that is a root of a polynomial with rational coefficients. We assign transcendentality 2 to dilogarithms Li_2 and transcendentality 1 to log's and π's. Finally, zeta functions ζ_x have transcendentality equal to x. Products of these functions have transcendentality equal to the sum of the corresponding transcendentalities. Each term in the expansion of scattering amplitudes and Wilson loops in $\mathcal{N} = 4$ super Yang-Mills has a fixed uniform degree of transcendentality (see for example the terms in the expansion (4.96), appearing in (4.97)-(4.100)).

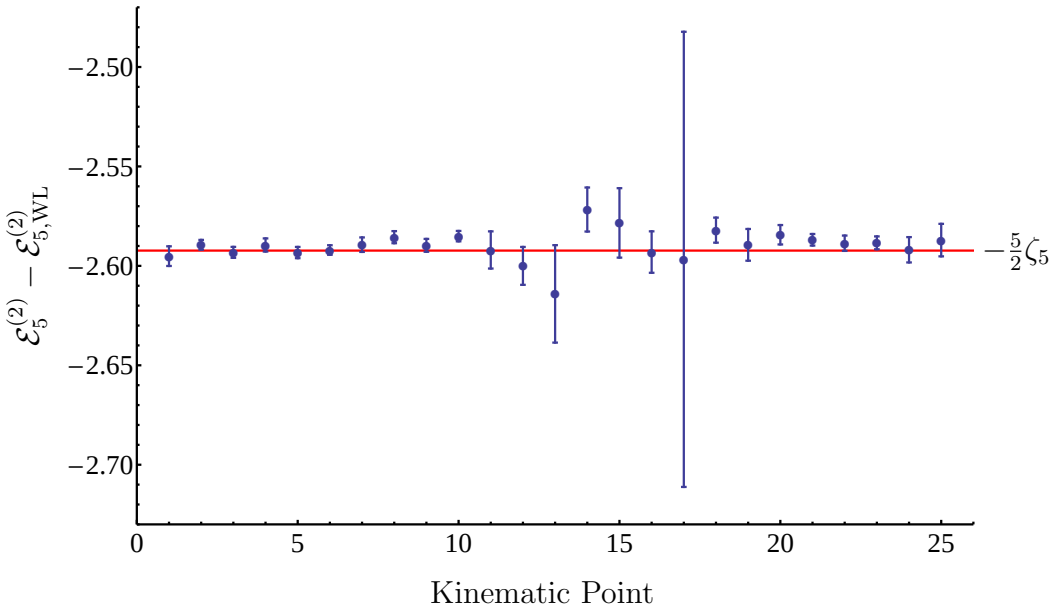

Figure 4.18: *Difference of the remainder functions* $\mathcal{E}_5^{(2)} - \mathcal{E}_{5,\mathrm{WL}}^{(2)}$. *The exact values together with their errors appear in Table 4.3.*

In the last column of Table 4.3 we give the distance of our results for the difference of remainders from the conjectured value in units of their standard deviation, while these values are plotted in Figure 4.19. We notice that all numerical results are within three standard deviations away from the conjectured value. From the histogram in Figure 4.20, we can see that these distances are normally distributed as expected.

For kinematic points 1, 4, 6 and 12 we have evaluated the remainder functions with even higher precision, and found agreement with the conjecture to 4 digits. These results are collected in Tables 4.4 and 4.5. A remark is in order here. By

#	$(s_{12}, s_{23}, s_{34}, s_{45}, s_{51})$	$\mathcal{E}_5^{(2)} - \mathcal{E}_{5,\mathrm{WL}}^{(2)}$	$\lvert\mathcal{E}_5^{(2)} - \mathcal{E}_{5,\mathrm{WL}}^{(2)} + \frac{5}{2}\zeta_5\rvert/\sigma$
1	$(-1,-1,-1,-1,-1)$	-2.5951 ± 0.0049	0.564
2	$(-1,-1,-2,-1,-1)$	-2.5894 ± 0.0025	1.2
3	$(-1,-2,-2,-1,-1)$	-2.5932 ± 0.0027	0.32
4	$(-1,-2,-3,-4,-5)$	-2.5895 ± 0.0033	0.853
5	$(-1,-1,-3,-1,-1)$	-2.5933 ± 0.0028	0.35
6	$(-1,-2,-1,-2,-1)$	-2.5920 ± 0.0024	0.120
7	$(-1,-3,-3,-1,-1)$	-2.5893 ± 0.0036	0.82
8	$(-1,-2,-3,-2,-1)$	-2.5856 ± 0.0030	2.2
9	$(-1,-3,-2,-5,-4)$	-2.5897 ± 0.0032	0.82
10	$(-1,-3,-1,-3,-1)$	-2.5851 ± 0.0026	2.8
11	$(-1,-4,-8,-16,-32)$	-2.5920 ± 0.0093	0.034
12	$(-1,-8,-4,-32,-16)$	-2.6000 ± 0.0095	0.808
13	$(-1,-10,-100,-10,-1)$	-2.614 ± 0.024	0.89
14	$(-1,-100,-10,-100,-1)$	-2.572 ± 0.011	1.9
15	$(-1,-1,-100,-1,-1)$	-2.578 ± 0.017	0.80
16	$(-1,-100,-1,-100,-1)$	-2.593 ± 0.010	0.071
17	$(-1,-100,-100,-1,-1)$	-2.60 ± 0.11	0.039
18	$(-1,-100,-10,-100,-10)$	-2.5820 ± 0.0063	1.6
19	$\left(-1,-\frac{1}{4},-\frac{1}{9},-\frac{1}{16},-\frac{1}{25}\right)$	-2.5894 ± 0.0080	0.36
20	$\left(-1,-\frac{1}{9},-\frac{1}{4},-\frac{1}{25},-\frac{1}{16}\right)$	-2.5844 ± 0.0049	1.6
21	$\left(-1,-1,-\frac{1}{4},-1,-1\right)$	-2.5869 ± 0.0029	1.9
22	$\left(-1,-\frac{1}{4},-\frac{1}{4},-1,-1\right)$	-2.5886 ± 0.0038	0.96
23	$\left(-1,-\frac{1}{4},-1,-\frac{1}{4},-1\right)$	-2.5884 ± 0.0032	1.2
24	$\left(-1,-\frac{1}{4},-\frac{1}{9},-\frac{1}{4},-1\right)$	-2.5919 ± 0.0064	0.064
25	$\left(-1,-\frac{1}{9},-\frac{1}{4},-\frac{1}{9},-1\right)$	-2.5870 ± 0.0082	0.65

Table 4.3: *Difference of the five-point amplitude and Wilson loop two-loop remainder functions at $\mathcal{O}(\epsilon)$, and its distance from $-\frac{5}{2}\zeta_5 \sim -2.592319$ in units of σ, the standard deviation reported by the CUBA numerical integration package [123].*

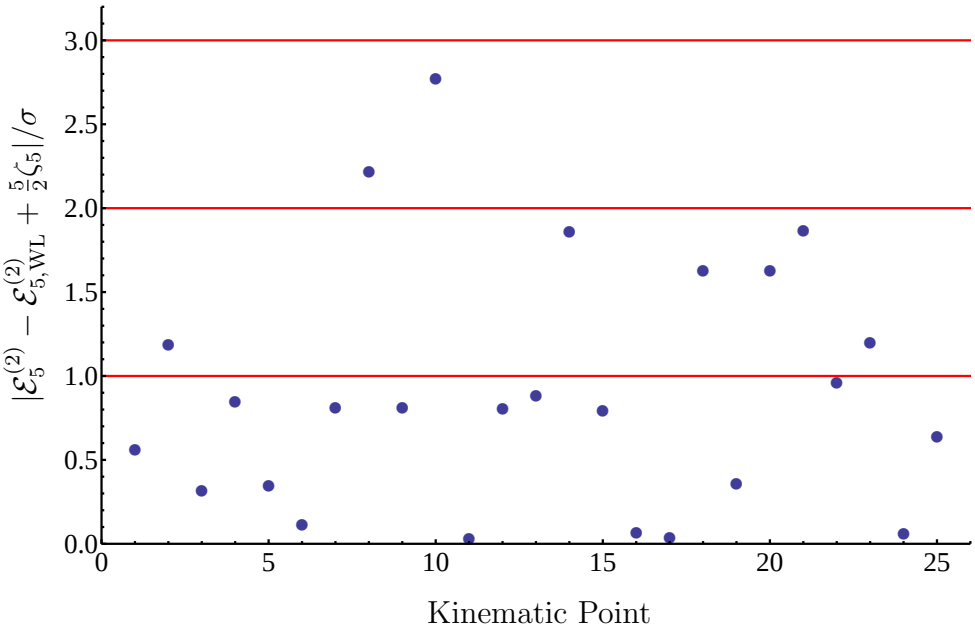

Figure 4.19: *Distance of the difference of the five-point amplitude and Wilson loop two-loop remainder functions at $\mathcal{O}(\epsilon)$, from $-\frac{5}{2}\zeta_5 \sim -2.592319$ in units of σ, the standard deviation reported by the CUBA numerical integration package [123]. The exact values are given in the last column of Table 4.3.*

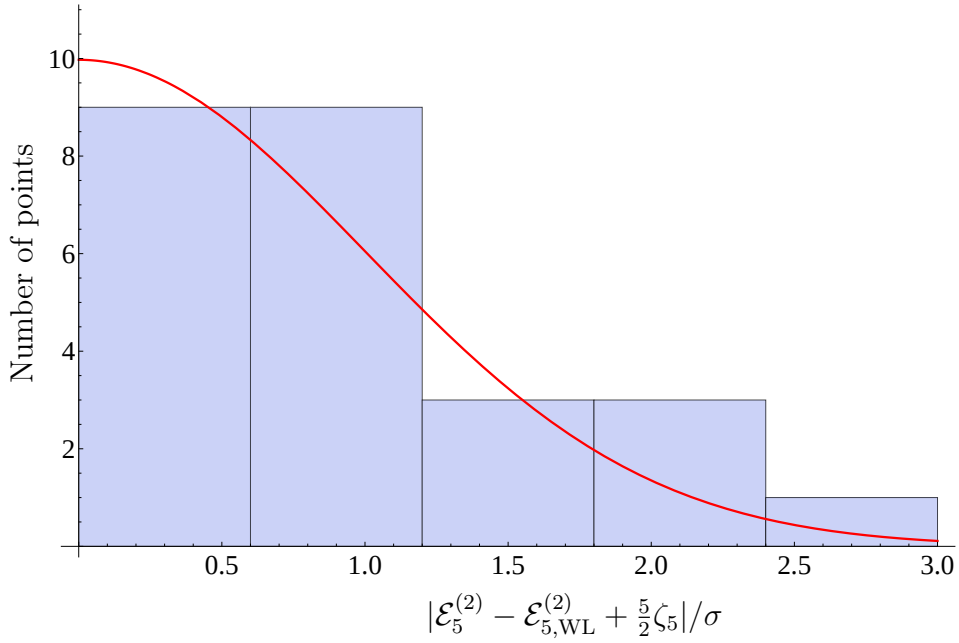

Figure 4.20: *A histogram for the 25 distances of our results from the conjectured value $-\frac{5}{2}\zeta_5$ (see Figure 4.20), compatible with a normal distribution.*

#	$(s_{12}, s_{23}, s_{34}, s_{45}, s_{51})$	$\mathcal{E}_5^{(2)}$	$\mathcal{E}_{5,\mathrm{WL}}^{(2)}$
1	$(-1,-1,-1,-1,-1)$	-8.463173 ± 0.000047	-5.8705280 ± 0.0000068
4	$(-1,-2,-3,-4,-5)$	-6.234809 ± 0.000032	-3.642125 ± 0.000018
6	$(-1,-2,-1,-2,-1)$	-8.142702 ± 0.000023	-5.5500050 ± 0.0000092
12	$(-1,-8,-4,-32,-16)$	-11.991985 ± 0.000089	-9.398659 ± 0.000084

Table 4.4: *High precision values of the $\mathcal{O}(\epsilon)$ five-point remainders for amplitudes ($\mathcal{E}_5^{(2)}$) and Wilson loops ($\mathcal{E}_{5,WL}^{(2)}$).*

#	$(s_{12}, s_{23}, s_{34}, s_{45}, s_{51})$	$\mathcal{E}_5^{(2)} - \mathcal{E}_{5,\mathrm{WL}}^{(2)}$	$\lvert\mathcal{E}_5^{(2)} - \mathcal{E}_{5,\mathrm{WL}}^{(2)} + \frac{5}{2}\zeta_5\rvert/\sigma$
1	$(-1,-1,-1,-1,-1)$	-2.592645 ± 0.000048	6.8
4	$(-1,-2,-3,-4,-5)$	-2.592697 ± 0.000036	10
6	$(-1,-2,-1,-2,-1)$	-2.592697 ± 0.000025	15
12	$(-1,-8,-4,-32,-16)$	-2.59333 ± 0.00012	8.3

Table 4.5: *High precision values of the difference of the five-point amplitude and Wilson loop two-loop remainder functions at $\mathcal{O}(\epsilon)$, and its distance from $-\frac{5}{2}\zeta_5 \sim -2.592319$ in units of σ, the standard deviation reported by the CUBA numerical integration package [123].*

increasing the precision, the mean value of the difference of remainders approaches the conjectured value, but we notice that in units of σ it drifts away from it, hinting at a potential underestimate of the errors. To test our error estimates we used the remainder functions $\mathcal{R}_5$ at $\mathcal{O}(\epsilon^0)$, that are known to vanish. Our analysis confirmed that, as we increase the desired precision, the actual precision of the mean value does increase, but on the other hand reported errors tend to become increasingly underestimated.

Chapter 5

Conclusions

In this thesis we have studied maximally supersymmetric theories via the study of perturbative scattering amplitudes, which provide a direct channel for the extraction of valuable information in any quantum field theory. We have demonstrated the simplicity of amplitudes in $\mathcal{N} = 4$ super Yang-Mills and $\mathcal{N} = 8$ supergravity, and the efficiency of on-shell methods in delivering their values by exploiting their analytic properties. We have studied relations between amplitudes in the two maximally supersymmetric theories, and the fascinating MHV amplitude/polygonal Wilson loop duality within maximal super Yang-Mills.

More specifically, in $\mathcal{N} = 8$ supergravity, we have shown in a number of cases how generalised unitarity can be used in order to generate new expressions for one-loop supercoefficients, and indicated how this applies in general. In particular, using recent results for tree amplitudes [42, 45], the one-loop supercoefficients take an intriguing form involving sums of squares of $\mathcal{N} = 4$ Yang-Mills one-loop expressions, times dressing factors. It seems likely that this structure will apply to all one-loop supercoefficients in $\mathcal{N} = 8$ supergravity. It is certainly of interest to take this further, proving more general results in detail, deriving algorithms which produce the loop dressing factors, and simplifying the expressions obtained when the solutions to the quadruple cut conditions for the loop momenta are inserted. For the MHV case, it was easy to eliminate the loop momenta from the expressions we derived, and thus find a direct correspondence with known results. It may be that a similar outcome can be attained for non-MHV cases. The loop momenta solutions are known explicitly, however the dressing factors entering non-MHV amplitudes are more complex.

It is intriguing that both tree-level superamplitudes and one-loop coefficients can be written in terms of squares of dual superconformal invariant quantities times

bosonic dressing factors. It would be interesting to understand what possible deeper reasons may underly these regularities. In this context, we note that in [68] it was shown that the dual superconformal invariant R-functions appearing in the NMHV amplitudes in $\mathcal{N} = 4$ SYM have a coplanar twistor-space localisation. It would be interesting if one could relate the simplicity of the tree-level and one-loop results in $\mathcal{N} = 8$ supergravity to simple twistor-space localisation properties. Interesting new ideas have been put forward recently [124, 125, 126] which in particular make a connection between on-shell recursion relations and twistor space [124, 125, 126, 127, 128].

In $\mathcal{N} = 4$ super Yang-Mills, we have studied for the first time the mysterious MHV amplitude/polygonal lightlike Wilson loop duality at two loops beyond the finite order in the dimensional regularisation parameter ϵ. We discover that, at four and five points, the duality persists at $\mathcal{O}(\epsilon)$: the remainder on the amplitude and Wilson loop side, agree up to a constant shift, that we determine. It would be very interesting to continue exploring this miraculous agreement and to understand the reason behind it. Dual conformal invariance cannot help in this regard since the symmetry is explicitly broken in dimensional regularisation, so it cannot say anything about terms of higher order in ϵ. Already starting from $\mathcal{O}(\epsilon^0)$ there must be some mechanism beyond dual conformal invariance at work. At five-points, it is an interesting open question whether the parity-odd terms cancel at $\mathcal{O}(\epsilon)$ as they do at $\mathcal{O}(\epsilon^0)$ [59].

Appendix A

Scalar box integrals

In this appendix we list all the scalar box integrals expanded in the dimensional regularisation parameter ϵ through $\mathcal{O}(\epsilon^0)$ [85].

The zero-mass box integral appears only in four-point amplitudes with massless particles and it is defined as follows

$\mathcal{I}^{0\mathrm{m}}(p_1,p_2,p_3,p_4) =$ 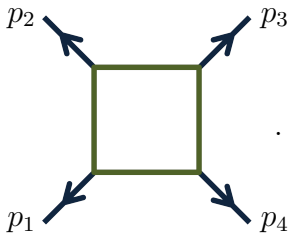

. (A.1)

Through $\mathcal{O}(\epsilon^0)$ this function is

$$\mathcal{I}^{0\mathrm{m}}(p_1,p_2,p_3,p_4) = \frac{r_\Gamma}{st}\left\{\frac{2}{\epsilon^2}\left[(-s)^{-\epsilon}+(-t)^{-\epsilon}\right] - \ln^2\left(\frac{-s}{-t}\right) - \pi^2\right\}, \tag{A.2}$$

where $s=(p_1+p_2)^2$ and $t=(p_2+p_3)^2$ are the usual Mandelstam variables, and the constant r_Γ is given in (3.5).

The one-mass scalar box contains a single massive corner and three massless corners, and it is defined in the following way

$\mathcal{I}^{1\mathrm{m}}(p,q,r,P) =$ 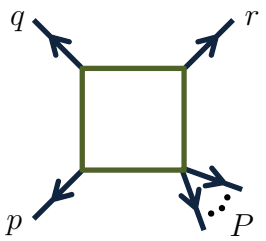

, (A.3)

while its expansion through $\mathcal{O}(\epsilon^0)$ is given by

$$\mathcal{I}^{\rm 1m}(p,q,r,P) = -\frac{2\,r_\Gamma}{st}\left\{-\frac{1}{\epsilon^2}\left[(-s)^{-\epsilon}+(-t)^{-\epsilon}-(-P^2)^{-\epsilon}\right]\right. \tag{A.4}$$
$$\left. +{\rm Li}_2\left(1-\frac{P^2}{s}\right)+{\rm Li}_2\left(1-\frac{P^2}{t}\right)+\frac{1}{2}\ln^2\left(\frac{s}{t}\right)+\frac{\pi^2}{6}\right\},$$

where $s=(p+q)^2$ and $t=(q+r)^2$.

The two-mass easy scalar box integral contains two non-adjacent massive corners as the one defined below

$$\mathcal{I}^{\rm 2me}(p,P,q,Q) = \tag{A.5}$$

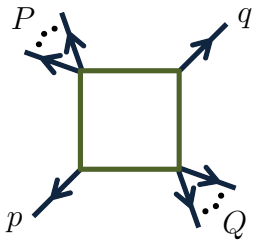

Its expansion up to finite terms is given by

$$\mathcal{I}^{\rm 2me}(p,P,q,Q) = \frac{-2\,r_\Gamma}{st-P^2Q^2}$$
$$\times\left\{-\frac{1}{\epsilon^2}\left[(-s)^{-\epsilon}+(-t)^{-\epsilon}-(-P^2)^{-\epsilon}-(-Q^2)^{-\epsilon}\right]\right.$$
$$+{\rm Li}_2\left(1-\frac{P^2}{s}\right)+{\rm Li}_2\left(1-\frac{P^2}{t}\right)+{\rm Li}_2\left(1-\frac{Q^2}{s}\right)$$
$$\left.+{\rm Li}_2\left(1-\frac{Q^2}{t}\right)-{\rm Li}_2\left(1-\frac{P^2Q^2}{st}\right)+\frac{1}{2}\ln^2\left(\frac{s}{t}\right)\right\}, \tag{A.6}$$

where $s=(p+P)^2$ and $t=(P+q)^2$.

The two-mass hard scalar box contains two adjacent massive corners as the one defined below

$$\mathcal{I}^{\rm 2mh}(p,q,P,Q) = \tag{A.7}$$

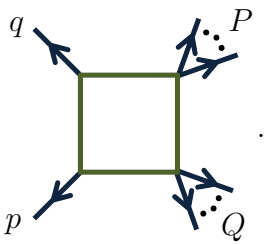

Its expansion up to finite terms is given by

$$\begin{aligned}\mathcal{I}^{\text{2mh}}(p,q,P,Q) = -\frac{2\,r_\Gamma}{st}\Bigg\{&-\frac{1}{\epsilon^2}\left[(-s)^{-\epsilon}+(-t)^{-\epsilon}-(-P^2)^{-\epsilon}-(-Q^2)^{-\epsilon}\right]\\&-\frac{1}{2\epsilon^2}\frac{(-P^2)^{-\epsilon}(-Q^2)^{-\epsilon}}{(-s)^{-\epsilon}}+\frac{1}{2}\ln^2\left(\frac{s}{t}\right)\\&+\text{Li}_2\left(1-\frac{P^2}{t}\right)+\text{Li}_2\left(1-\frac{Q^2}{t}\right)\Bigg\},\end{aligned} \tag{A.8}$$

where $s=(p+q)^2$ and $t=(q+P)^2$.

The three-mass scalar box contains a single massless corner. Defining this integral in the following way

$$\mathcal{I}^{\text{3m}}(p,P,Q,R) = \tag{A.9}$$

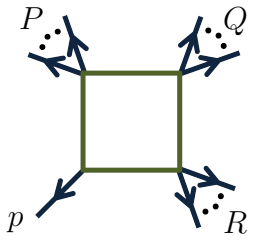

its expansion up to $\mathcal{O}(\epsilon^0)$ reads

$$\begin{aligned}\mathcal{I}^{\text{3m}}(p,P,Q,R) = \frac{-2\,r_\Gamma}{st-P^2R^2}&\\\times\Bigg\{&-\frac{1}{\epsilon^2}\left[(-s)^{-\epsilon}+(-t)^{-\epsilon}-(-P^2)^{-\epsilon}-(-Q^2)^{-\epsilon}-(-R^2)^{-\epsilon}\right]\\&-\frac{1}{2\epsilon^2}\frac{(-P^2)^{-\epsilon}(-Q^2)^{-\epsilon}}{(-t)^{-\epsilon}}-\frac{1}{2\epsilon^2}\frac{(-Q^2)^{-\epsilon}(-R^2)^{-\epsilon}}{(-s)^{-\epsilon}}+\frac{1}{2}\ln^2\left(\frac{s}{t}\right)\\&+\text{Li}_2\left(1-\frac{P^2}{s}\right)+\text{Li}_2\left(1-\frac{R^2}{t}\right)+\text{Li}_2\left(1-\frac{P^2R^2}{st}\right)\Bigg\},\end{aligned} \tag{A.10}$$

where $s=(p+P)^2$ and $t=(Q+R)^2$.

Finally, the four-mass scalar box integral contains four massive corners

$$\mathcal{I}^{\text{4m}}(P,Q,R,S) = \tag{A.11}$$

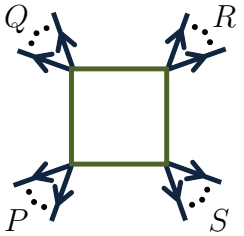

This is the only box function that is finite, and at $\mathcal{O}(\epsilon^0)$ it is given by

$$\begin{aligned}\mathcal{I}^{\text{4m}}(P,Q,R,S) = \frac{-r_\Gamma}{st\rho}\Bigg\{&-\text{Li}_2\left(\frac{1}{2}(1-\lambda_1+\lambda_2+\rho)\right)+\text{Li}_2\left(\frac{1}{2}(1-\lambda_1+\lambda_2-\rho)\right)\\&-\text{Li}_2\left(\frac{1}{2\lambda_1}(1-\lambda_1-\lambda_2-\rho)\right)+\text{Li}_2\left(\frac{1}{2\lambda_1}(1-\lambda_1-\lambda_2+\rho)\right)\\&-\frac{1}{2}\ln\left(\frac{\lambda_1}{\lambda_2^2}\right)\ln\left(\frac{1+\lambda_1-\lambda_2+\rho}{1+\lambda_1-\lambda_2-\rho}\right)\Bigg\},\end{aligned} \tag{A.12}$$

The function ρ is given by

$$\rho = \sqrt{1-2\lambda_1-2\lambda_2+\lambda_1^2-2\lambda_1\lambda_2+\lambda_2^2}, \tag{A.13}$$

where

$$\lambda_1 = \frac{P^2R^2}{st}, \qquad \lambda_2 = \frac{Q^2S^2}{st}, \tag{A.14}$$

while $s=(P+Q)^2$ and $t=(Q+R)^2$.

Appendix B

The finite part of the two-mass easy box function

We present two different forms for the finite part of the two mass easy box function, and more precisely the function $\mathcal{F}_\epsilon$, defined in (4.41). For more details we refer the reader to Appendix B of [14]. The first form is manifestly finite and it reads

$$\begin{aligned}\mathcal{F}_\epsilon(s,t,P^2,Q^2) &= \frac{(-a)^\epsilon}{2} \\ &\times \left[(-aP^2){}_3\mathrm{F}_2(1,1,1+\epsilon;2,2;1-aP^2) + (1-aQ^2){}_3\mathrm{F}_2(1,1,1+\epsilon;2,2;1-aQ^2)\right. \\ &\left.-(1-as){}_3\mathrm{F}_2(1,1,1+\epsilon;2,2;1-as) - (1-at){}_3\mathrm{F}_2(1,1,1+\epsilon;2,2;1-at)\right],\end{aligned} \tag{B.1}$$

where $a = u/(P^2Q^2 - st)$. Furthermore, since ${}_3\mathrm{F}_2(1,1,1+\epsilon;2,2;x) = \mathrm{Li}_2(x)/x$, this form directly leads to the expression derived in [129, 50] for the finite two-mass easy box function,

$$\mathcal{F}_{\epsilon=0}(s,t,P^2,Q^2) = \frac{1}{2}\left[\mathrm{Li}_2(1-aP^2) + \mathrm{Li}_2(1-aQ^2) - \mathrm{Li}_2(1-as) - \mathrm{Li}_2(1-at)\right]. \tag{B.2}$$

We also notice that the simple expansion

$$x \times {}_3\mathrm{F}_2(1,1,1+\epsilon;2,2;x) = \sum_{n=1}^{\infty} \epsilon^n S_{1\,n+1}(x), \tag{B.3}$$

gives a correspondingly simple expansion for the Wilson loop diagram in terms of Nielsen polylogarithms.

The more familiar looking second form for the two-mass easy box function is (see

(A.13) of [130])

$$\begin{aligned}
&\mathcal{F}_\epsilon(s,t,P^2,Q^2) \;= -\frac{1}{2\epsilon^2} \\
&\times \left[\left(\frac{a}{1-aP^2}\right)^{\epsilon} {}_2\mathrm{F}_1\left(\epsilon,\epsilon;1+\epsilon;\tfrac{1}{(1-aP^2)}\right) + \left(\frac{a}{1-aQ^2}\right)^{\epsilon} {}_2\mathrm{F}_1\left(\epsilon,\epsilon;1+\epsilon;\tfrac{1}{(1-aQ^2)}\right) \right. \\
&- \left(\frac{a}{1-as}\right)^{\epsilon} {}_2\mathrm{F}_1\left(\epsilon,\epsilon;1+\epsilon;\tfrac{1}{(1-as)}\right) - \left(\frac{a}{1-at}\right)^{\epsilon} {}_2\mathrm{F}_1\left(\epsilon,\epsilon;1+\epsilon;\tfrac{1}{(1-at)}\right) \\
&\left. +\epsilon(-a)^{\epsilon}\left(\log(1-aP^2)+\log(1-aQ^2)-\log(1-as)-\log(1-at)\right)\right]. \qquad \text{(B.4)}
\end{aligned}$$

This second form was derived in [130, 8] except for the last line which is an additional correction term needed to obtain the correct analytic continuation in all regimes. The identity

$$\frac{(1-aP^2)(1-aQ^2)}{(1-as)(1-at)} = 1, \qquad \text{(B.5)}$$

implies that if all the arguments of the logs are positive then this additional term vanishes, but for example if we have $1-aP^2, 1-aQ^2 > 0$ and $1-as, 1-at < 0$ then the additional term gives (taking care of the appropriate analytic continuation in (4.42)) $\mathrm{sgn}(a)2\pi i(-a)^{\epsilon}/\epsilon$. This becomes important when considering this expression at four and five points in the Euclidean regime.

Acknowledgements

I would like to thank my supervisors and collaborators Bill Spence and Gabriele Travaglini for their guidance, their collaboration and their patience. I thank Andreas Brandhuber, Paul Heslop, Dung Nguyen, and Marcus Spradlin for the privilege of collaboration with them on research that is part of this thesis.

I am grateful to Queen Mary, University of London, for funding my research, my studies, and my training through a college studentship. I am also grateful to the Centre for Research in String Theory for generous travel funds.

I would like to thank the QMUL High Throughput Computing Facility and the London Grid, especially Alex Martin and Christopher Walker, for providing us with the necessary computer power for our high precision numerical evaluations. I would also like to thank Terry Arter, Alex Owen and Cozmin Timis for technical assistance. I am indebted to Konstantinos Anagnostopoulos for teaching a Computational Techniques course during my undergraduate degree, that gave strong foundations to my programming skills, and proved extremely valuable for producing numerical results that appear on this thesis.

I would like to thank the String Theory group in Queen Mary, the staff in the Physics department, the PhD students and the undergraduate students, for discussions, their support and numerous other memorable moments on and off campus, during seminars, coffee and lunch breaks, graduate lectures, journal clubs, labs, tutorials, dinners, nights out in London and conference trips. To name a few, I thank Kathy Boydon, Tom Brown, Vincenzo Calo, Paola Ferrario, George Georgiou, Valeria Gili, Bill Gillin, Dimitrios Korres, Daniel Koschade, Theo Kreouzis, Andrew Low, Roger Massey, Moritz McGarrie, Cristina Monni, Jazmina Moura, Adele Nasti, Jurgis Pasukonis, Sanjaye Ramgoolam, Rodolfo Russo, Kate Shine, Steve Thomas, David Turton and Max Vincon. Finally, I would like to thank Zvi Bern, Tristan Dennen, Yu-tin Huang, Harald Ita, Kemal Ozeren and the Theoretical Elementary Particles group at University of California, Los Angeles for their hospitality during the last months of my PhD studies.

I would like to thank all the staff at the front office of the IT services of QMUL, where I worked on Wednesday mornings and where part of this thesis was written.

I would like to thank my friends and especially my housemates Alexandra, Beth, Paul, Philip, Steph and Steph for sharing a house that I could call home. Finally, I would like to thank all my salsa friends, and the Latin Collective, who made my evenings much more fun during my last and most busy year of my PhD.

Finally, I would like to thank my family, my grand parents, my uncle Takis Stathopoulos, my brother Ioannis and my parents, for their support and unconditional love.

Bibliography

[1] M. F. Sohnius and P. C. West, "Conformal Invariance in N=4 Supersymmetric Yang-Mills Theory," *Phys. Lett.* **B100** (1981) 245.

[2] S. Mandelstam, "Light Cone Superspace and the Ultraviolet Finiteness of the N=4 Model," *Nucl. Phys.* **B213** (1983) 149–168.

[3] P. S. Howe, K. S. Stelle, and P. C. West, "A Class of Finite Four-Dimensional Supersymmetric Field Theories," *Phys. Lett.* **B124** (1983) 55.

[4] P. S. Howe, K. S. Stelle, and P. K. Townsend, "Miraculous Ultraviolet Cancellations in Supersymmetry Made Manifest," *Nucl. Phys.* **B236** (1984) 125.

[5] Z. Bern and D. A. Kosower, "The Computation of loop amplitudes in gauge theories," *Nucl. Phys.* **B379** (1992) 451–561.

[6] Z. Bern, A. De Freitas, L. J. Dixon, and H. L. Wong, "Supersymmetric regularization, two-loop QCD amplitudes and coupling shifts," *Phys. Rev.* **D66** (2002) 085002, `hep-ph/0202271`.

[7] J. M. Drummond, G. P. Korchemsky, and E. Sokatchev, "Conformal properties of four-gluon planar amplitudes and Wilson loops," *Nucl. Phys.* **B795** (2008) 385–408, `0707.0243`.

[8] A. Brandhuber, P. Heslop, and G. Travaglini, "MHV Amplitudes in N=4 Super Yang-Mills and Wilson Loops," *Nucl. Phys.* **B794** (2008) 231–243, `0707.1153`.

[9] J. M. Drummond, J. Henn, G. P. Korchemsky, and E. Sokatchev, "On planar gluon amplitudes/Wilson loops duality," *Nucl. Phys.* **B795** (2008) 52–68, `0709.2368`.

[10] J. M. Drummond, J. Henn, G. P. Korchemsky, and E. Sokatchev, "Conformal Ward identities for Wilson loops and a test of the duality with gluon amplitudes," *Nucl. Phys.* **B826** (2010) 337–364, 0712.1223.

[11] J. M. Drummond, J. Henn, G. P. Korchemsky, and E. Sokatchev, "The hexagon Wilson loop and the BDS ansatz for the six- gluon amplitude," *Phys. Lett.* **B662** (2008) 456–460, 0712.4138.

[12] J. M. Drummond, J. Henn, G. P. Korchemsky, and E. Sokatchev, "Hexagon Wilson loop = six-gluon MHV amplitude," *Nucl. Phys.* **B815** (2009) 142–173, 0803.1466.

[13] A. Brandhuber, P. Heslop, V. V. Khoze, and G. Travaglini, "Simplicity of Polygon Wilson Loops in N=4 SYM," *JHEP* **01** (2010) 050, 0910.4898.

[14] A. Brandhuber, P. Heslop, P. Katsaroumpas, D. Nguyen, B. Spence, M. Spradlin, and G. Travaglini, "A Surprise in the Amplitude/Wilson Loop Duality," *JHEP* **07** (2010) 080, 1004.2855.

[15] J. M. Maldacena, "The large N limit of superconformal field theories and supergravity," *Adv. Theor. Math. Phys.* **2** (1998) 231–252, hep-th/9711200.

[16] E. Witten, "Anti-de Sitter space and holography," *Adv. Theor. Math. Phys.* **2** (1998) 253–291, hep-th/9802150.

[17] L. F. Alday and J. M. Maldacena, "Gluon scattering amplitudes at strong coupling," *JHEP* **06** (2007) 064, 0705.0303.

[18] R. Britto, F. Cachazo, and B. Feng, "New Recursion Relations for Tree Amplitudes of Gluons," *Nucl. Phys.* **B715** (2005) 499–522, hep-th/0412308.

[19] R. Britto, F. Cachazo, B. Feng, and E. Witten, "Direct Proof Of Tree-Level Recursion Relation In Yang- Mills Theory," *Phys. Rev. Lett.* **94** (2005) 181602, hep-th/0501052.

[20] Z. Bern, L. J. Dixon, and D. A. Kosower, "One-loop amplitudes for e+ e- to four partons," *Nucl. Phys.* **B513** (1998) 3–86, hep-ph/9708239.

[21] R. Britto, F. Cachazo, and B. Feng, "Generalized unitarity and one-loop amplitudes in N = 4 super-Yang-Mills," *Nucl. Phys.* **B725** (2005) 275–305, hep-th/0412103.

[22] J. Bedford, A. Brandhuber, B. J. Spence, and G. Travaglini, "A recursion relation for gravity amplitudes," *Nucl. Phys.* **B721** (2005) 98–110, hep-th/0502146.

[23] F. Cachazo and P. Svrcek, "Tree level recursion relations in general relativity," hep-th/0502160.

[24] P. Benincasa, C. Boucher-Veronneau, and F. Cachazo, "Taming tree amplitudes in general relativity," *JHEP* **11** (2007) 057, hep-th/0702032.

[25] N. Arkani-Hamed and J. Kaplan, "On Tree Amplitudes in Gauge Theory and Gravity," *JHEP* **04** (2008) 076, 0801.2385.

[26] N. Arkani-Hamed, F. Cachazo, and J. Kaplan, "What is the Simplest Quantum Field Theory?," 0808.1446.

[27] Z. Bern, L. J. Dixon, and R. Roiban, "Is N = 8 supergravity ultraviolet finite?," *Phys. Lett.* **B644** (2007) 265–271, hep-th/0611086.

[28] Z. Bern *et al.*, "Three-Loop Superfiniteness of N=8 Supergravity," *Phys. Rev. Lett.* **98** (2007) 161303, hep-th/0702112.

[29] Z. Bern, J. J. Carrasco, D. Forde, H. Ita, and H. Johansson, "Unexpected Cancellations in Gravity Theories," *Phys. Rev.* **D77** (2008) 025010, 0707.1035.

[30] Z. Bern, J. J. M. Carrasco, and H. Johansson, "Progress on Ultraviolet Finiteness of Supergravity," 0902.3765.

[31] Z. Bern, L. J. Dixon, M. Perelstein, and J. S. Rozowsky, "Multi-leg one-loop gravity amplitudes from gauge theory," *Nucl. Phys.* **B546** (1999) 423–479, hep-th/9811140.

[32] Z. Bern, N. E. J. Bjerrum-Bohr, and D. C. Dunbar, "Inherited twistor-space structure of gravity loop amplitudes," *JHEP* **05** (2005) 056, hep-th/0501137.

[33] N. E. J. Bjerrum-Bohr, D. C. Dunbar, and H. Ita, "Six-point one-loop N = 8 supergravity NMHV amplitudes and their IR behaviour," *Phys. Lett.* **B621** (2005) 183–194, hep-th/0503102.

[34] N. E. J. Bjerrum-Bohr, D. C. Dunbar, H. Ita, W. B. Perkins, and K. Risager, "The no-triangle hypothesis for N = 8 supergravity," *JHEP* **12** (2006) 072, hep-th/0610043.

[35] N. E. J. Bjerrum-Bohr and P. Vanhove, "Explicit Cancellation of Triangles in One-loop Gravity Amplitudes," *JHEP* **04** (2008) 065, 0802.0868.

[36] S. Badger, N. E. J. Bjerrum-Bohr, and P. Vanhove, "Simplicity in the Structure of QED and Gravity Amplitudes," *JHEP* **02** (2009) 038, 0811.3405.

[37] Z. Bern, J. J. Carrasco, L. J. Dixon, H. Johansson, and R. Roiban, "The Ultraviolet Behavior of N=8 Supergravity at Four Loops," *Phys. Rev. Lett.* **103** (2009) 081301, 0905.2326.

[38] G. Chalmers, "On the finiteness of N = 8 quantum supergravity," hep-th/0008162.

[39] M. B. Green, J. G. Russo, and P. Vanhove, "Non-renormalisation conditions in type II string theory and maximal supergravity," *JHEP* **02** (2007) 099, hep-th/0610299.

[40] M. B. Green, J. G. Russo, and P. Vanhove, "Ultraviolet properties of maximal supergravity," *Phys. Rev. Lett.* **98** (2007) 131602, hep-th/0611273.

[41] N. Berkovits, "New higher-derivative R**4 theorems," *Phys. Rev. Lett.* **98** (2007) 211601, hep-th/0609006.

[42] H. Elvang and D. Z. Freedman, "Note on graviton MHV amplitudes," *JHEP* **05** (2008) 096, 0710.1270.

[43] F. A. Berends, W. T. Giele, and H. Kuijf, "On relations between multi - gluon and multigraviton scattering," *Phys. Lett.* **B211** (1988) 91.

[44] M. Spradlin, A. Volovich, and C. Wen, "Three Applications of a Bonus Relation for Gravity Amplitudes," *Phys. Lett.* **B674** (2009) 69–72, 0812.4767.

[45] J. M. Drummond, M. Spradlin, A. Volovich, and C. Wen, "Tree-Level Amplitudes in N=8 Supergravity," *Phys. Rev.* **D79** (2009) 105018, 0901.2363.

[46] A. Brandhuber, P. Heslop, and G. Travaglini, "A note on dual superconformal symmetry of the N=4 super Yang-Mills S-matrix," *Phys. Rev.* **D78** (2008) 125005, 0807.4097.

[47] J. M. Drummond and J. M. Henn, "All tree-level amplitudes in N=4 SYM," *JHEP* **04** (2009) 018, 0808.2475.

[48] J. M. Drummond, J. Henn, G. P. Korchemsky, and E. Sokatchev, "Generalized unitarity for N=4 super-amplitudes," 0808.0491.

[49] G. Georgiou and V. V. Khoze, "Tree amplitudes in gauge theory as scalar MHV diagrams," *JHEP* **05** (2004) 070, hep-th/0404072.

[50] A. Brandhuber, B. J. Spence, and G. Travaglini, "One-loop gauge theory amplitudes in N = 4 super Yang-Mills from MHV vertices," *Nucl. Phys.* **B706** (2005) 150–180, hep-th/0407214.

[51] M. Bianchi, H. Elvang, and D. Z. Freedman, "Generating Tree Amplitudes in N=4 SYM and N = 8 SG," *JHEP* **09** (2008) 063, 0805.0757.

[52] H. Elvang, D. Z. Freedman, and M. Kiermaier, "Recursion Relations, Generating Functions, and Unitarity Sums in N=4 SYM Theory," *JHEP* **04** (2009) 009, 0808.1720.

[53] H. Elvang, D. Z. Freedman, and M. Kiermaier, "Proof of the MHV vertex expansion for all tree amplitudes in N=4 SYM theory," *JHEP* **06** (2009) 068, 0811.3624.

[54] Z. Bern, J. J. M. Carrasco, H. Ita, H. Johansson, and R. Roiban, "On the Structure of Supersymmetric Sums in Multi-Loop Unitarity Cuts," *Phys. Rev.* **D80** (2009) 065029, 0903.5348.

[55] P. Katsaroumpas, B. Spence, and G. Travaglini, "One-loop N=8 supergravity coefficients from N=4 super Yang-Mills," *JHEP* **08** (2009) 096, 0906.0521.

[56] H. Kawai, D. C. Lewellen, and S. H. H. Tye, "A Relation Between Tree Amplitudes of Closed and Open Strings," *Nucl. Phys.* **B269** (1986) 1.

[57] C. Anastasiou, Z. Bern, L. J. Dixon, and D. A. Kosower, "Planar amplitudes in maximally supersymmetric Yang-Mills theory," *Phys. Rev. Lett.* **91** (2003) 251602, hep-th/0309040.

[58] F. Cachazo, M. Spradlin, and A. Volovich, "Iterative structure within the five-particle two-loop amplitude," *Phys. Rev.* **D74** (2006) 045020, hep-th/0602228.

[59] Z. Bern, M. Czakon, D. A. Kosower, R. Roiban, and V. A. Smirnov, "Two-loop iteration of five-point N = 4 super-Yang-Mills amplitudes," *Phys. Rev. Lett.* **97** (2006) 181601, hep-th/0604074.

[60] M. Spradlin, A. Volovich, and C. Wen, "Three-Loop Leading Singularities and BDS Ansatz for Five Particles," *Phys. Rev.* **D78** (2008) 085025, 0808.1054.

[61] L. F. Alday and J. Maldacena, "Comments on gluon scattering amplitudes via AdS/CFT," *JHEP* **11** (2007) 068, 0710.1060.

[62] Z. Bern *et al.*, "The Two-Loop Six-Gluon MHV Amplitude in Maximally Supersymmetric Yang-Mills Theory," *Phys. Rev.* **D78** (2008) 045007, 0803.1465.

[63] V. Del Duca, C. Duhr, and V. A. Smirnov, "An Analytic Result for the Two-Loop Hexagon Wilson Loop in N = 4 SYM," *JHEP* **03** (2010) 099, 0911.5332.

[64] V. Del Duca, C. Duhr, and V. A. Smirnov, "The Two-Loop Hexagon Wilson Loop in N = 4 SYM," *JHEP* **05** (2010) 084, 1003.1702.

[65] J.-H. Zhang, "On the two-loop hexagon Wilson loop remainder function in N=4 SYM," 1004.1606.

[66] A. B. Goncharov, M. Spradlin, C. Vergu, and A. Volovich, "Classical Polylogarithms for Amplitudes and Wilson Loops," 1006.5703.

[67] J. M. Drummond, J. Henn, V. A. Smirnov, and E. Sokatchev, "Magic identities for conformal four-point integrals," *JHEP* **01** (2007) 064, hep-th/0607160.

[68] J. M. Drummond, J. Henn, G. P. Korchemsky, and E. Sokatchev, "Dual superconformal symmetry of scattering amplitudes in N=4 super-Yang-Mills theory," *Nucl. Phys.* **B828** (2010) 317–374, 0807.1095.

[69] M. L. Mangano and S. J. Parke, "Multi-Parton Amplitudes in Gauge Theories," *Phys. Rept.* **200** (1991) 301–367, hep-th/0509223.

[70] M. E. Peskin and D. V. Schroeder, "An Introduction to quantum field theory,". Reading, USA: Addison-Wesley (1995) 842 p.

[71] L. H. Ryder, "Quantum Field Theory,". Cambridge, Uk: Univ. Pr. (1985) 443p.

[72] L. J. Dixon, "Calculating scattering amplitudes efficiently," `hep-ph/9601359`.

[73] F. A. Berends, R. Kleiss, P. De Causmaecker, R. Gastmans, and T. T. Wu, "Single Bremsstrahlung Processes in Gauge Theories," *Phys. Lett.* **B103** (1981) 124.

[74] P. De Causmaecker, R. Gastmans, W. Troost, and T. T. Wu, "Multiple Bremsstrahlung in Gauge Theories at High- Energies. 1. General Formalism for Quantum Electrodynamics," *Nucl. Phys.* **B206** (1982) 53.

[75] R. Kleiss and W. J. Stirling, "Spinor Techniques for Calculating p anti-p $\to$ W+- / Z0 + Jets," *Nucl. Phys.* **B262** (1985) 235–262.

[76] Z. Xu, D.-H. Zhang, and L. Chang, "Helicity Amplitudes for Multiple Bremsstrahlung in Massless Nonabelian Gauge Theories," *Nucl. Phys.* **B291** (1987) 392.

[77] J. F. Gunion and Z. Kunszt, "Improved Analytic Techniques for Tree Graph Calculations and the G g q anti-q Lepton anti-Lepton Subprocess," *Phys. Lett.* **B161** (1985) 333.

[78] E. Witten, "Perturbative gauge theory as a string theory in twistor space," *Commun. Math. Phys.* **252** (2004) 189–258, `hep-th/0312171`.

[79] S. J. Parke and T. R. Taylor, "An Amplitude for n Gluon Scattering," *Phys. Rev. Lett.* **56** (1986) 2459.

[80] F. A. Berends and W. T. Giele, "Recursive Calculations for Processes with n Gluons," *Nucl. Phys.* **B306** (1988) 759.

[81] L. Mason and D. Skinner, "Gravity, Twistors and the MHV Formalism," *Commun. Math. Phys.* **294** (2010) 827–862, `0808.3907`.

[82] V. P. Nair, "A current algebra for some gauge theory amplitudes," *Phys. Lett.* **B214** (1988) 215.

[83] Z. Bern, "Perturbative quantum gravity and its relation to gauge theory," *Living Rev. Rel.* **5** (2002) 5, gr-qc/0206071.

[84] Z. Bern, L. J. Dixon, D. C. Dunbar, and D. A. Kosower, "One-Loop n-Point Gauge Theory Amplitudes, Unitarity and Collinear Limits," *Nucl. Phys.* **B425** (1994) 217–260, hep-ph/9403226.

[85] Z. Bern, L. J. Dixon, D. C. Dunbar, and D. A. Kosower, "Fusing gauge theory tree amplitudes into loop amplitudes," *Nucl. Phys.* **B435** (1995) 59–101, hep-ph/9409265.

[86] N. E. J. Bjerrum-Bohr and P. Vanhove, "Absence of Triangles in Maximal Supergravity Amplitudes," *JHEP* **10** (2008) 006, 0805.3682.

[87] K. Risager, "Unitarity and On-Shell Recursion Methods for Scattering Amplitudes," 0804.3310.

[88] A. Denner, U. Nierste, and R. Scharf, "A Compact expression for the scalar one loop four point function," *Nucl. Phys.* **B367** (1991) 637–656.

[89] N. I. Usyukina and A. I. Davydychev, "An Approach to the evaluation of three and four point ladder diagrams," *Phys. Lett.* **B298** (1993) 363–370.

[90] Z. Bern, L. J. Dixon, and D. A. Kosower, "Dimensionally regulated pentagon integrals," *Nucl. Phys.* **B412** (1994) 751–816, hep-ph/9306240.

[91] R. Roiban, M. Spradlin, and A. Volovich, "Dissolving N = 4 loop amplitudes into QCD tree amplitudes," *Phys. Rev. Lett.* **94** (2005) 102002, hep-th/0412265.

[92] C. F. Berger *et al.*, "An Automated Implementation of On-Shell Methods for One- Loop Amplitudes," *Phys. Rev.* **D78** (2008) 036003, 0803.4180.

[93] M. T. Grisaru, H. N. Pendleton, and P. van Nieuwenhuizen, "Supergravity and the s matrix," *Phys. Rev. D* **15** (Feb, 1977) 996.

[94] M. T. Grisaru and H. N. Pendleton, "Some properties of scattering amplitudes in supersymmetric theories," *Nuclear Physics B* **124** (1977), no. 1, 81 – 92.

[95] S. Catani, "The singular behaviour of QCD amplitudes at two-loop order," *Phys. Lett.* **B427** (1998) 161–171, hep-ph/9802439.

[96] G. F. Sterman and M. E. Tejeda-Yeomans, "Multi-loop amplitudes and resummation," *Phys. Lett.* **B552** (2003) 48–56, hep-ph/0210130.

[97] D. A. Kosower and P. Uwer, "One-Loop Splitting Amplitudes in Gauge Theory," *Nucl. Phys.* **B563** (1999) 477–505, hep-ph/9903515.

[98] Z. Bern, V. Del Duca, W. B. Kilgore, and C. R. Schmidt, "The infrared behavior of one-loop QCD amplitudes at next-to-next-to-leading order," *Phys. Rev.* **D60** (1999) 116001, hep-ph/9903516.

[99] F. Cachazo, M. Spradlin, and A. Volovich, "Leading Singularities of the Two-Loop Six-Particle MHV Amplitude," *Phys. Rev.* **D78** (2008) 105022, 0805.4832.

[100] J. G. M. Gatheral, "Exponentiation of eikonal cross sections in nonabelian gauge theories," *Physics Letters B* **133** (1983), no. 1-2, 90 – 94.

[101] J. Frenkel and J. C. Taylor, "Nonabelian eikonal exponentiation," *Nucl. Phys.* **B246** (1984) 231.

[102] G. P. Korchemsky and G. Marchesini, "Structure function for large x and renormalization of Wilson loop," *Nucl. Phys.* **B406** (1993) 225–258, hep-ph/9210281.

[103] E. Gardi, E. Laenen, G. Stavenga, and C. D. White, "Webs in multiparton scattering using the replica trick," *JHEP* **11** (2010) 155, 1008.0098.

[104] I. A. Korchemskaya and G. P. Korchemsky, "On lightlike Wilson loops," *Phys. Lett.* **B287** (1992) 169–175.

[105] C. Anastasiou, A. Brandhuber, P. Heslop, V. V. Khoze, B. Spence, and G. Travaglini, "Two-Loop Polygon Wilson Loops in N=4 SYM," *JHEP* **05** (2009) 115, 0902.2245.

[106] P. Heslop and V. V. Khoze, "Regular Wilson loops and MHV amplitudes at weak and strong coupling," *JHEP* **06** (2010) 037, 1003.4405.

[107] Z. Bern, L. J. Dixon, and V. A. Smirnov, "Iteration of planar amplitudes in maximally supersymmetric Yang-Mills theory at three loops and beyond," *Phys. Rev.* **D72** (2005) 085001, hep-th/0505205.

[108] M. B. Green, J. H. Schwarz, and L. Brink, "N=4 Yang-Mills and N=8 Supergravity as Limits of String Theories," *Nucl. Phys.* **B198** (1982) 474–492.

[109] Z. Bern, L. J. Dixon, D. C. Dunbar, and D. A. Kosower, "One-loop self-dual and N = 4 superYang-Mills," *Phys. Lett.* **B394** (1997) 105–115, hep-th/9611127.

[110] Z. Bern, J. S. Rozowsky, and B. Yan, "Two-loop four-gluon amplitudes in N = 4 super-Yang- Mills," *Phys. Lett.* **B401** (1997) 273–282, hep-ph/9702424.

[111] Z. Bern, J. Rozowsky, and B. Yan, "Two-loop N = 4 supersymmetric amplitudes and QCD," hep-ph/9706392.

[112] M. Czakon, "Automatized analytic continuation of Mellin-Barnes integrals," *Comput. Phys. Commun.* **175** (2006) 559–571, hep-ph/0511200.

[113] A. V. Smirnov and V. A. Smirnov, "On the Resolution of Singularities of Multiple Mellin- Barnes Integrals," *Eur. Phys. J.* **C62** (2009) 445–449, 0901.0386.

[114] G. Georgiou, "Null Wilson loops with a self-crossing and the Wilson loop/amplitude conjecture," *JHEP* **09** (2009) 021, 0904.4675.

[115] S. Sarkar, "Dimensional Regularization and Broken Conformal Ward Identities," *Nucl. Phys.* **B83** (1974) 108.

[116] D. Mueller, "Conformal constraints and the evolution of the nonsinglet meson distribution amplitude," *Phys. Rev.* **D49** (1994) 2525–2535.

[117] D. Mueller, "Restricted conformal invariance in QCD and its predictive power for virtual two-photon processes," *Phys. Rev.* **D58** (1998) 054005, hep-ph/9704406.

[118] A. V. Belitsky and D. Mueller, "Broken conformal invariance and spectrum of anomalous dimensions in QCD," *Nucl. Phys.* **B537** (1999) 397–442, hep-ph/9804379.

[119] V. M. Braun, G. P. Korchemsky, and D. Mueller, "The uses of conformal symmetry in QCD," *Prog. Part. Nucl. Phys.* **51** (2003) 311–398, hep-ph/0306057.

[120] N. Berkovits and J. Maldacena, "Fermionic T-Duality, Dual Superconformal Symmetry, and the Amplitude/Wilson Loop Connection," *JHEP* **09** (2008) 062, 0807.3196.

[121] N. Beisert, R. Ricci, A. A. Tseytlin, and M. Wolf, "Dual Superconformal Symmetry from AdS5 x S5 Superstring Integrability," *Phys. Rev.* **D78** (2008) 126004, 0807.3228.

[122] V. A. Smirnov, "Evaluating Feynman integrals," *Springer Tracts Mod. Phys.* **211** (2004) 1–244.

[123] T. Hahn, "CUBA: A library for multidimensional numerical integration," *Comput. Phys. Commun.* **168** (2005) 78–95, hep-ph/0404043.

[124] L. Mason and D. Skinner, "Scattering Amplitudes and BCFW Recursion in Twistor Space," 0903.2083.

[125] N. Arkani-Hamed, F. Cachazo, C. Cheung, and J. Kaplan, "The S-Matrix in Twistor Space," *JHEP* **03** (2010) 110, 0903.2110.

[126] A. Hodges, "Eliminating spurious poles from gauge-theoretic amplitudes," 0905.1473.

[127] A. P. Hodges, "Twistor diagrams for all tree amplitudes in gauge theory: A helicity-independent formalism," hep-th/0512336.

[128] B. Chen and J.-B. Wu, "Tree-level Split Helicity Amplitudes in Ambitwistor Space," *Phys. Rev.* **D80** (2009) 125031, 0905.0522.

[129] G. Duplancic and B. Nizic, "Dimensionally regulated one-loop box scalar integrals with massless internal lines," *Eur. Phys. J.* **C20** (2001) 357–370, hep-ph/0006249.

[130] A. Brandhuber, B. Spence, and G. Travaglini, "From trees to loops and back," *JHEP* **01** (2006) 142, hep-th/0510253.